

ASSESSMENT OF SAFE AQUIFER YIELD WITHIN THE SALT BASIN IN NEW MEXICO AND TEXAS.

by

Elizabeth Evenocheck

Submitted in Partial Fulfillment
of the Requirements for the Degree of
Master of Science in Hydrology



New Mexico Institute of Mining and Technology
Socorro, New Mexico
September, 2021

ACKNOWLEDGMENTS

This project was funded by the Bureau of Reclamation and was conducted in coordination with the New Mexico Interstate Stream Committee, New Mexico Bureau of Geology and Mineral Resources, the U.S. Geological Survey, and S.S. Papadopoulos & Associates, Inc.

I would like to express my appreciation for my advisor Dr. Mark Person who has taught me so much, always found time to answer questions, and goes above and beyond for his students. I have been fortunate to get to learn from such a great scientist, professor, and person.

Thank you to Gilbert Barth, Jessica Rogers, and those behind the scenes at S.S. Papadopoulos & Associates, Inc. for providing insights on model construction and taking the time to teach me how everything worked.

Thank you to Marissa Fichera for your roles in developing these models and always being willing to chat about the Salt Basin, Beth Ann Eberle for being a great research project buddy, and Shari Kelley for getting me out of the office and in the field.

Thank you to the NMT graduate student and Socorro, NM community, without them this thesis would not have been completed.

Thank you to my family and friends who have supported me in every endeavor I have taken including this one. In particular, thank you to my parents who let me move back home during a global pandemic and made sure I had the resources and support to continue research.

Finally, thank you to Spencer Hollingworth, Isabel Morris, Scott Roberts, Koa, and the Ultra-Mafic intramural soccer team.

This dissertation was typeset with \LaTeX^1 by the author.

¹The \LaTeX document preparation system was developed by Leslie Lamport as a special version of Donald Knuth's \TeX program for computer typesetting. \TeX is a trademark of the American Mathematical Society. The \LaTeX macro package for the New Mexico Institute of Mining and Technology dissertation format was written by John W. Shipman.

ABSTRACT

The goals of this study are to refine water budget estimates and determine safe aquifer yield for the Salt Basin, located in south central New Mexico and west Texas. A secondary goal is to determine if a hypothetical well field on the New Mexico side of the basin can produce between 66,345 to 127,072 acre-feet of water while maintaining safe aquifer yield. The Salt Basin has a footprint of ~14,000 km², is sparsely populated, semi-arid, and hydrologically closed. We developed a series of three-dimensional numerical groundwater flow models to address these questions. We developed a predevelopment steady-state model and a historical transient model that included pumping from 1948 to 2020. Pumping scenarios were run with the historical transient model to test hypothetical well field affects on the Salt Basin aquifer. The predevelopment steady state model was calibrated using recharge rates of 40,000, 60,000, and 80,000 acre-feet/year.

In the historical transient model, we assumed an average recharge rate of 61,259 acre-feet/year. The historical transient model was able to reproduce regional water table maps as well as observed well hydrograph data. Using water budget calculations and assuming a recharge rate of about 60,000 acre-feet/year we estimate the safe aquifer yield to be valued between 64,000 to 67,000 acre-feet/year. The safe aquifer yield estimate would change if recharge rates or climatic conditions in the Salt Basin changed.

Simulation of hypothetical well fields indicates that additional pumping will capture water from groundwater storage and/or evapotranspiration. In the historical transient model there was a total of about 5,700,000 acre-feet of pumping for the entire simulation of 72 years. For the hypothetical well field pumping scenarios, pumping an additional 127,072 acre-feet from 1969 to 1974 lowered total evapotranspiration for the entire simulation between 15,107 and 1,150 acre-feet. Pumping an additional 66,345 acre-feet during years with high runoff (eight years from 1972 to 2014) lowered total evapotranspiration for the entire simulation between 3,939 and 185 acre-feet. The pumping volume not taken from evapotranspiration was from reductions in groundwater storage. Pumping from new well fields resulted in a maximum drawdown in New Mexico of 25 meters. Drawdowns >1 meter can reach a radius of 35 km from the hypothetical well fields. The change in flux of groundwater crossing from NM to TX is the least for the Crow Flats well field; with only a 65 acre-feet decrease from the historical model for the entire model simulation. This represents ~0.05% of the additional water pumped. Although drawdown and state line flux results showed promise for some hypothetical well fields, based on the safe aquifer yield estimate, it was found that pumping any additional water from any hypothetical well field could not maintain safe aquifer yield. Our analysis did not take into consideration the

effects of salt water upconing on safe aquifer yield.

Keywords: Salt Basin; Safe Aquifer Yield; Groundwater Flow Model; Recharge; Evapotranspiration; Closed Basin

CONTENTS

	Page
LIST OF TABLES	viii
LIST OF FIGURES	x
CHAPTER 1. INTRODUCTION	1
CHAPTER 2. BACKGROUND	4
CHAPTER 3. METHODS	12
3.1 Model Framework	12
3.2 Model Inputs	14
3.3 Model Calibration	16
3.4 Pumping Scenarios	18
CHAPTER 4. RESULTS	26
4.1 Predevelopment Steady-State Model: 3 Levels of Recharge	26
4.2 Predevelopment Steady-State Model	27
4.3 Historical Transient Model	28
4.4 Pumping Scenarios	30
CHAPTER 5. DISCUSSION	53
5.1 Predevelopment Steady-State Model	53
5.2 Historical Transient Model	56
5.3 Pumping Scenarios	58
5.4 Uncertainties and Improvements	60
CHAPTER 6. CONCLUSIONS	62
REFERENCES	65

APPENDIX A. SALT BASIN GEOLOGY	72
A.1 Stratigraphy	72
A.1.1 Neogene Alluvial and Bolson Deposits	72
A.1.2 Tertiary Intrusions	73
A.1.3 Cretaceous Units	73
A.1.4 Permian Shelf Facies	73
A.1.5 Permian Shelf-Margin Facies	74
A.1.6 Permian Basin Facies	75
A.1.7 Later Paleozoic Units	75
A.1.8 Early Paleozoic Units	76
A.1.9 Precambrian Units	76
A.2 Structure	76
A.2.1 Pennsylvania to Early Permian	77
A.2.2 Mid-to-Late Permian	77
A.2.3 Late Cretaceous	78
A.2.4 Cenozoic	78
APPENDIX B. PAST GROUNDWATER MODELS OF THE SALT BASIN	81
B.1 Mayer and Sharp (1995) - The Role of Fractures in Regional Groundwater Flow	81
B.2 John Shomaker & Associates, Inc. (2002)	83
B.2.1 Finch (2002) - Hydrogeologic framework of the Salt Basin and development of three-dimensional ground-water flow model	83
B.2.2 Shomaker (2002) - Hypothetical well fields in Salt Basin and pipeline to Pecos River	85
B.3 Hutchison (2008) - Preliminary Groundwater Flow Model, Dell City Area, Hudspeth and Culberson Counties, Texas	86
B.4 John Shomaker & Associates, Inc (2010) – Revised Hydrogeologic Framework and Groundwater-Flow Model of the Salt Basin Aquifer in Southeastern New Mexico and Part of Texas	87
B.5 Ritchie (2011) - Hydrogeologic Framework and Development of a Three-dimensional Finite Difference Groundwater-Flow Model of the Salt Basin, New Mexico and Texas	89
B.6 Past Model Summary	90

LIST OF TABLES

Table	Page
3.1 Initial hydraulic conductivities and vertical anisotropies assigned to geologic zones. These values are the initial parameters from Ritchie (2011). Initial S_y and S_s were suggested by S.S. Papadopoulos & Associates, Inc. based on Shomaker [2010]. S_y is specific yield, S_s is specific storage. Categorized by geologic unit. Figure 3.2 – 3.4 show distribution of geologic zones listed here.	19
3.2 Years and pumping rates of extra pumping in acre-feet/year and m^3/day for the hypothetical Scenario 1 simulations. A total of pumping is 127,072 acre-feet (157 million m^3) for the entire six years of additional pumping. Pumping rates come from Shomaker [2002].	20
3.3 Years and pumping rates of extra pumping in acre-feet/year and m^3/day for the hypotheical Scenario 2 simulations. A total of 66,345 acre-feet (82 million m^3) was added to the years indicated and those years were times with higher than average runoff.	20
4.1 Table of hydraulic conductivities and vertical anisotropies data for the three levels of recharge rates. Average indicates, averages of the value for each geology zone polygon, and does not account for area covered by each geologic zone polygon.	31
4.2 Table of flow budget parameters for three levels of recharge with the predevelopment steady-state model used to decide the predevelopment recharge rate. In m^3/day and acre-feet/year.	32
4.3 Statistics on the observed versus computed water levels for the predevelopment steady-state recharge model using three levels of recharge. Water levels not used in the PEST calibration were not used to compute the statistics. Mean Error is observed minus computed water levels.	33
4.4 Statistics on the observed versus computed ^{14}C ages for the predevelopment steady-state recharge model using three levels of recharge. Observed ^{14}C ages from Sigstedt [2010].	34
4.5 Hydraulic conductivities and vertical anisotropies assigned to geologic zones for the predevelopment steady-state and historical transient models, categorized by geologic unit.	34

4.6	Flow budget (in acre-feet/year and m ³ /day) of the predevelopment steady-state model.	35
4.7	Diffuse recharge rates for each diffuse recharge polygon in the predevelopment steady-state model.	36
4.8	S _y and S _s used in the historical transient model. S _y is specific yield, S _s is specific storage, categorized by geologic unit. Figure 3.2 – 3.4 show the distribution of geologic zones listed here.	36
4.9	Average parameters for the flow budget (in acre-feet/year and m ³ /day) for the historical transient model from 1948 to 2020.	37
4.10	Flow budget for the historical transient model and the difference between the total volume in acre-feet and m ³ for the hypothetical pumping scenario flow budget and the historical model flow budget. All values are totals from 1948 to 2020. This table shows that the additional pumping takes water from evapotranspiration and storage.	38
4.11	Sum of subsurface water flux across the state line from New Mexico to Texas for the entire transient model run (1948 – 2020), and the difference of the model scenario sum of subsurface water flowing across the state line from New Mexico to Texas minus the historical transient model sum. Values in acre-feet and m ³	39
B.1	General information about each Salt Basin model's purpose and results.	92
B.2	Hydraulic conductivity, recharge and discharge data for each Salt Basin model. Abbreviations: FEM = Finite element model; FDM = finite difference model.	93

LIST OF FIGURES

Figure	Page
Figure 2.1 Location of prominent features in the Salt Basin. Black outline is the current model boundary. Red line is the Victorio Flexure.	7
Figure 2.2 Predevelopment (blue) and current (red) 50 meter water table contours and 5 meter contours in the salt flats in the Salt Basin. Developed in this study. Gray polygon is the area near Dell City with greater than 1 meter of drawdown from the predevelopment to current observed water tables. The current observed water table is based on some older observed water levels but they were outside the Dell City area where water levels are assumed to have not changed much.	8
Figure 2.3 Locations of the monitoring wells in Dell City, TX area that have at least one water level measurement for each decade from pre-1950 to 2010's. The data from these wells are presented in the hydrographs in Figure 2.4. Wells are labeled with their well ID.	9
Figure 2.4 Hydrographs of water levels (m) for thirteen wells in Dell City, TX that have at least one water level measurement for each decade from pre-1950 to 2010's. Their locations shown on Figure 2.3. This figure shows 15 – 20 meters of drawdown from 1948 to 2020.	10
Figure 2.5 Graphical summary of model parameters used in prior studies of the Salt Basin. The blue lines denote the hydraulic conductivity range used by Mayer and Sharp Jr [1995], Shomaker [2002], Hutchison [2008], Shomaker [2010], Ritchie [2011], and this model. Blue circles indicate steady-state recharge, red squares indicate steady-state discharge, green circles indicate average transient recharge, and pink squares indicate average transient discharge. Mayer and Sharp Jr [1995]'s hydraulic conductivities are actually transmissivity values so the location of the blue line could be different. This figure shows how the flow budget parameters of prior models of the Salt Basin compare. They are all similar except for the high values in Hutchison [2008] and the low values in Ritchie [2011]. Hutchison [2008] values include their high underflow values.	11

Figure 3.1 Current model grid outline with all boundary conditions symbolized by color of grid cell. Diffuse recharge (colored polygons), depression-focused recharge (blue lines), evapotranspiration (ET Zone, gray polygon), specified flux boundaries (purple boundary cells), general head boundaries (brown boundary cells), and no flow boundaries (red boundary cells) are shown.	21
Figure 3.2 Map of model geologic zonation in layer 1 (left) and layer 2 (right). Labels indicate the geologic zone number. Colors indicate the geologic unit.	22
Figure 3.3 Map of final model geologic zonation in layer 3 (left) and layer 4 (right). Labels indicate the geologic zone number. Colors indicate the geologic unit.	22
Figure 3.4 Map of final model geologic zonation in layer 5 (left) and layer 6 (right). Labels indicate the geologic zone number. Colors indicate the geologic unit.	23
Figure 3.5 Locations of irrigation and DCMI pumping wells in the current transient model. Red model cells have a pumping well in the first layer. Yellow model cells have a pumping well in the second layer. Blue model cells have a pumping well in the third layer. Orange model cells have a pumping well in layers 1 and 2. Purple model cells have a pumping well in layers 1 and 3. Green model cells have a pumping well in layers 2 and 3.	24
Figure 3.6 Location of wells for the three hypothetical pumping scenario well fields. Red squares make up the Crow Flats well field in model layer 3. Blue squares make up the Otero Break well field in model layer 2. Green squares make up the Piñon Creek well field in model layer 2.	25
Figure 4.1 Observed versus computed water levels for the three predevelopment steady-state recharge model scenarios. Water levels not used in the PEST calibration were not used to compute the statistics.	40
Figure 4.2 Graph of the computed versus observed ^{14}C ages for the three preliminary predevelopment steady-state model. Observed ^{14}C ages measured by Sigstedt [2010].	41
Figure 4.3 Distribution of hydraulic conductivities for the predevelopment steady-state and historical transient model for layer 1 (left) and layer 2 (right).	42
Figure 4.4 Distribution of hydraulic conductivities for the predevelopment steady-state and historical transient model for layer 3 (left) and layer 4 (right).	42
Figure 4.5 Distribution of hydraulic conductivities for the predevelopment steady-state and historical transient model for layer 5 (left) and layer 6 (right).	43

Figure 4.6 Distribution of depression-focused recharge in SFR segments in the predevelopment steady-state model. Color denotes amount of recharge from SFR segment. In acre-feet/year and m^3/day	44
Figure 4.7 Observed and modeled predevelopment water table contour map (in meters). Observed water table contours are denoted by solid blue contour elevation, labels are in meters. Model computed water table contours are denoted by red dashed lines. Black points are locations of observed predevelopment water levels used to create predevelopment observed water table contours. Both set of water table contours developed in this study. The contour interval is 50 meter. This figure shows a relatively good fit between the observed and model predevelopment water tables, and that some of the larger discrepancies may simply reflect interpolation of observed data across regions with only sparse data.	45
Figure 4.8 (top) Evapotranspiration, pumping, total recharge, and net storage through time of transient model (1948 to 2020). (bottom) Diffuse recharge, underflow, depression-focused recharge, total discharge, and difference between total recharge and total discharge through time of transient model.	46
Figure 4.9 Observed versus computed well hydrographs in the Salt Basin (b-d). Locations of four wells displayed as black dots in Figure 4.9a. Black lines show computed water levels through time for the well. Points are observed water levels. Red points have a >2.5m residual. Yellow points have a 2.5m to 1m residual. Green points have a <1m residual.	47
Figure 4.10 Initial (red dashed line) and final 2020 (blue and bolded labels) transient model water table contours. The initial water table contour map is from the predevelopment steady-state model. 50 m contour interval and 5 m contour interval in the salt flats.	48
Figure 4.11 Drawdown contours for Scenario 1 (additional 127,072 acre-feet of pumping) water table compared to the historical transient model water table (m) for the three pumping scenarios in the year with the most drawdown, 1974. Crow Flats drawdown contours are red, Otero Break drawdown contours are blue, and Piñon Creek drawdown contours are green.	49
Figure 4.12 Drawdown contours for Scenario 2 (additional 66,345 acre-feet of pumping) water table compared to the historical transient model water table (m) for the three pumping scenarios in the year with the most drawdown, 2014. Crow Flats drawdown contours are red, Otero Break drawdown contours are blue, and Piñon Creek drawdown contours are green.	50
Figure 4.13 Annual subsurface flux of water across the state line from New Mexico to Texas through the entire transient model run, in acre-feet/year.	51

Figure 4.14 Transient water levels for the historical transient model and the six pumping scenario models. Color denotes the model scenario. Well ID is in bottom left of each graph. Top left is a map of model grid and locations of wells plotted in figure. Well ST-00021 is near the Piñon Creek well field. Well ST-00015 is within the Crow Flats well field. Well NM-00183 is within the Otero Break well field. Water levels are in meters.	52
Figure A.1 Generalized surface geology map of the Salt Basin study area. Modified from [Kelley et al., 2020].	79
Figure A.2 General structures within the Salt Basin. Structures grouped by age, Cenozoic (green), Late Cretaceous (blue), Mid-to Late Permian (red), and Pennsylvanian to Permian (yellow). Pennsylvanian to Permian structures extend into Texas, but we did not gather data for Texas. (Modified from Ritchie [2011]).	80
Figure B.1 Boundaries of the five models discussed in this report along with this studies model boundary. Boundaries made from geo-referencing report boundaries into GIS.	94
Figure B.2 Transmissivity zones used in the model that was found to be most accurate when compared to observed data. The highest transmissivity zone contains the Otero Break. Modified from [Mayer and Sharp Jr, 1995].	95
Figure B.3 Outline of model domain used by Finch [2002]. The red dots are recharge wells that simulate recharge and inflow from other basins. The blue cells represent groundwater discharge by evapotranspiration. Modified from [Finch, 2002]. The green lines denote a no-flux boundary condition.	96
Figure B.4 Computed drawdown resulting from pumping from 1945 – 2000. Maximum drawdown is 100 ft. Contours intervals are 10 ft. Modified from [Finch, 2002].	97
Figure B.5 Net-difference in ground-water flow from NM to TX from 1945 – 2000. (Modified from Shomaker [2002]).	98
Figure B.6 Model simulated net-difference in groundwater flow from NM to TX as a result of different pumping scenarios. (Modified from Shomaker [2002]).	99
Figure B.7 Locations of the potential well fields represented in Shomaker (2002). The light purple indicates the well fields in the Otero Break, Crow Flats, and Fourmile Draw. Modified from [Shomaker, 2002].	100
Figure B.8 Maximum simulated drawdown due to historical pumping with a hypothetical well field near Otero Break (scenario (1)). Drawdowns were calculated from pre-development conditions. Contour intervals of 10 ft. Maximum drawdown of about 100 ft. Modified from [Shomaker, 2002].	101

Figure B.9 Maximum simulated drawdown due to historical pumping with a hypothetical well field near Crow Flats. Drawdowns were calculated from pre-development conditions. Contour intervals of 10 ft. Maximum drawdown of 100 ft. Modified from [Shomaker, 2002].	102
Figure B.10 Drawdowns for the structural model from pumping from 1948 - 2002. Drawdown follows the Otero Break north-northwestward. Maximum drawdown of 50 ft. Contour intervals of 10 ft. The anisotropy used in the model is illustrated by the yellow arrows. Modified from Hutchison [2008].	103
Figure B.11 Drawdowns for the geochemistry model from pumping from 1948 - 2002. Drawdown follows the Otero Break north-northwestward. Maximum drawdown of 50 ft. Contour intervals of 10 ft. The location of the Otero Break and Diablo Plateau are also shown. Modified from Hutchison [2008].	104
Figure B.12 Drawdowns for the hybrid model from pumping from 1948 - 2002. Drawdown follows the Otero Break north-northwestward. Maximum drawdown of 40 ft. Contour intervals of 10 ft. Modified from Hutchison [2008].	105
Figure B.13 Shomaker [2010] [orange] and Shomaker [2002] [green] model boundaries. Modified from [Shomaker, 2010] and [Shomaker, 2002]	106
Figure B.14 Shomaker [2010] model boundary (orange), model sinkholes (blue), and major flow paths (arrows). Modified from [Shomaker, 2010].	107
Figure B.15 Shomaker [2010] location of recharge and evapotranspiration. Injection well recharge is in dark blue, areal recharge is light blue, and the light red is evapotranspiration. Modified from Shomaker [2010].	108
Figure B.16 Model simulated drawdown after running the historical transient model from 1948 to 2009. Contour intervals of 10 ft. Maximum drawdown of 90 ft. Modified from [Shomaker, 2010].	109
Figure B.17 Ritchie [2011] Salt Basin groundwater flow model boundary.	110

This dissertation is accepted on behalf of the faculty of the Institute by the following committee:

Mark Person

Academic and Research Advisor

Andre Ritchie

Shari Kelley

Alex Rinehart

I release this document to the New Mexico Institute of Mining and Technology.

Elizabeth Evenocheck

July 21, 2021

CHAPTER 1

INTRODUCTION

Safe aquifer yield is the maximum pumping rate for which the consequences are considered acceptable [Alley et al., 1999]. Consequences could be water level declines affecting current pumping operations, reduced stream flow, and degradation of water quality [Pauloo et al., 2021]. Recharge is usually thought to be the sole component that determines safe aquifer yield. However, Bredehoeft [2002] argued that determining safe aquifer yields depends on many factors, most importantly on the “capture” from pumping. Capture is the difference between the change in recharge and the change in discharge. Capture considers the dynamics of the entire groundwater flow system. Many groundwater models are developed in an effort to understand the dynamics of a specific groundwater system [Mercer and Faust, 1980]. To determine safe groundwater yield, the groundwater flow dynamics are numerically represented and used to determine how a groundwater system reaches equilibrium with changing hydrologic stresses and aquifer parameters [Bredehoeft, 2002]. Recharge is an important component to a groundwater model but all components that help determine the system dynamics of the aquifer, such as hydraulic conductivity, storativity, discharge, and boundary conditions are critical. Setting pumping equal to the recharge underestimates safe aquifer yield. Pumping can end up reducing discharge (streamflow, transpiration, or evaporation from a salt flat) or storage. Understanding the transient dynamics of an aquifer is critical when determining safe aquifer yields.

Estimating the water budget in closed basins is difficult. There is no surface water discharge from rivers that can be measured, so both recharge and evapotranspiration must be estimated. Estimating recharge is difficult because it is hard to identify and quantify the recharge mechanisms for a given area, the spatial distribution of recharge is highly variable, and there is a lack of hydrogeological data [Sophocleous, 2004]. Depression-focused recharge is best quantified with physical measurements, such as seepage meters in streambeds or stream gauges [Sophocleous, 2004, Xu, 2018]. The Salt Basin is lacking in these measurements. Estimates of depression-focused recharge based on ephemeral channel width is another, less accurate method [Tillery, 2011]. Evapotranspiration has similar difficulties, but specifically in a semi-arid environment, a large proportion precipitation goes directly to evapotranspiration and the evapotranspiration rates are very dynamic, which makes them hard to quantify [Jovanovic and Israel, 2012].

Many closed basins in the southwest United States are being heavily pumped and have experienced water level declines, subsidence, and desertification. Las

Vegas Valley, NV has experienced these problems, with 85 meters of water level decline and 1.5 meters of land subsidence from 1912 to 1981 [Morgan and Dettinger, 1994]. A groundwater flow model was developed to help make decisions about the groundwater management of the area [Morgan and Dettinger, 1994]. Another example is in Owens Valley, CA where surface water flows have been diverted and routed to Los Angeles and the basin has been over pumped to the point where the water levels dropped below the plant root zone. This is adversely affecting the phreatophytic vegetation and causing desertification [Harrington and Steinwand, 2004]. A groundwater model of the basin was developed to help manage pumping to prevent adverse changes to vegetation [Harrington and Steinwand, 2004].

This study focuses on the Salt Basin which is a large, hydrologically closed, semi-arid, sparsely populated basin stretching from southern New Mexico into northwestern Texas. The Salt Basin lies within Hudspeth County and Culberson County, TX and Otero County, Chaves County, Eddy County, NM. The largest population center is Dell City, TX, which had 537 residents in 2020 [US-Census-Bureau, 2020]. This is a small town that is located near the NM-TX border and is dependent on pumping from Salt Basin aquifers for agriculture production. This study estimated recharge, evapotranspiration, and safe aquifer yield. A secondary goal was to determine if pumping from hypothetical well fields under two different scenarios will exceed safe aquifer yields. In order to address these questions, several 3D finite difference groundwater flow models were been developed of the Salt Basin.

Three steady-state groundwater flow models were developed each having different recharge rates of about 40,000, 60,000, and 80,000 acre-feet/year (135,000, 203,000, and 270,000 m³/day). These models were calibrated manually and using the parameter estimation code, PEST [Doherty and Hunt, 2010]. The recharge, evapotranspiration, hydraulic conductivity, and streambed conductance were varied during the calibration. Advective ages computed using the calibrated predevelopment steady-state models were compared to ¹⁴C ages. The 60,000 acre-feet/year (203,000 m³/day) steady-state model was chosen for further calibration and as a starting point for the historical transient model. The 60,000 acre-feet/year (203,000 m³/day) recharge model was chosen because of the water level fit and prior studies of the Salt Basin suggesting a similar recharge rate. The historical transient model was calibrated with observed water levels to find values for specific storage, specific yield, hydraulic conductivity, evapotranspiration, and streambed conductance. The changes to hydraulic conductivity, evapotranspiration, and streambed conductance were applied to the predevelopment steady-state model. The historical transient model was then used to run the hypothetical pumping scenarios.

This thesis continues with a review of Salt Basin geology, historical water-level changes, and prior Salt Basin groundwater modeling studies. Groundwater flow governing equations, boundary and initial conditions are discussed next, followed by methods to develop the groundwater model inputs, model calibration, and pumping scenarios. The results of the predevelopment steady-state and transient model calibration and pumping scenarios are described. The discussion section

examines simulated-recharge values and compares them to independent estimates of aquifer recharge and evapotranspiration and whether simulated hypothetical pumping scenarios indicate a potential to exceed basin safe aquifer yield. Findings are summarized in a conclusions section. Appendices are included in the back of the thesis, providing detailed information regarding the geology of the Salt Basin and a review of prior Salt Basin groundwater models.

CHAPTER 2

BACKGROUND

The Salt Basin is approximately 14,000 square km (5,000 square miles), contains high mountains on its margins, grassy plains, arid desert, and a large salt flat. Water enters the aquifer system from diffuse recharge in the mountains and by depression-focused recharge in ephemeral streams and arroyos. Groundwater flows down hydraulic gradients and can be focused into structural features. The groundwater flows to the salt flats where it is evapoconcentrated to levels above halite saturation. Around the margins of the salt flat, variable density flow may be important. Figure 2.1 shows prominent Salt Basin features.

The Salt Basin is a geologically complex region. It has experienced three major tectonic events, as well as several transgressions and regressions of the sea during the Paleozoic and Mesozoic Eras. Paleozoic limestone and sandstone permeability was largely derived from fracturing related to the Ancestral Rocky Mountains and Laramide orogenies, as well as the Basin and Range extensional tectonics. Above these units are sandstone, limestone, dolomite, and shale of Permian age. These units are the primary water bearing strata in the Salt Basin. The two major units that make up the aquifer system are the Victorio Peak Limestone (dolomites and limestones) and the Bone Spring Formation (limestones), which together is referred to as the Bone Spring-Victorio Peak aquifer. In the southwestern Salt Basin, there are several laccolith, sill, and dike Tertiary intrusions. At the land surface, Permian through Quaternary units crop out. For further information on the geology of the Salt Basin, see the Salt Basin Geology section in the appendix and Kelley et al. [2020].

The Salt Basin has a wide range of climatic zones leading to differences in evapotranspiration and recharge rates. In the lowlands near Dell City the annual precipitation rate was about 247 mm/year from 1981 to 2010, whereas the Sacramento Mountains near Cloudcroft, NM received about 901 mm/year (PRISM precipitation data). Temperature also varies spatially. Dell City's average temperature from 1981 to 2010 was about 16.4 °C while the Sacramento Mountains averaged about 7.1 °C (PRISM temperature data). Because of the relatively high temperatures and low precipitation rates, no recharge was predicted to occur in the lowlands, based on a modified Thornthwaite equation [Thornthwaite, 1948]. In the Sacramento Mountains the annual recharge was predicted based on the Thornthwaite equation to be about 423 mm/year. The environment has also changed temporally, during the last glacial maximum pluvial lakes formed in both the lowlands and uplands of the Salt Basin [Wilkins, 1997].

Predevelopment conditions, before the mid 1940's when significant agricultural pumping began in the Salt Basin, pumping was not a significant component of the basin water budget and existing wells were more widely dispersed throughout the Salt Basin. Prior to agricultural pumping, the water table elevations resembled a subdued replica of the land surface [Toth, 1963]. Larger increases in Dell City agricultural pumping began around 1960. This concentrated pumping created a large cone of depression in the Salt Basin (Figure 2.2).

The locations of wells with water level measurements in Dell City, TX, specifically wells with water level data for at least each decade, are plotted in Figure 2.3. The water level data for the wells in Figure 2.3 were plotted as hydrographs in Figure 2.4. These hydrographs show that there has been a general downward trend in water levels except for an interval that recorded a brief increase in the mid 1980's to early 1990's, which are years with increased precipitation and decreased pumping rates. From 1949 to 2019, there has been a 15 to 20 meter decline in water levels (Figure 2.4). This indicates that the groundwater may already be unsustainably pumped in Dell City, TX. Sustainable safe aquifer yield remains an important unresolved question for Salt Basin ranchers.

The Salt Basin has been intensively studied by four prior groups, all of whom developed hydrologic models to quantify the Salt Basin hydrodynamics. Mayer and Sharp Jr [1995] concluded that the Salt Basin has highly variable transmissivities due to fracturing in the basin. They found a north-northwest trending fracture zone that directs flow from the Sacramento Mountains towards the Dell City, TX area. Shomaker [2002] concluded that additional pumping in New Mexico, at either existing wells or new well fields, will ultimately decrease the amount of water flowing into Texas and increase drawdowns around Dell City. Hutchison [2008] developed structural, geochemical, and hybrid transient groundwater flow models to study the effects of groundwater withdrawals from the Dell City, Texas area. These authors concluded from the three different models that the groundwater production of the Dell City, TX area ranges from 54,000 to 95,000 acre-feet/year ($183,000$ to $321,000 \text{ m}^3/\text{day}$). They also found the average total inflow into the Salt Basin ranged from 87,000 to 114,000 acre-feet/year ($294,000$ to $385,000 \text{ m}^3/\text{day}$), the average evapotranspiration ranged from 49,000 to 67,000 acre-feet/year ($166,000$ to $226,000 \text{ m}^3/\text{day}$), and the total pumping was $\sim 88,000$ acre-feet/year ($297,000 \text{ m}^3/\text{day}$). Shomaker (2010) developed another transient historical groundwater model and found a total inflow into the Salt Basin of 61,723 acre-feet/year, pumping averaged to 89,257 acre-feet/year ($302,000 \text{ m}^3/\text{day}$), and the upper 300 meters of the aquifer has about 37.9 million acre-feet (46.7 billion m^3) of water. Ritchie [2011] and Sigstedt [2010] quantified recharge rates using a detailed steady-state 3D groundwater flow model calibrated to ^{14}C age data. They found a recharge rate of 15,000 acre-feet/year ($51,000 \text{ m}^3/\text{day}$), which is far lower than prior models.

In regards to the past models of the Salt Basin, Mayer and Sharp Jr [1995] and Hutchison [2008] used transient one layer models, while Shomaker [2002] and Shomaker [2010] used models with four layers and Ritchie [2011] used a

steady-state six layer model. The hydrostratigraphic frameworks were determined for Mayer and Sharp Jr [1995] and two of Hutchison [2008]'s models by structural features. Hutchison [2008] also constructed frameworks from geochemistry data. Shomaker [2002] determined their framework by decreasing hydraulic conductivity with depth. Shomaker [2010] and Ritchie [2011] used a simplification of a 16-layer hydrostratigraphic framework developed by Ritchie [2011]. To determine recharge, Mayer and Sharp Jr [1995] and Druhan et al. [2008] used the Eakin and Maxey [1949] approach, Shomaker [2002] used the surplus-precipitation method, Shomaker [2010] used Stephens [2010a]'s areal recharge results, potential recharge calculations, and Tillery [2011] runoff values. Ritchie [2011] used Stephens [2010a]'s net infiltration data and Shomaker [2010]'s watersheds for one model and elevations, recharge data from Newton et al. [2012], and precipitation data for the other model. In general, recharge was dependent on elevation for all prior models. Evapotranspiration was applied to the salt flats for all prior models. Mayer and Sharp Jr [1995] used irrigation pumping rates from Ashworth [1995], Shomaker [2002] used irrigation pumping data from NMOSE WATERS database, Bjorklund [1957], Scalapino [1950], and Ashworth [1995]. Hutchison [2008] developed pumping from irrigated acreage estimates from Groeneveld and Baugh [2002] and crop duties. Shomaker [2010] used pumping from Hutchison [2008].

The prior models of the Salt Basin had varying levels of complexity and variable parameter ranges (Figure 2.5). Mayer and Sharp Jr [1995], Shomaker [2002], and Shomaker [2010] all used steady-state recharge, steady-state discharge, and average transient recharge of around 60,000 acre-feet/year (203,000 m³/day). Shomaker [2002] and Shomaker [2010] used average transient recharge rates of around 95,000 acre-feet/year (321,000 m³/day). Hutchison [2008], including their high underflow values, used the largest values for all parameters with a steady-state recharge and discharge around 88,000 acre-feet/year (297,000 m³/day), an average transient recharge rate of 97,000 acre-feet/year (328,000 m³/day) and an average transient discharge of 146,000 acre-feet/year (493,000 m³/day). Ritchie [2011] used the lowest steady-state recharge and discharge rates of 15,000 acre-feet/year (51,000 m³/day). Hydraulic conductivity ranges differed with Shomaker [2002] with the smallest range and Ritchie [2011] with the largest range, including the lowest hydraulic conductivity by two magnitudes. For more detailed information on the prior models of the Salt Basin, see the Past Groundwater Flow Models of the Salt Basin section in the appendix.



Figure 2.1: Location of prominent features in the Salt Basin. Black outline is the current model boundary. Red line is the Victorio Flexure.

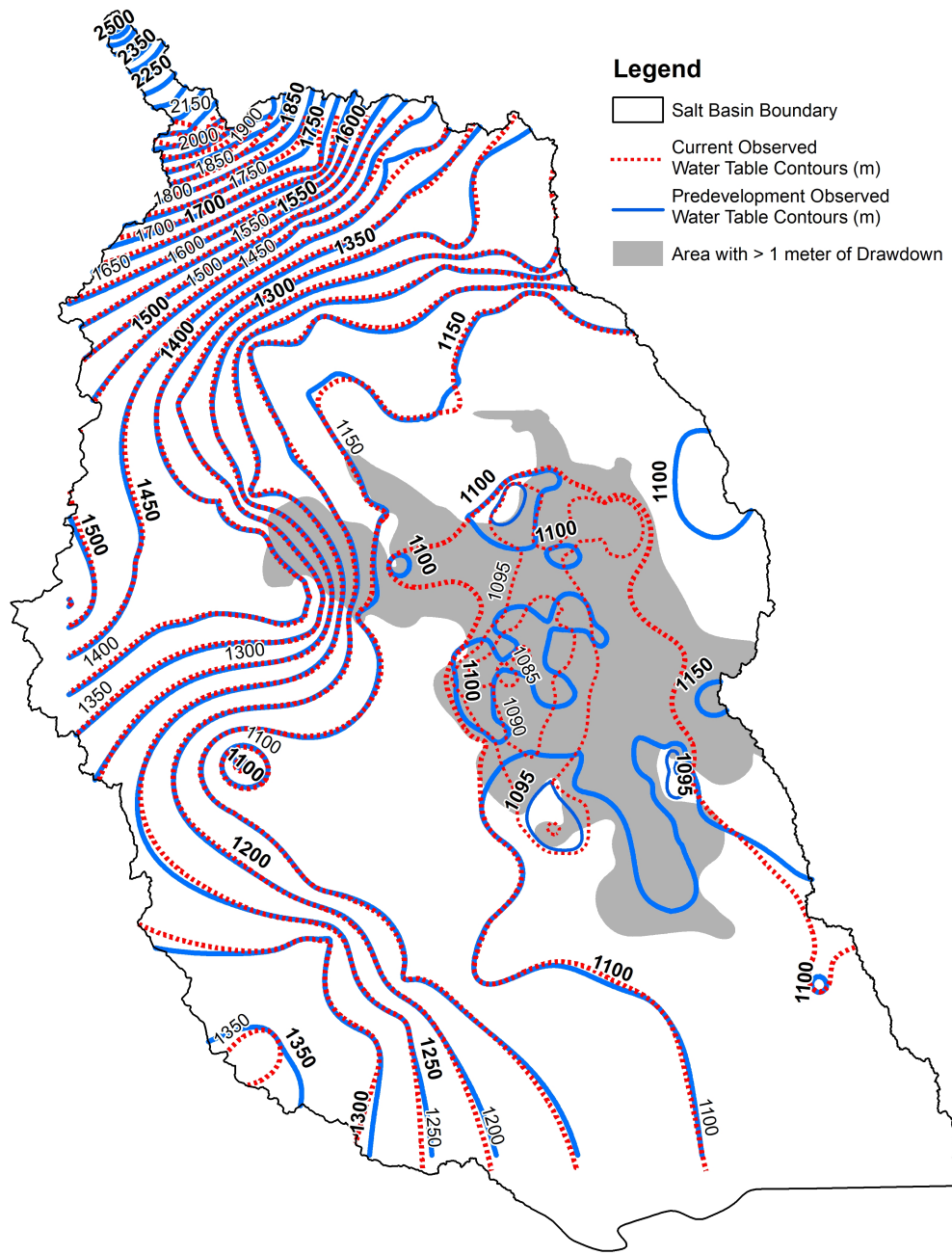


Figure 2.2: Predevelopment (blue) and current (red) 50 meter water table contours and 5 meter contours in the salt flats in the Salt Basin. Developed in this study. Gray polygon is the area near Dell City with greater than 1 meter of drawdown from the predevelopment to current observed water tables. The current observed water table is based on some older observed water levels but they were outside the Dell City area where water levels are assumed to have not changed much.

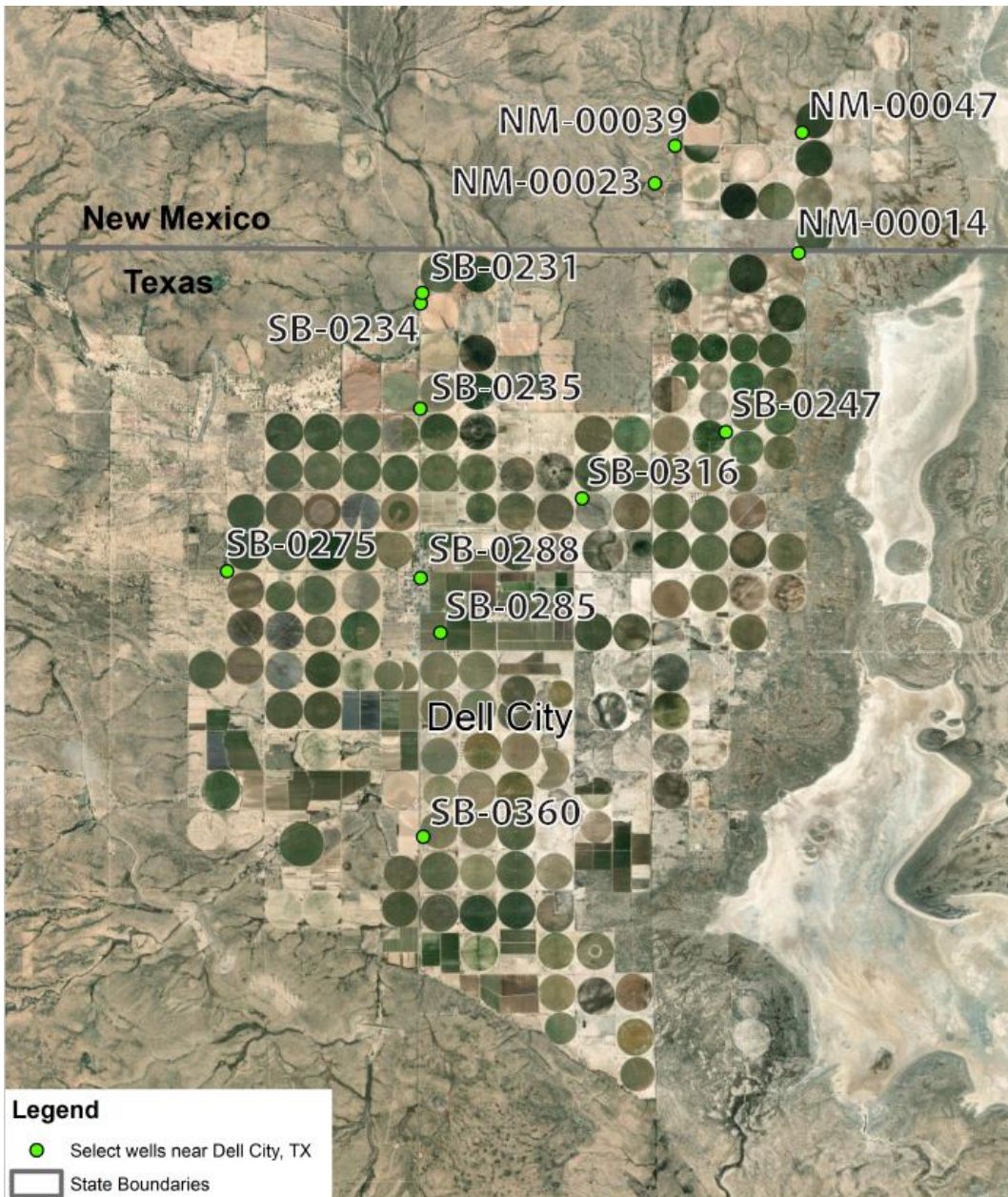


Figure 2.3: Locations of the monitoring wells in Dell City, TX area that have at least one water level measurement for each decade from pre-1950 to 2010's. The data from these wells are presented in the hydrographs in Figure 2.4. Wells are labeled with their well ID.

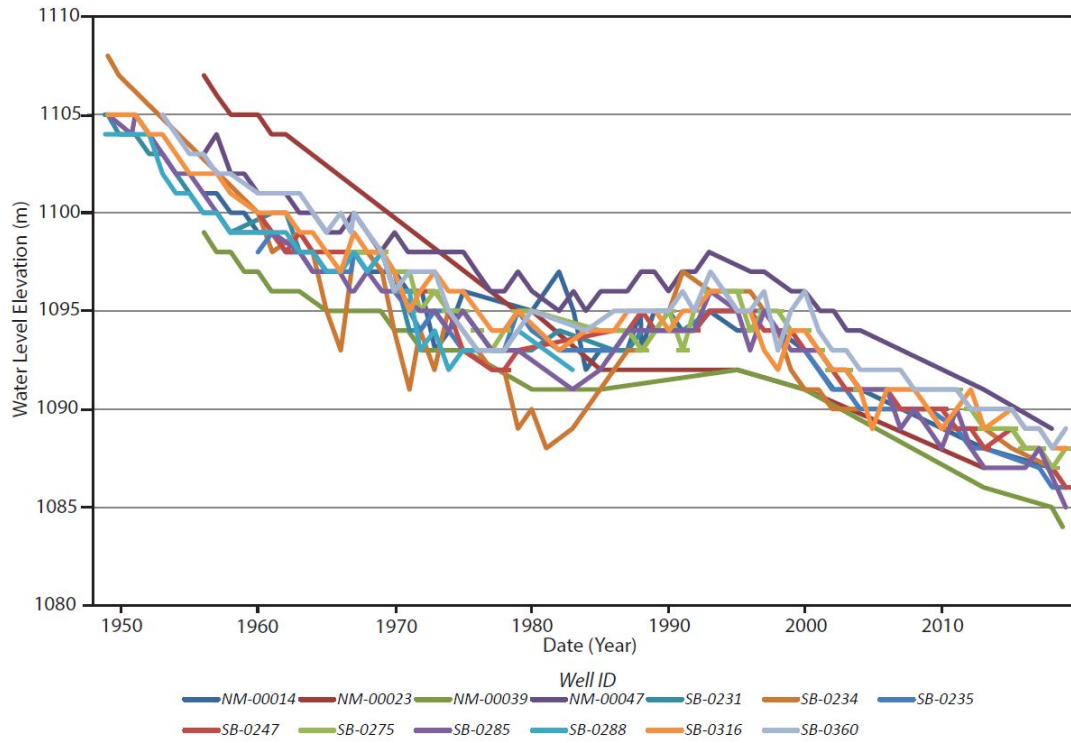


Figure 2.4: Hydrographs of water levels (m) for thirteen wells in Dell City, TX that have at least one water level measurement for each decade from pre-1950 to 2010's. Their locations shown on Figure 2.3. This figure shows 15 – 20 meters of drawdown from 1948 to 2020.

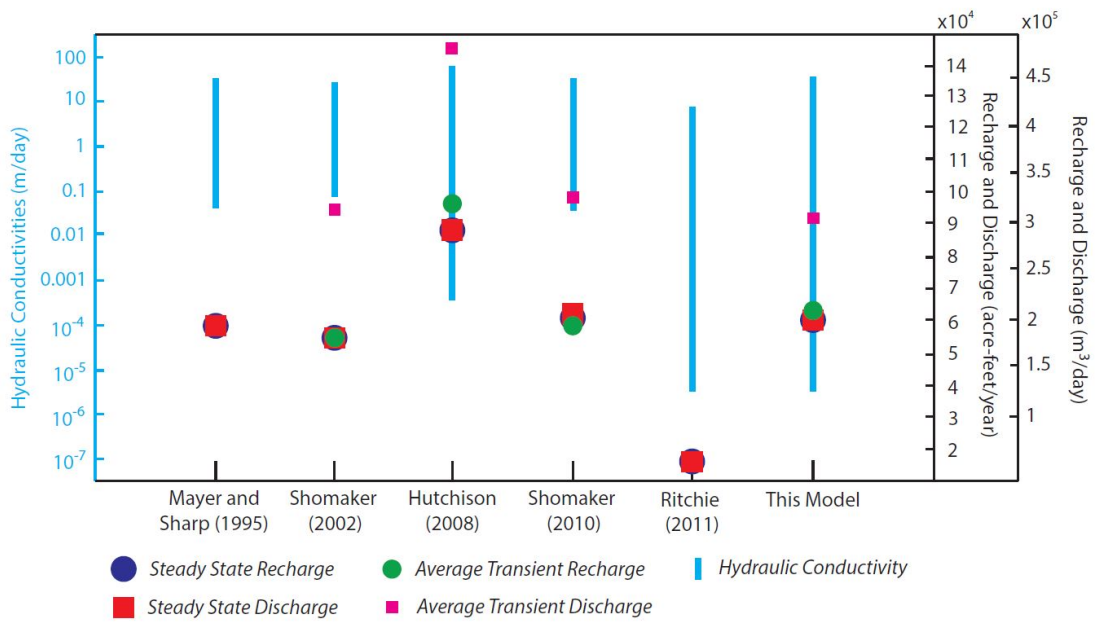


Figure 2.5: Graphical summary of model parameters used in prior studies of the Salt Basin. The blue lines denote the hydraulic conductivity range used by Mayer and Sharp Jr [1995], Shomaker [2002], Hutchison [2008], Shomaker [2010], Ritchie [2011], and this model. Blue circles indicate steady-state recharge, red squares indicate steady-state discharge, green circles indicate average transient recharge, and pink squares indicate average transient discharge. Mayer and Sharp Jr [1995]'s hydraulic conductivities are actually transmissivity values so the location of the blue line could be different. This figure shows how the flow budget parameters of prior models of the Salt Basin compare. They are all similar except for the high values in Hutchison [2008] and the low values in Ritchie [2011]. Hutchison [2008] values include their high underflow values.

CHAPTER 3

METHODS

To better understand recharge, evapotranspiration, and groundwater availability in the Salt Basin and determine the impacts of a hypothetical well field, a series of groundwater flow models were constructed. A predevelopment steady-state and several transient groundwater flow models were developed. The predevelopment steady-state model was constructed to estimate hydraulic conductivities, recharge, evapotranspiration, and underflow. Except for depression-focused recharge, these parameters were then held constant for the historical transient model, which also had time-varying pumping. The historical transient model was then used to evaluate potential for safe yield for a series of hypothetical pumping scenarios in the NM portion of the Salt Basin.

The models were developed using Groundwater Modeling System (GMS), which is a pre- and post-processor for MODFLOW. MODFLOW was developed by the U.S. Geological Survey and the specific formulation used in this study was MODFLOW-NWT. MODFLOW-NWT is a Newton-Raphson formulation for MODFLOW-2005 which is used to model groundwater flow in unconfined geologic units [Niswonger and Pradic, 2005]. The three-dimensional movement of groundwater through a porous media, which is solved by MODFLOW is described by the following equation:

$$\frac{\partial}{\partial x} \left(K_{xx} \frac{\partial h}{\partial x} \right) + \frac{\partial}{\partial y} \left(K_{yy} \frac{\partial h}{\partial y} \right) + \frac{\partial}{\partial z} \left(K_{zz} \frac{\partial h}{\partial z} \right) + W = S_s \frac{\partial h}{\partial t} \quad (3.1)$$

where K_{xx} , K_{yy} , and K_{zz} are the values of hydraulic conductivity along the \bar{x} , \bar{y} , \bar{z} directions, h is the freshwater hydraulic head, W is a volumetric flux per unit volume representing sources and/or sinks, S_s is the specific storage of the porous media, and t is time [Harbaugh, 2005].

3.1 Model Framework

The model has six layers with a model grid made up of 1,000 m by 1,000 m finite difference cells. The active cells create a grid of 176 rows and 135 columns. Figure 3.1 shows the active model grid outline. Layer 1 is modeled as unconfined with a saturated thickness of 0 to ~550 meters. Layers 2 - 6 are assigned a layer

type of confined. The only confining unit in layers 2 – 6 is a low permeability Cretaceous unit in the southwestern Salt Basin. The majority of layers 2 – 6 is made up of Permian and Paleozoic and earlier units. Only the top layer is assigned unconfined because of computing constraints. But, because the water table does not go below the bottom of layer 1 except for one or two cells, layers 2 - 6 can be assigned as confined, even though they are unconfined in reality, without divergence in model solutions.

The hydrostratigraphic framework model used in this study was highly influenced by the 3D hydrogeologic framework of Ritchie [2011]. He used structural features from geologic maps, lithologic facies, compiled data from oil-and-gas exploratory wells, and surface geologic exposure information. Compared to Ritchie [2011] the current model is nearly identical except for minor changes to a "state line fault", addition of the Capitan Reef Complex, and minor modifications of geology zones for simplification and model calibration. The current model extends the southern boundary ~30km farther south than Ritchie [2011]. The current model uses one geologic zone for each geologic unit except for the Permian geologic unit, which has many geologic subunits because of the wide expansion of the Permian units throughout the Salt Basin and the variability in properties of different rock types and fracture density (see the Salt Basin Geology Appendix). If the Permian unit only had one zone, it would be difficult to fit observed data and the model would be too simple to accomodate the spatial differences in hydraulic response to historical stresses. There is one confining unit in the southwestern Salt Basin, the low permeability Cretaceous unit (Geologic Zone 2). The crystalline basement was lumped into the Paleozoic and earlier group, with layer 6 being completely crystalline basement. Faulting in the Salt Basin has increased permeability, creating flow paths, and causing the aquifer to be less connected across some of this faulting. Geologic zones were spatially adjusted to improve parameter flexibility required to better fit observed water levels during the calibration process. Each geologic zone had unique values of hydraulic conductivity, vertical anisotropy, S_y , and S_s for each model layer. Due to the lack of porosity data, a uniform value of 0.15 was used for all the geologic units, which was close to Ritchie [2011]'s average porosity model values. S_y and S_s are only used in the transient models. The geologic zone assignments and initial parameters are in Table 3.1 and Figures 3.2 – 3.4.

The model boundary follows the surface water divide around the entirety of the model except for the southeastern portion, which follows the groundwater divide of the Victorio Flexure. The Victorio Flexure is a large fault that crosses the Salt Basin graben, which lies beneath the salt flats. The boundary was divided into segments based on the internal Salt Basin HUC 10 watersheds, except for the northern boundary and southeastern groundwater divide. The northern and portions of the northeastern and southwestern boundary were assigned specified flux boundaries (Figure 3.1). The northern boundary had the largest flux, with an initial value of 5,000 acre-feet/year ($17,000 \text{ m}^3/\text{day}$), simulating underflow from the adjacent Peñasco Basin. Flow is believed to come from the Peñasco Basin because head gradients show water flowing into the Salt Basin [Shomaker, 2010].

The other segments were assigned initial fluxes of about 15 acre-feet/year (51 m³/day) and were selected to represent water table mounding found in observed water levels. The southeastern groundwater divide section of the boundary was a general head boundary with a conductance of 0.0001 m/day (Figure 3.1). This boundary condition was imposed to help with convergence and to see which direction water was flowing across the groundwater divide. The goal was to have no flow through the general head boundary. All of the boundary fluxes were applied to layer 1. All other layers were assigned no flux boundary conditions.

3.2 Model Inputs

Our model had both diffuse and depression-focused recharge. Diffuse recharge was applied to the model using the Recharge package in MODFLOW where Python Recharge Assessment for New Mexico Aquifers (PyRANA) spatially determined there to be diffuse recharge at high elevations [Cadol et al., 2020]. PyRANA is a program that estimates soil water holding capacity and runoff in New Mexico and generates an improved recharge rate for groundwater modeling [Cadol et al., 2020]. Depression-focused recharge was applied to ephemeral streams and arroyos throughout the model using the Streamflow Routing (SFR2) package in MODFLOW Niswonger and Prudic [2005]. To determine the recharge rate in the Salt Basin, three different recharge rates were considered in the predevelopment steady-state model; about 40,000, 60,000, and 80,000 acre-feet/year (135,000, 203,000, and 270,000 m³/day) of recharge. These values were chosen because they span the range of prior Salt Basin model recharge rates. Also, Stephens [2010a] developed a basin-scale balance model that evaluated precipitation, evapotranspiration, and recharge. They used a groundwater model to estimate an average recharge of 63,000 acre-feet/year (213,000 m³/day) with a low precipitation year having 37,000 (125,000) and a high precipitation year having 82,000 acre-feet/year (277,000 m³/day) of recharge.

The recharge rate in the predevelopment steady-state model that had the best statistical fit to observed data or support from other studies of the Salt Basin was used as a starting point for the historical transient model. For the historical transient model, diffuse recharge remained constant through time while depression-focused recharge had an annual scaling factor determined by PRISM and Hutchison [2008] precipitation data. Stream flow in the SFR's is routed based on the continuity equation which assumes steady uniform flow. Volumetric inflow is equal to volumetric outflow plus the net of all sources and sinks along the channel. Simulated water seepage out of a stream to the aquifer when the water table is below the stream bottom is computed by:

$$q = \frac{K}{m}(h_s - h_b) \quad (3.2)$$

q is the infiltration rate, K is the saturated hydraulic conductivity of the streambed, h_s is the hydraulic head in the stream at the top of the streambed, and h_b is the

hydraulic head at the bottom of the streambed, and m is the thickness of the streambed [Niswonger and Prudic, 2005].

All stream segments were given an initial stream conductance of 1 m/day. In the predevelopment steady-state model, all water in the streams entered the aquifer. In the transient models, all water in the streams entered the aquifer except for a few limited events with high runoff volumes. This was intended to represent the part of the ponded flow that does not infiltrate and was lost to evaporation. Figure 3.1 shows the distribution of recharge.

Evapotranspiration is only applied to the salt flats (Figure 3.1). This is because it was the only place that the water table was historically close enough to the surface to be available for evaporation. Also, during high precipitation events surface water flows to the salt flats, pools on the ground surface, and evaporates. The transpiration in the model is accounted for by the reduction of recharge rates. An initial evapotranspiration rate of 80 in/year (5.5 mm/day) was used with an extinction depth of 10 meters, as determined by PyRANA and gridMET. gridMET is a dataset of daily meteorological data [Abatzoglou et al., 2014]. Evapotranspiration is applied to the model using the MODFLOW EVT package. The package uses an evapotranspiration surface elevation, an extinction depth, and a maximum evapotranspiration rate to simulate evapotranspiration [Banta, 2000]. For each cell with evapotranspiration applied, if the water table is below the extinction depth, no water was removed from the model. If the water table is at or above the evapotranspiration surface elevation, water is removed from the model at the maximum evapotranspiration rate. If the water table is somewhere in between, water is removed from the model at a linear decay rate with depth.

Pumping was only applied to the transient model. There were two groups of pumping wells; irrigation and DCMI (domestic, commercial, municipal, and industrial). Pumping in both groups was consumptive pumping, precluding the need to specifically model return flow to the aquifer. Hypothetical well field pumping scenarios will be discussed in the Pumping Scenarios section. Irrigation pumping was estimated using the normalized difference vegetation index (NDVI), the Blaney-Criddle method, and pumping volumes reported in Shomaker [2010]. The Blaney-Criddle method is a temperature based crop evapotranspiration algorithm [Blaney and Criddle, 1962]. NDVI quantifies vegetation greenness and produces maps showing vegetation density and health [USGS, 2021]. The NDVI maps were used to determine where irrigation was occurring in the Salt Basin and ultimately determined the simulated spatial distribution. The spatial distribution of NDVI is used instead of well locations because of the lack of pumping data for wells in the Salt Basin. The NDVI is also used in the Blaney-Criddle calculations, which determined irrigation pumping volumes from 1984 to 2020. The pumping rates reflect consumptive pumping, only representing the net aquifer extraction: pumping rate minus return flow to the aquifer. Pre-1984, irrigation pumping volumes are from Shomaker [2010]'s 2010 model. Pre-1984 irrigation pumping is distributed using a combination of the NDVI irrigation pumping footprints and the original Shomaker [2010] well locations. From 1948 to 1999, the irrigation pumping is applied evenly over the yearly stress periods. For irrigation

pumping during the seasonal stress periods from 2000 to 2020, all of the irrigation for the year is applied in the irrigation season (March to October) and no irrigation is applied in the non-irrigation season (November to February). The DCMI pumping is derived from data from the New Mexico Water Rights Reporting System (NMWRRS) database and Texas Water Development Board (TWDB). For the NMWRRS pumping wells, 50% of pumping returned to the aquifer was assumed. A 50% return flow is higher than what has been assumed in some prior studies (e.g. Konikow and Bredehoeft [1974]). Pumping rates were not available for the TWDB wells, so a pumping rate of 3 acre-feet/year ($10 \text{ m}^3/\text{day}$) is assumed, based on typical pumping allowances for New Mexico wells. Again, 50% return flow from the pumping back to the aquifer was assumed. This leads to pumping rates of 1.5 acre-feet/year ($5 \text{ m}^3/\text{day}$) for the TWDB DCMI wells. The DCMI pumping is year-round, so the pumping rate was constant through both annual and seasonal stress periods. Locations of the irrigation and DCMI pumping wells are presented in Figure 3.5.

3.3 Model Calibration

The predevelopment steady-state model was calibrated to observed water levels and calculated stream fluxes, then compared to ^{14}C ages. The transient model was only manually calibrated to observed water levels. Three recharge rates were considered in the predevelopment steady-state model. Models with about 40,000, 60,000, and 80,000 acre-feet/year (135,000, 203,000, and 270,000 m^3/day) of recharge. These recharge values fall within the range of recharge used in prior models of the Salt Basin (15,000 to 88,000 acre-feet/year or 51,000 to 297,000 m^3/day). The three predevelopment steady-state models with different recharge rates were first manually calibrated, changing diffuse recharge, depression-focused recharge, hydraulic conductance, streambed conductivity, evapotranspiration, and underflow to get a better fit to observed water levels and calculated stream fluxes. Then the predevelopment steady-state models were processed using Parameter Estimation (PEST) refine the fit between observed and simulated water levels (not calculated stream fluxes or ^{14}C ages) by changing diffuse recharge, hydraulic conductivities, streambed conductance, evapotranspiration, and underflow. Water levels were given different weights based on measurement confidence. The PEST objective function is the squared sum of weighted residuals:

$$\phi = \sum_m \left(h_m^{sim} - h_m^{obs} \right)^2 * w_m \quad (3.3)$$

Where ϕ is the objective function to be minimized, h_m^{obs} is the measured value of observation m , h_m^{sim} is the simulated value corresponding to observation m , w_m is the weight of the m^{th} observation, and m is the total number of observations [Hill and Tiedeman, 2006].

PEST minimizes the objective function by calculating finite-difference approximations to the sensitivity (derivative) of each adjustable parameter with respect to every observation. Based on these sensitivities, PEST estimates a series of potential parameter adjustments and goes through the process of evaluating adjustments to identify a combination providing the most improvement in the objective function. The process of calculating sensitivities, estimating potential parameter change and refining the parameter values is repeated, or iterated, until the objective function has reached a minimum value. In some instances, the minimum value of the objective function does not yield parameters that are representative of the geologic/hydrologic conditions requiring careful inspection of successive iterations to identify a parameter set consistent with geologic/hydrologic conceptual model while providing improvement in the objective function.

Not all water level measurements were used in the model calibration. Water level measurements with metadata depicting possible discrepancies or issues during measurements, measurements that are obviously outliers, measurements that were spatially too close together, and for the predevelopment steady-state model, measurements that were showing affects of pumping were removed. The weighting for the water level observation data was not uniform while conducting PEST runs. Observed water levels were not weighted as heavily or were excluded from PEST calibration if the water level diverged from the pattern of observed water levels around it or a lack of geologic formation data and model geology resolution made fitting the gradient of the water level too difficult.

Stream conductance was calibrated using flux targets consistent with the general conceptual model of Salt Basin stream flow presented by Tillery [2011]. Upstream portions of each stream tend to increase in total flow (net gains), while downstream portions tend to have net losses with the final portion of the mapped stream channel losing virtually all remaining flow, representing the high infiltration capacity of the fractured Permian system in the vicinity of each stream terminus. While observed ^{14}C ages were not used in manual or PEST calibrations of the predevelopment steady-state model they were used to evaluate if simulated travel times had the potential to be consistent with the general trends of ^{14}C ages. This approach was implemented due to a lack of porosity data and low sensitivity to changes in model parameter values, leading to a low confidence in the modeled ^{14}C age accuracy. The observed ^{14}C ages were from Sigstedt [2010].

Based on the statistics and prior work in the Salt Basin, the 60,000 acre-feet/year of recharge predevelopment steady-state model was selected for further calibration. This choice is discussed in the results section. The 60,000 acre-feet/year predevelopment steady-state model was used as a starting point for the historical transient model. The historical transient model was manually calibrated to water levels to get better values for hydraulic conductivities, specific storage, specific yield, evapotranspiration, and stream conductances. Changes in hydraulic conductivity, streambed conductance, and evapotranspiration from the calibration of the historical transient model were applied to the predevelopment steady-state model. The historical transient model was then used to assess the impact of three hypothetical well fields situated within the New Mexico side of the Salt Basin.

3.4 Pumping Scenarios

Six hypothetical pumping scenarios were tested using the historical transient model (Figure 3.6). Each pumping scenario was added to the historical transient model. That is, additional pumping wells were added to the historical pumping wells during specific time intervals. Three well field locations were considered, with two pumping schemes (Scenario 1 and Scenario 2) for each location, totaling six pumping scenario simulations. The Otero Break and Crow Flats locations are consistent with locations previously simulated by Shomaker [2002] while the Piñon Creek location was chosen because it was on New Mexico state land and may be a location more conducive to transbasin transfers. Minor adjustments were made to Shomaker [2002] well field locations were positioned to make sure the wells were in a productive geologic formation. The hypothetical Piñon Creek well field footprint was suggested by S.S. Papadopoulos & Associates, Inc., and consisted of five areas near Piñon Creek on NM state lands. The hypothetical locations provide the opportunity to examine impacts of spatial and geologic contrasts and provide the opportunity to evaluate the simulated response. The five areas were intersected with the current model grid to assign pumping to model cells. For each of the hypothetical well fields, the well model layer was assigned based on the deepest model layer with productive geologic formations. This was layer 2 for the Otero Break and Piñon Creek well fields and layer 3 for the Crow Flats well field (Figure 3.2 through Figure 3.4 show geology for model layers). Pumping volumes were distributed evenly through all of the wells in the hypothetical well field being pumped.

Scenario 1 represents the pumping needed to make up for the Pecos River Compact shortages of water going from New Mexico to Texas in six historical years with the worst delivery shortfalls (1969 to 1974). The Pecos River Compact is an interstate compact between New Mexico and Texas that allocates the waters of the Pecos River between the states [ISC, 1949]. Presumably the produced water from the scenario would be transferred via a pipeline discharging to the Pecos River. The well fields were pumped from 1969 to 1974 with a total of 127,072 acre-feet (157 million m³) for the entire six years of additional pumping. Limiting Scenario 1 pumping to a single six year time period provides the opportunity to examine long term response from the individual six-year augmentation effort. The pumping for Scenario 1 simulates the worst case scenario, pumping the large volumes of water for several years in a row. Table 3.2 has the annual additional pumping rates for the Scenario 1 models.

Scenario 2 was developed to have additional pumping in years with higher than normal runoff. The pumping volumes were suggested by S.S. Papadopoulos & Associates, Inc. The first step to determine suggested pumping volumes was summing the predevelopment steady-state runoff volumes from drainages on the New Mexico side of the Salt Basin. The total predevelopment steady-state runoff in New Mexico was 9,375 acre-feet/year (32,000 m³/day). A threshold of about 20% greater than this was chosen, 11,000 acre-feet/year (37,000 m³/day). Years with more than 15,100 acre-feet/year (51,000 m³/day) of runoff were selected for

extra pumping. The extra pumping volume per year was the runoff exceeding the threshold of 11,000 acre-feet. Based on these criteria, additional pumping was applied for Scenario 2 in 1972, 1974, 1985, 1993, 2006, 2008, 2013, and 2014 totaling to 66,345 acre-feet (82 million m³) over the entire 8 years (Table 3.3). Scenario 2 pumping is the best case scenario, pumping low volumes of water in years with high recharge.

The hypothetical pumping scenarios were not run into the future because of the many unknowns including projected temperature increases and uncertainty regarding future pumping stresses [Gutzler, 2005]. It was decided that looking at hypothetical pumping scenarios in the past would be equally beneficial.

Geologic Unit	Geologic Zones	Hydraulic Conductivity (m/day)	Vertical Anisotropy	S_y	S_s (1/m)
Cenozoic alluvium (Layer 1)	8	1	100	0.1	n/a
Cenozoic intrusions	3	0.0001	1000	0.01	1×10^{-6}
Cretaceous	105	0.01	100	0.01	1×10^{-6}
low permeability Cretaceous	2	0.000001	1000	0.01	1×10^{-6}
Permian	6, 7, 8, 10, 107, 110, 205, 207, 210, 307, 310, 407, 410, 507, 607	0.01 - 10	10 - 100	0.1 – 0.01	1×10^{-6}
Paleozoic and Earlier	4	0.001	1000	0.01	1×10^{-6}

Table 3.1: Initial hydraulic conductivities and vertical anisotropies assigned to geologic zones. These values are the initial parameters from Ritchie (2011). Initial S_y and S_s were suggested by S.S. Papadopoulos & Associates, Inc. based on Shomaker [2010]. S_y is specific yield, S_s is specific storage. Categorized by geologic unit. Figure 3.2 – 3.4 show distribution of geologic zones listed here.

Transient Model Year	Additional Pumping Rate	
Units	(acre-feet/year)	(m³/day)
1969	27,449	92,763
1970	24,555	82,980
1971	21,960	74,211
1972	18,372	62,086
1973	22,060	74,548
1974	12,676	42,839

Table 3.2: Years and pumping rates of extra pumping in acre-feet/year and m³/day for the hypothetical Scenario 1 simulations. A total of pumping is 127,072 acre-feet (157 million m³) for the entire six years of additional pumping. Pumping rates come from Shomaker [2002].

Transient Model Year	Additional Pumping Rate	
Units	(acre-feet/year)	(m³/day)
1972	6,532	22,074
1974	11,848	40,039
1985	6,652	22,480
1993	6,341	21,429
2006	13,107	44,294
2008	9,215	31,141
2013	4,495	15,190
2014	8,152	27,549

Table 3.3: Years and pumping rates of extra pumping in acre-feet/year and m³/day for the hypothetical Scenario 2 simulations. A total of 66,345 acre-feet (82 million m³) was added to the years indicated and those years were times with higher than average runoff.

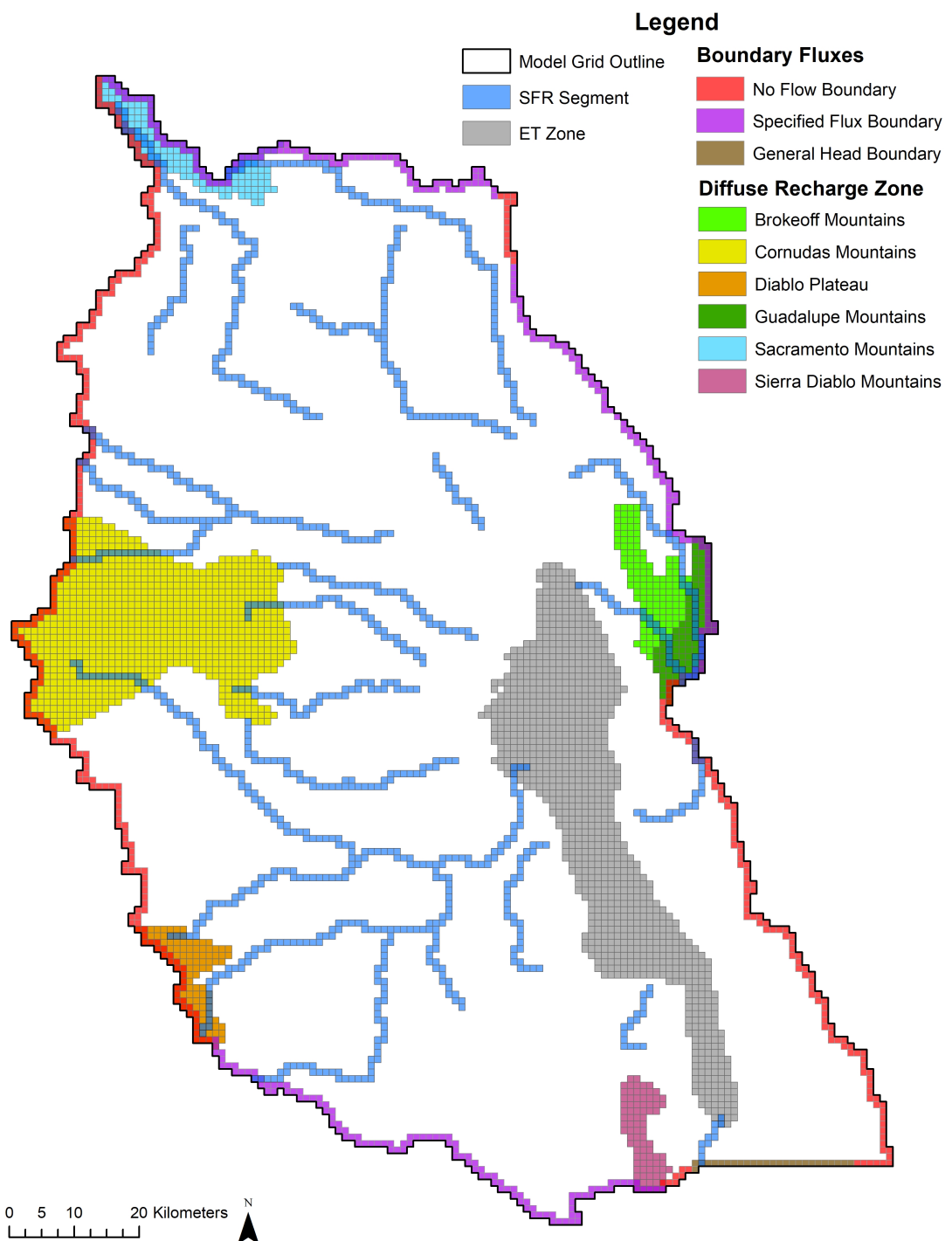


Figure 3.1: Current model grid outline with all boundary conditions symbolized by color of grid cell. Diffuse recharge (colored polygons), depression-focused recharge (blue lines), evapotranspiration (ET Zone, gray polygon), specified flux boundaries (purple boundary cells), general head boundaries (brown boundary cells), and no flow boundaries (red boundary cells) are shown.

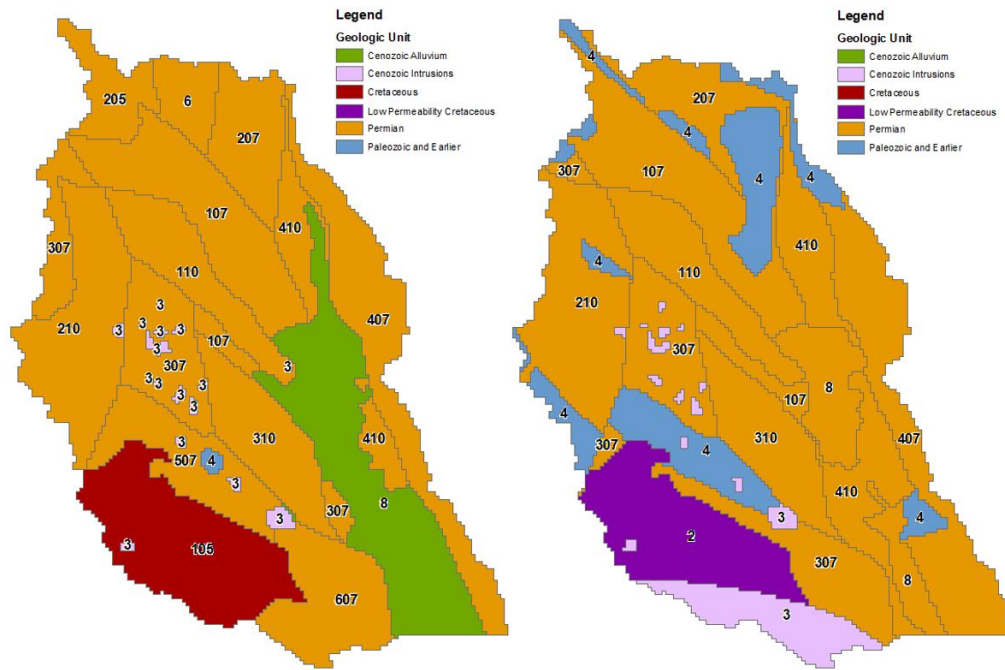


Figure 3.2: Map of model geologic zonation in layer 1 (left) and layer 2 (right). Labels indicate the geologic zone number. Colors indicate the geologic unit.

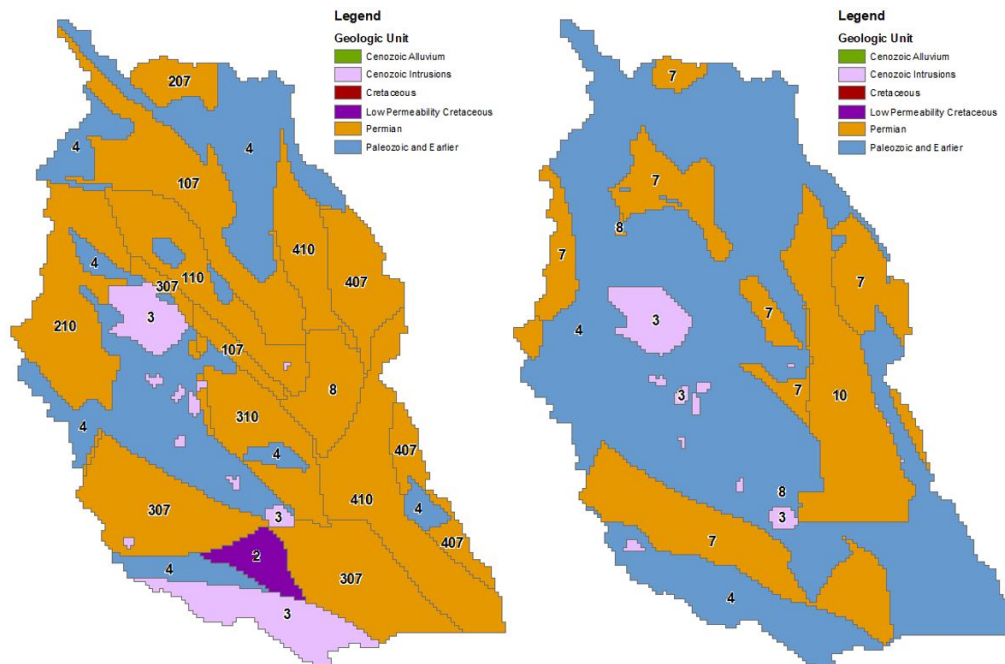


Figure 3.3: Map of final model geologic zonation in layer 3 (left) and layer 4 (right). Labels indicate the geologic zone number. Colors indicate the geologic unit.

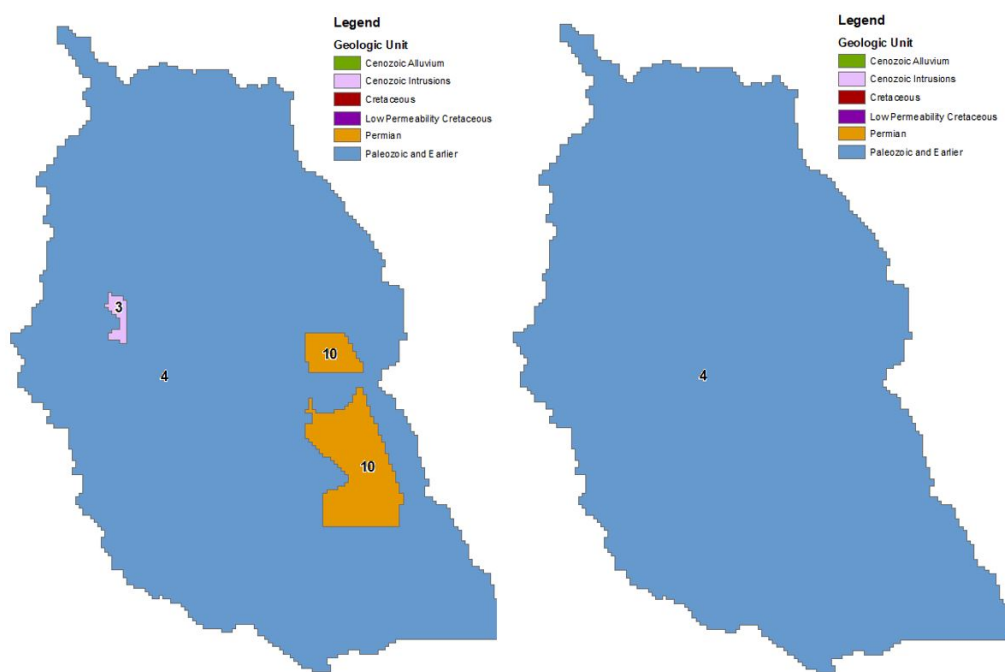


Figure 3.4: Map of final model geologic zonation in layer 5 (left) and layer 6 (right). Labels indicate the geologic zone number. Colors indicate the geologic unit.

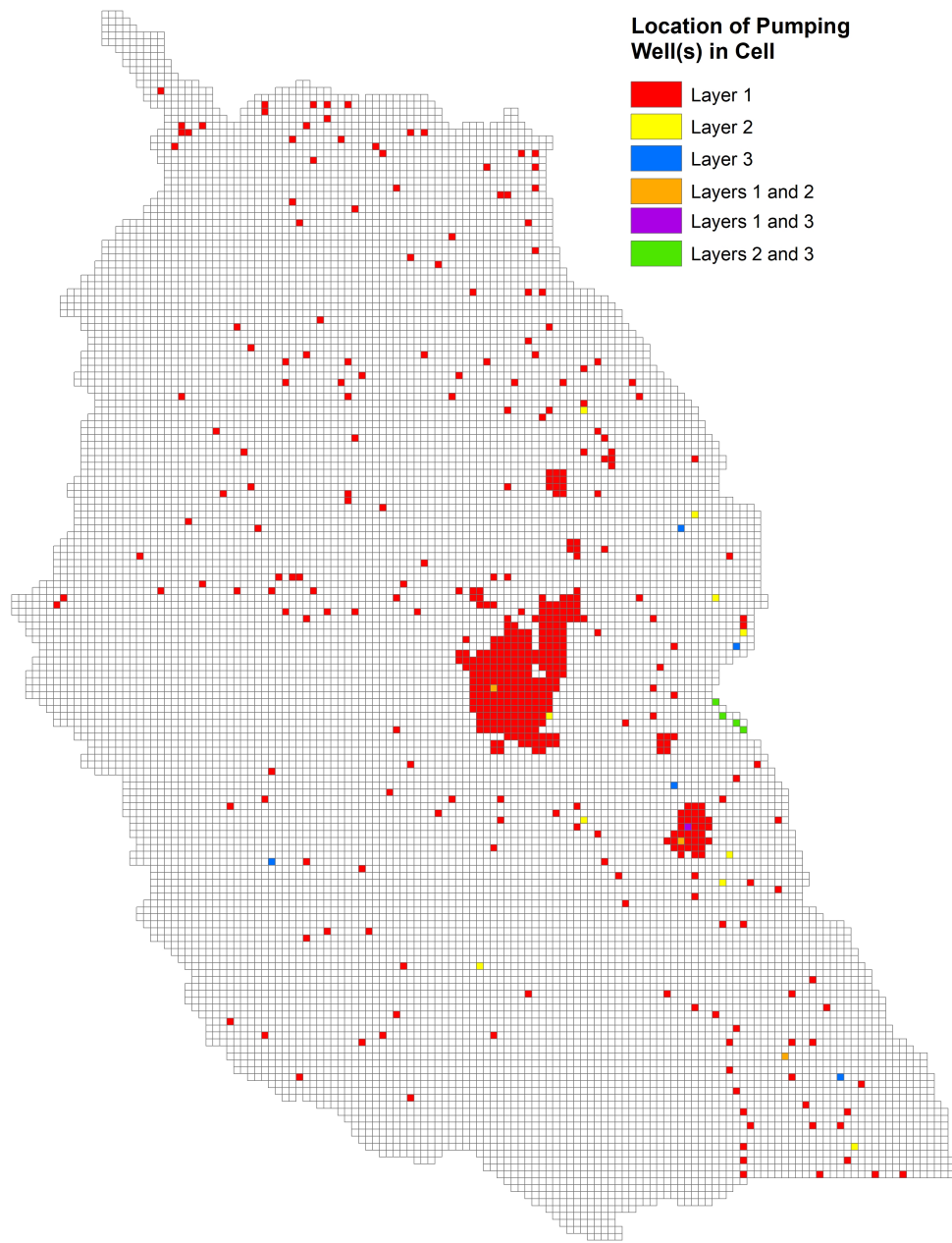


Figure 3.5: Locations of irrigation and DCMI pumping wells in the current transient model. Red model cells have a pumping well in the first layer. Yellow model cells have a pumping well in the second layer. Blue model cells have a pumping well in the third layer. Orange model cells have a pumping well in layers 1 and 2. Purple model cells have a pumping well in layers 1 and 3. Green model cells have a pumping well in layers 2 and 3.

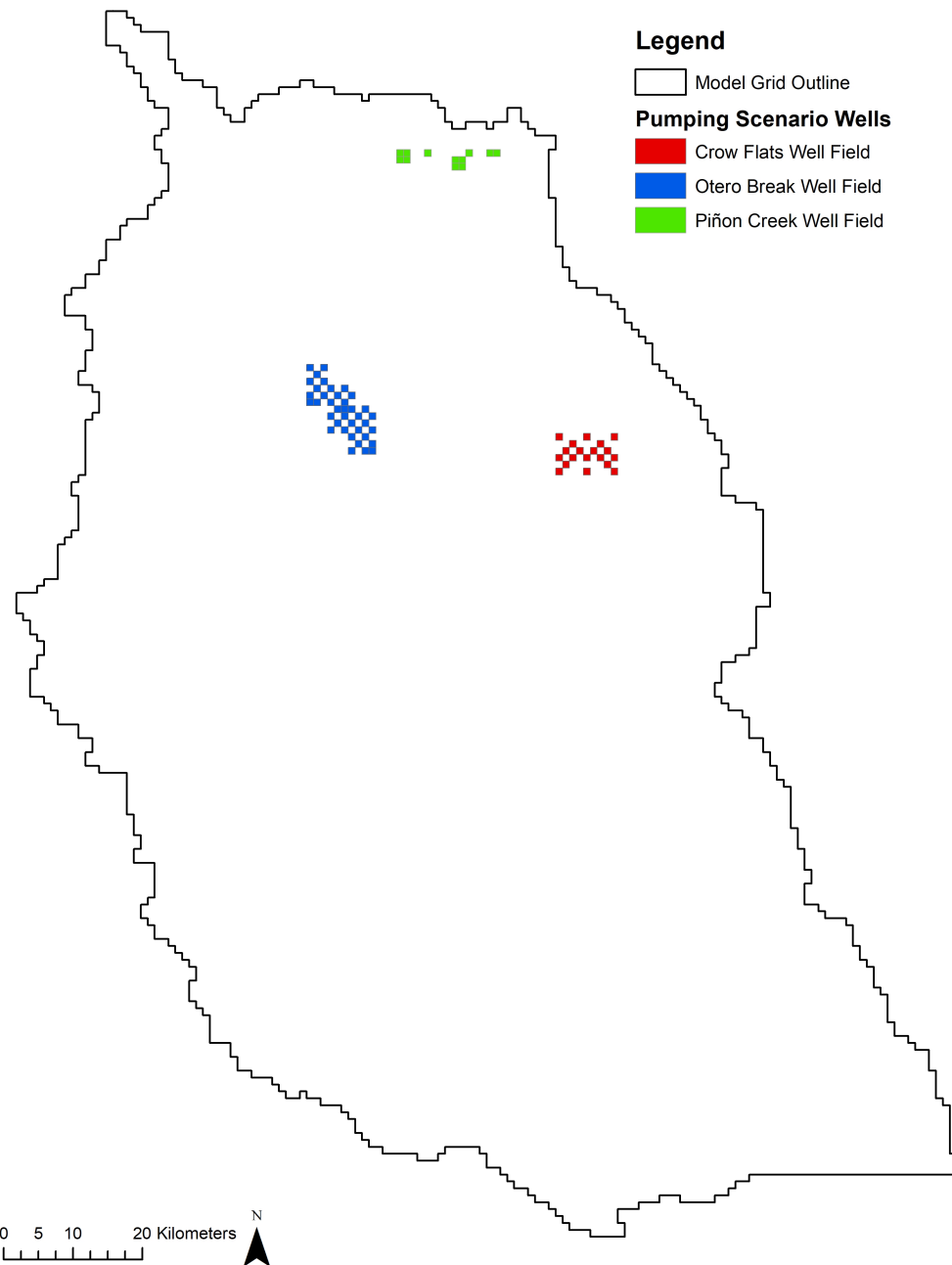


Figure 3.6: Location of wells for the three hypothetical pumping scenario well fields. Red squares make up the Crow Flats well field in model layer 3. Blue squares make up the Otero Break well field in model layer 2. Green squares make up the Piñon Creek well field in model layer 2.

CHAPTER 4

RESULTS

4.1 Predevelopment Steady-State Model: 3 Levels of Recharge

To find a predevelopment steady-state model and determine a recharge rate for the Salt Basin, three predevelopment steady-state models with different recharge rates were considered: about 40,000, 60,000, and 80,000 acre-feet/year (135,000, 203,000, and 270,000 m³/day) of recharge. These values were chosen because they span the range of prior Salt Basin model recharge rates. Also, Stephens [2010a] developed a basin-scale balance model that evaluated precipitation, evapotranspiration, and recharge. They found a groundwater model estimated recharge of 63,000 acre-feet/year (213,000 m³/day) with a low precipitation year having 37,000 (125,000) and a high precipitation year having 82,000 acre-feet/year (277,000 m³/day) of recharge. Evapotranspiration is a good approximation of recharge assuming a steady-state condition for closed basins. Stephens [2010b] studied the evaporation from the playa deposit core samples in the salt flats and found an average of 28,300 acre-feet/year (96,000 m³/day) of evapotranspiration. Stephens [2010b] described potential factors that might cause this estimate to be too low, making 28,300 acre-feet/year (96,000 m³/day) a minimum. PyRANA estimated the total diffuse and depression-focused recharge to be 34,000 to 68,000 acre-feet/year.

Hydraulic conductivity and vertical anisotropy ranges and averages for each of the predevelopment steady-state recharge model are in Table 4.1. The hydraulic conductivity and vertical anisotropy increase with increased recharge rate.

Table 4.2 shows the flow budget for the predevelopment steady-state model with three levels of recharge. The majority of the recharge is from diffuse recharge. Diffuse recharge is 47%, 67%, and 56% of the total recharge for the 40,000, 60,000, and 80,000 acre-feet/year (135,000, 203,000, and 270,000 m³/day) models respectively. Depression-focused recharge from ephemeral streams and arroyos is the next largest contributor to recharge coming in at 46%, 29%, and 41% for recharge of 40,000, 60,000, and 80,000 acre-feet/year (135,000, 203,000, and 270,000 m³/day) respectively. The rest of the recharge comes from underflow from adjacent basins, coming in at 7%, 4%, and 3% for recharge of 40,000, 60,000, and 80,000 acre-feet/year (135,000, 203,000, and 270,000 m³/day), respectively.

For the predevelopment steady-state model, all of the discharge results from

evapotranspiration in the salt flats. The evapotranspiration rate for the three levels of recharge is reduced to 1.45 mm/day with a 10 meter extinction depth.

For each of the three levels of recharge the predevelopment steady-state model has relatively good fit between observed versus computed heads (Table 4.3 and Figure 4.1). The R-squared values for all three levels of recharge models were above 0.992, which suggests there was a substantial correlation and therefore a good fit of observed to computed heads. The mean error for all three recharges was negative, meaning on average the computed head was larger than the observed heads. It is a common calibration metric to determine if a model fit is good if the Root Mean Square Error (RMSE) is <10% the range of the observed values. For all three levels of recharge, the predevelopment steady-state model RMSE was well below the 10% observed value range. The 60,000 acre-feet/year (203,000 m³/day) of recharge model had a slightly better R-squared and RMSE value compared to the other two recharge rates. The 40,000 acre-feet/year (135,000 m³/day) of recharge model had the smallest mean error. The selection and weighting of observed water levels is discussed in the methods section.

All three predevelopment steady-state models had similar quality of fit between the observed ¹⁴C ages and computed MODPATH ages (Table 4.4 and Figure 4.2). The observed ¹⁴C ages were from Sigstedt [2010]. Because of the lack of porosity data and quality checks on flow paths, this data was not used to determine which model was better or to refine model parameters. All three predevelopment steady-state models had poor statistical fits to ¹⁴C ages, but the 60,000 acre-feet/year (203,000 m³/day) of recharge model had the best R-squared and RMSE values. The ~80,000 acre-feet/year (270,000 m³/day) of recharge model had the best mean error. The 40,000 acre-feet/year (135,000 m³/day) of recharge model had the worst R-squared, mean error, and RMSE, with the mean error and RMSE being almost double the other two predevelopment steady-state models. A poor fit of advective travel times to ¹⁴C is not uncommon. In this study it could be due to the lack of quality checks on the MODFLOW flow paths or from young and old water mixing in the highly fractured Salt Basin [Kreitler et al., 1987]. Sanford [2011] found a poor fit between advective groundwater ages to correct ¹⁴C data for their model of the Albuquerque basin.

4.2 Predevelopment Steady-State Model

The findings from the preliminary predevelopment steady-state models along with field based studies [Stephens, 2010a] suggests that the ~60,000 acre-feet/year (203,000 m³/day) of recharge model is the most reasonable of the physical system. This model underwent further calibration in PEST and was updated with changes from the historical transient model calibration to create the predevelopment steady-state model.

Table 4.5 shows a more detailed view at the hydraulic conductivities used in the ~60,000 acre-feet/year (203,000 m³/day) predevelopment recharge model. Figures 4.3 - 4.5 show the hydraulic conductivity distribution for the six layers in the predevelopment 60,000 acre-feet/year (203,000 m³/day) recharge model. These values were also used in the historical transient model. The hydraulic conductivity across the entire model stayed within an order of a magnitude compared to the initial hydraulic conductivity ranges.

Table 4.6 shows the flow budget for the predevelopment steady-state model. Total recharge is made up of 67% diffuse recharge, 29% depression-focused recharge, and 4% underflow from adjacent basins. Evapotranspiration is the only discharge in the model and is approximately equivalent to total recharge. During further calibration after the predevelopment recharge rate selection, the evapotranspiration extinction depth decreased to five meters.

Table 4.7 shows the distribution of diffuse recharge in the predevelopment steady-state model. Each diffuse recharge polygon has a unique recharge. The Cornudas Mountains and Sacramento Mountains have the highest percent of diffuse recharge volume. The Sierra Diablo Mountains, Brokeoff Mountains, Diablo Plateau, and Guadalupe Mountains all have similar recharge volumes of under 3,000 acre-feet/year (or 9,500 m³/day). The locations of the recharge polygons are in Figure 3.1.

Figure 4.6 gives a detailed view at the distribution of depression-focused recharge in the predevelopment steady-state model. The Sacramento River, Piñon Creek, Shiloh Draw, and sections of the Antelope Gulch produce the most depression-focused recharge with over 1,200 acre-feet/year (4,000 m³/day) each (Figure 4.6). Stream conductance values were calibrated with PEST to a model wide maximum of 1.62 m/day, minimum of 0.0000305 m/day, average of 0.0860 m/day, and a median of 0.00675 m/day. All of the runoff that is inputted into the streams enters the aquifer.

For the predevelopment steady-state model, all of the discharge came from evapotranspiration with a rate of 1.45 mm/day and a five meter extinction depth. The extinction depth decreased from the predevelopment steady-state model with three levels of recharge after further model calibrations.

The predevelopment steady-state model water table contours had a relatively good fit to the observed predevelopment water table contours (Figure 4.7). There are similar head gradients and water table mounding between the two sets of contours in the Sacramento Mountains area, the Cornudas Mountains, the Diablo Plateau, and the Sierra Diablo Mountains area. The salt flats water table is flat in both water table contour maps.

4.3 Historical Transient Model

The historical transient model had time-varying depression-focused recharge and pumping. All other model parameters, including diffuse recharge, hydraulic

conductivity, evapotranspiration, underflow, and stream conductance were held constant. The calibrated values of S_y and S_s are in Table 4.8.

Table 4.9 shows the average flow budget values for the historical transient model from 1948 to 2020. The average recharge rate for the historical transient model was 61,259 acre-feet/year ($207,019 \text{ m}^3/\text{day}$). This increase from the predevelopment steady-state model is from depression-focused recharge which varied with annual precipitation rates. Over the course of the transient simulation period, evapotranspiration decreased substantially from the predevelopment steady-state model. The historical transient model total recharge is 29,336 acre-feet/year ($99,138 \text{ m}^3/\text{day}$), which is less than the average total discharge. On average, the storage change decreased by 26,732 acre-feet/year ($87,958 \text{ m}^3/\text{day}$).

Figure 4.8 displays the changes in variables through the entire historical transient model simulation. Depression-focused recharge and pumping varies with each annual or seasonal stress period. The evapotranspiration rate generally decreases through time, starting at $\sim 57,000$ acre-feet/year ($193,000 \text{ m}^3/\text{day}$) in 1948 and declining to $\sim 3,000$ acre-feet/year ($10,000 \text{ m}^3/\text{day}$) at the end of the transient run (2020). This is due to the lowering of the water table in the lowlands below the evapotranspiration extinction depth of five meters. Total recharge stays under 80,000 acre-feet/year ($270,000 \text{ m}^3/\text{day}$) except for five years of high precipitation (1974, 2006, 2008, 2013, and 2014). After 1985, the net storage starts to oscillate over the zero change in storage line. Between 1948 and 1984 changes in storage were predominantly negative with a maximum annual change in storage of $-100,000$ acre-feet/year ($-338,000 \text{ m}^3/\text{day}$). Between 1985 and 2020 there were many years having less than 20,000 acre-feet/year ($68,000 \text{ m}^3/\text{day}$) of storage declines. Some years during this period had aquifer storage changes that were positive (increased storage) which correlated to years with high recharge or low pumping.

The transient model was calibrated to observed water level trends. Figure 4.9 shows four observed versus computed water level graphs for four wells. These wells had the longest time series of observations in the Salt Basin. The wells are all located near Dell City, TX. No wells outside the Dell City area had a large number of water level measurements temporally spaced out. For these wells, the computed water levels were lower than the observed water levels. However, the general trend of a decrease in water levels from 1948 to ~ 1980 , an increase from ~ 1980 to ~ 2000 , and then a decrease from ~ 2000 to today was reproduced.

Figure 4.10 presents the predevelopment model computed steady-state water table versus the final water table contours at the termination of the transient model in the year 2020. In the predevelopment steady-state model water table contours, the lowest water levels are in the salt flats. In the final transient model water table contours, a cone of depression has formed under Dell City.

4.4 Pumping Scenarios

All of the proposed hypothetical pumping scenarios added additional net amounts of produced water at the three proposed NM well fields, 127,072 and 66,345 acre-feet (157 million and 82 million m³) total for 1948 to 2020 for Scenarios 1 and 2, respectively.

The most drawdown was seen in 1974 for Scenario 1, which had a total of 127,072 acre-feet (157 million m³) additional pumping and 2014 for Scenario 2, which had a total of 66,345 acre-feet (82 million m³) additional pumping. When pumped a total additional 127,072 acre-feet (157 million m³) (Scenario 1), drawdown reaches over six meters for the Crow Flats and Otero Break well fields and over 25 meters for the Piñon Creek well field. When pumped a total additional 66,345 acre-feet (82 million m³) (Scenario 2), the Crow Flats and Otero Break well fields reach a drawdown of over two meters and Piñon Creek well field was over 10 meters. For the higher additional pumping volume (Scenario 1), additional drawdown was greater than a meter in 1974, laterally extending 16 to 32 km away from the Crow Flats well field, 8 to 35 km away from the Otero Break well field, and 13 to 20 km from the Piñon Creek well field (Figure 4.11). For the lower additional pumping volume (Scenario 2), additional pumping drawdown was a greater than a meter in 2014, laterally extending 11 to 29 km away from the Crow Flats well field, 6 to 23 km away from the Otero Break well field, and 17 to 24 km from the Piñon Creek well field (Figure 4.12). For the Crow Flats drawdown with higher additional pumping volume (Scenario 1), there was a small three meter deep pocket of drawdown within Dell City. The higher additional pumping volume (Scenario 1) in the Otero Break caused drawdown that extends towards Dell City and also had a small one meter pocket of drawdown near the town. Beyond the one meter of drawdown contour, there were <1 meter decreases in water level sporadically throughout the basin for all pumping scenarios.

For all six pumping scenarios the evapotranspiration and net storage decreases (Table 4.10). Due to declining water levels, total evapotranspiration through the entire model run decreases.

When compared to the historical transient model, all hypothetical pumping scenario models have a modest decrease in subsurface water flowing from New Mexico into Texas. This can be seen by the computed state line flux into Texas (Table 4.11). The state line flux for the entire model run decreased the most for Crow Flats well field pumping a total additional 127,072 acre-feet (157 million m³) (Scenario 1) with a decrease of 65 acre-feet (80,176 m³). The smallest decrease was for the Piñon Creek well field pumping a total of 66,345 acre-feet (82 million m³) (Scenario 2) with a decrease of 2 acre-feet (2,467 m³). Figure 4.13 presents a graph of the flux across the state line through the time of the transient model scenarios. From 1970 to 2008 the Crow Flats Scenario 1 and Otero Break Scenario 1 have the largest decrease in state line flux. After 2008, all model scenarios have similar decreases in state line fluxes.

In order to assess the impacts of the pumping scenarios, water levels were monitored at wells near the three proposed pumping well fields and spaced out

across the model domain. The monitoring wells were actual wells in the Salt Basin. Figure 4.14 presents the computed water levels through time for these wells. Well ST-00015 is in the Crow Flats well field, NM-00183 is in the Otero Break well field, and ST-00021 is near the Piñon Creek well field. Overall, wells near the well fields are highly affected by the additional pumping and all wells across the entire basin are slightly affected. Scenario 1 (127,072 acre-feet (157 million m³) of additional pumping) water levels have a maximum drawdown around 1975, which was the end of the six year additional pumping period, and then partially recovers towards the historic water level, but does not completely recover by 2020. Scenario 2 (66,345 acre-feet (82 million m³) of additional pumping) water levels diverge from the historic water level around 1974 and continue to increase distance from the historic water levels, making jumps during pumping years, through the end of the transient model.

Model Scenario Recharge Rate (acre-feet/year)	Hydraulic Conductivity Range (m/day)	Hydraulic Conductivity Average (m/day)	Vertical Anisotropy Range	Vertical Anisotropy Average
~40,000	1.4E-06 to 21.8	0.93	0.353 to 1000	152.6
~60,000	2.0E-06 to 31.4	1.7	0.353 to 2084	175.4
~80,000	3.2E-06 to 44.3	3.2	0.353 to 2329	179.3

Table 4.1: Table of hydraulic conductivities and vertical anisotropies data for the three levels of recharge rates. Average indicates, averages of the value for each geology zone polygon, and does not account for area covered by each geologic zone polygon.

Units	Total Recharge	Total Discharge	Diffuse Recharge	Depression Focused Recharge	Underflow	Evapotranspiration
(acre-feet/year)	37,092	37,085	17,315	17,223	2,554	37,085
m ³ /day	125,349	125,325	58,514	58,203	8,631	125,325
(acre-feet/year)	59,753	59,745	39,853	17,223	2,677	59,745
m ³ /day	201,929	201,902	134,679	58,203	9,047	201,902
(acre-feet/year)	80,417	80,409	45,193	32,609	2,615	80,409
m ³ /day	271,761	271,734	152,725	110,199	8,837	271,734

Table 4.2: Table of flow budget parameters for three levels of recharge with the predevelopment steady-state model used to decide the predevelopment recharge rate. In m³/day and acre-feet/ year.

Model Scenario Recharge Rate (acre-feet/year)	R-Squared	Mean Error (m) (Obs - Comp)	RMSE (m)	10% of Observed Value Range (m)
~40,000	0.992	-2.02	20.8	158.0
~60,000	0.993	-3.25	20.0	158.0
~80,000	0.992	-3.57	22.2	158.0

Table 4.3: Statistics on the observed versus computed water levels for the predevelopment steady-state recharge model using three levels of recharge. Water levels not used in the PEST calibration were not used to compute the statistics. Mean Error is observed minus computed water levels.

Model Scenario Recharge Rate (acre-feet/year)	R-Squared	Mean Error (m) (Obs - Comp)	RMSE (m)	10% of Observed Value Range (m)
~40,000	0.0098	-26,506	35,715	1500
~60,000	0.0122	-9,949	17,169	1500
~80,000	0.0103	-9,379	17,631	1500

Table 4.4: Statistics on the observed versus computed ^{14}C ages for the predevelopment steady-state recharge model using three levels of recharge. Observed ^{14}C ages from Sigstedt [2010].

Geologic Unit	Geologic Zones	Hydraulic Conductivity (m/day)	Vertical Anisotropy
Cenozoic alluvium (Layer 1)	8	25.68	8.689
Cenozoic intrusions	3	0.0001 to 0.0003	92.78 to 1000
Cretaceous	105	0.0371	56.42
low permeability Cretaceous	2	3.11E-06	92.78 to 1000
Permian	6, 7, 8, 10, 107, 110, 205, 207, 210, 307, 310, 407, 410, 507, 607	0.0011 to 41.4	7.804 to 2084
Paleozoic and Earlier	4	0.0003 to 0.0311	0.358 to 1000

Table 4.5: Hydraulic conductivities and vertical anisotropies assigned to geologic zones for the predevelopment steady-state and historical transient models, categorized by geologic unit.

Units	Total Recharge	Total Discharge	Diffuse Recharge	Depression Focused Recharge	Underflow	Evapotranspiration
acre-feet/year	60,487	60,474	40,446	17,479	2,562	60,474
m³/day	204,410	204,366	136,683	59,069	8,658	204,366

Table 4.6: Flow budget (in acre-feet/year and m³/day) of the predevelopment steady-state model.

Diffuse Recharge Polygon	Predevelopment Recharge Rate	
Unit	acre-feet/year	m ³ /day
Cornudas Mountains	20,617	69,672
Sacramento Mountains	9,554	32,288
Sierra Diablo Mountains	2,792	9,432
Brokeoff Mountains	2,646	8,942
Diablo Plateau	2,484	8,395
Guadalupe Mountains	2,353	7,949
Sum of All Diffuse Recharge	40,446	136,678

Table 4.7: Diffuse recharge rates for each diffuse recharge polygon in the predevelopment steady-state model.

Geologic Unit	Geologic Zones	Calibrated S _y (only Layer 1)	Calibrated S _s (1/m)
Cenozoic alluvium (Layer 1)	8	0.05	n/a
Cenozoic intrusions	3	0.01	1 × 10 ⁻⁶
Cretaceous	105	0.01	1 × 10 ⁻⁶
low permeability Cretaceous	2	n/a	1 × 10 ⁻⁶
Permian	6, 7, 8, 10, 107, 110, 205, 207, 210, 307, 310, 407, 410, 507, 607	0.01 – 0.1	1 × 10 ⁻⁶
Paleozoic and Earlier	4	0.01	1 × 10 ⁻⁶

Table 4.8: S_y and S_s used in the historical transient model. S_y is specific yield, S_s is specific storage, categorized by geologic unit. Figure 3.2 – 3.4 show the distribution of geologic zones listed here.

Unit	Average Total Recharge	Average Total Discharge	Average Diffuse Recharge	Average Depression Focused Recharge	Average Underflow	Average Evapo-transpiration	Average Pumping	Average Storage Change
acre-feet/ year	61,259	90,595	40,446	18,251	2,562	11,067	79,529	-26,732
m ³ /day	207,019	306,157	136,683	61,677	8,658	37,400	268,760	-90,338

Table 4.9: Average parameters for the flow budget (in acre-feet/year and m³/day) for the historical transient model from 1948 to 2020.

		IN	IN	IN	OUT	OUT	OUT	OUT	OUT	OUT
Model Name / Calculation	Boundary Flux In	Diffuse Recharge	Depression Focused Recharge	Total Recharge	Pumping	Evapotranspiration	General Head Boundary Flux Out	Total Head Boundary Flux Out	Discharge	Net Storage
Units	acre-feet	acre-feet	acre-feet	acre-feet	acre-feet	acre-feet	acre-feet	acre-feet	acre-feet	m ³
Historical Model	184,622	2,914,057	1,313,278	4,411,957	5,731,962	820,476	882	6,553,320	2,141,345	
Crow Flats Scenario 1 - Historical Model	0	0	0	0	0	1,01E+09	-15,107	1,09E+06	8,08E+09	2,64E+09
Otero Break Scenario 1 - Historical Model	0	0	0	0	0	1,57E+08	-1,86E+07	-6,17E+03	1,38E+08	-1,38E+08
Pinon Creek Scenario 1 - Historical Model	0	0	0	0	0	1,57E+08	-8,349	-3	118,720	-118,722
Crow Flats Scenario 2 - Historical Model	0	0	0	0	0	1,57E+03	-1,150	0	125,922	-125,917
Otero Break Scenario 2 - Historical Model	0	0	0	0	0	1,57E+08	-1,42E+06	0,00E+00	1,55E+08	-1,55E+08
Pinon Creek Scenario 2 - Historical Model	0	0	0	0	0	66,345	-3,939	-1	62,406	-62,405

Table 4.10: Flow budget for the historical transient model and the difference between the total volume in acre-feet and m³ for the hypothetical pumping scenario flow budget and the historical model flow budget. All values are totals from 1948 to 2020. This table shows that the additional pumping takes water from evapotranspiration and storage.

Pumping Scenario	Total State Line Flux For Entire Transient Model Run	Model Scenario Total State Line Flux - Historical Transient Model Total State Line Flux
Units	acre-feet	m ³
Historical Transient Model	3,177	3.92E+06
Crow Flats Scenario 1	3,112	3.84E+06
Otero Break Scenario 1	3,118	3.85E+06
Piñon Creek Scenario 1	3,166	3.91E+06
Crow Flats Scenario 2	3,147	3.88E+06
Otero Break Scenario 2	3,154	3.89E+06
Piñon Creek Scenario 2	3,175	3.92E+06

Table 4.11: Sum of subsurface water flux across the state line from New Mexico to Texas for the entire transient model run (1948 – 2020), and the difference of the model scenario sum of subsurface water flowing across the state line from New Mexico to Texas minus the historical transient model sum. Values in acre-feet and m³.

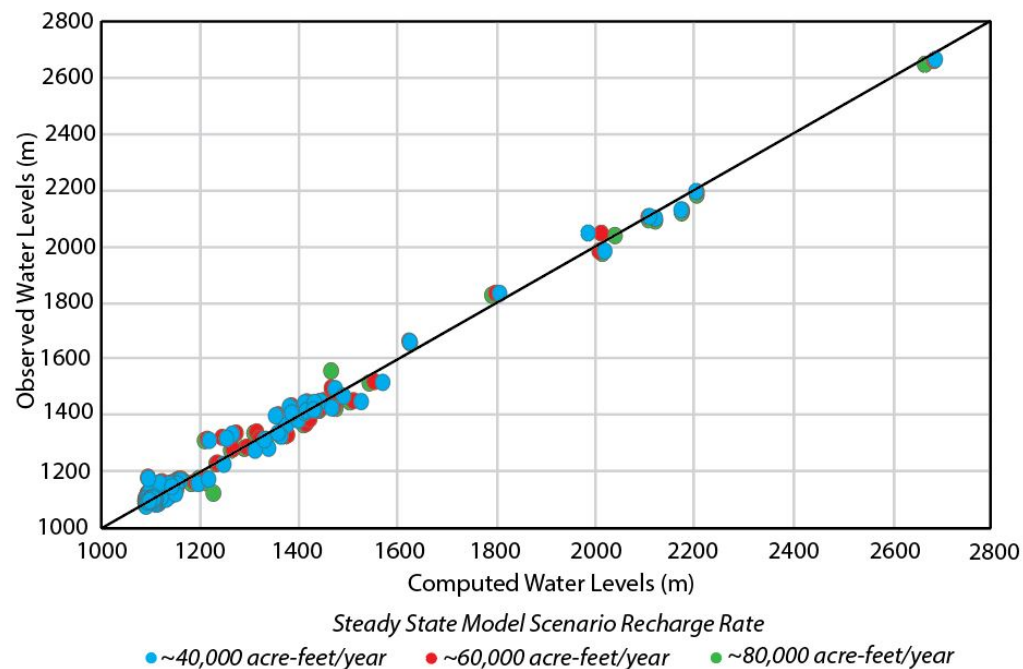


Figure 4.1: Observed versus computed water levels for the three predevelopment steady-state recharge model scenarios. Water levels not used in the PEST calibration were not used to compute the statistics.

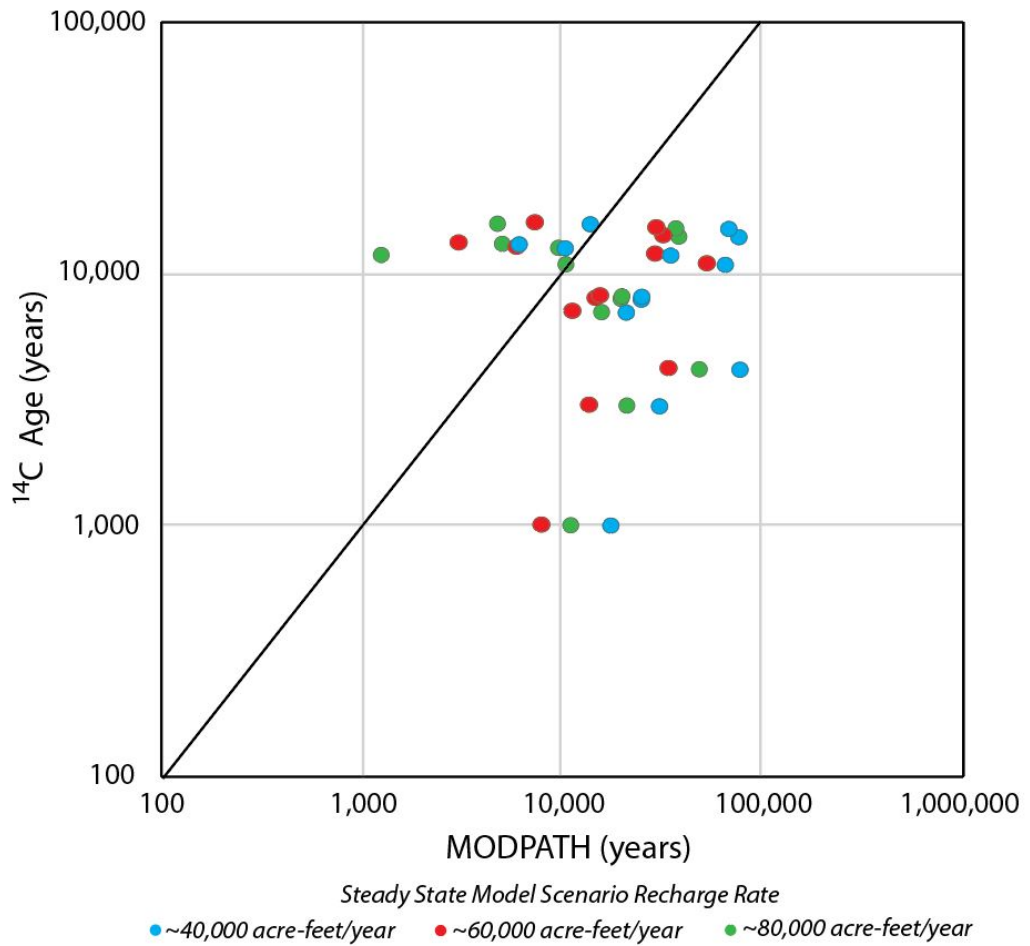


Figure 4.2: Graph of the computed versus observed ^{14}C ages for the three preliminary predevelopment steady-state model. Observed ^{14}C ages measured by Sigstedt [2010].

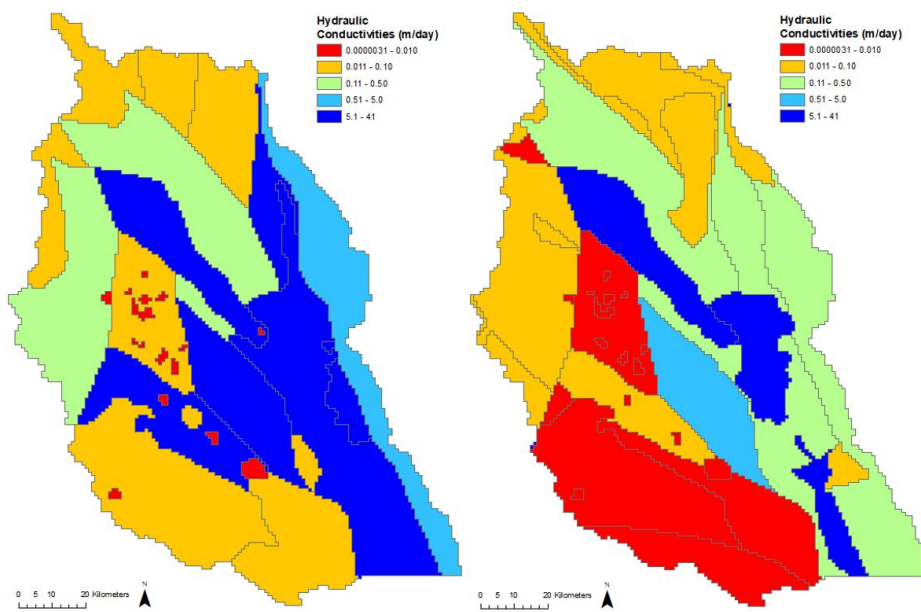


Figure 4.3: Distribution of hydraulic conductivities for the predevelopment steady-state and historical transient model for layer 1 (left) and layer 2 (right).

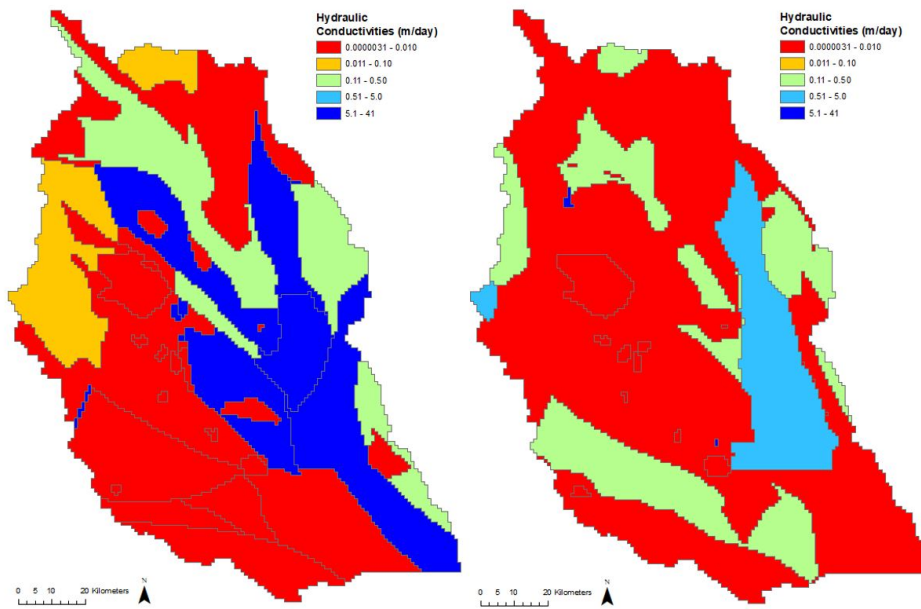


Figure 4.4: Distribution of hydraulic conductivities for the predevelopment steady-state and historical transient model for layer 3 (left) and layer 4 (right).

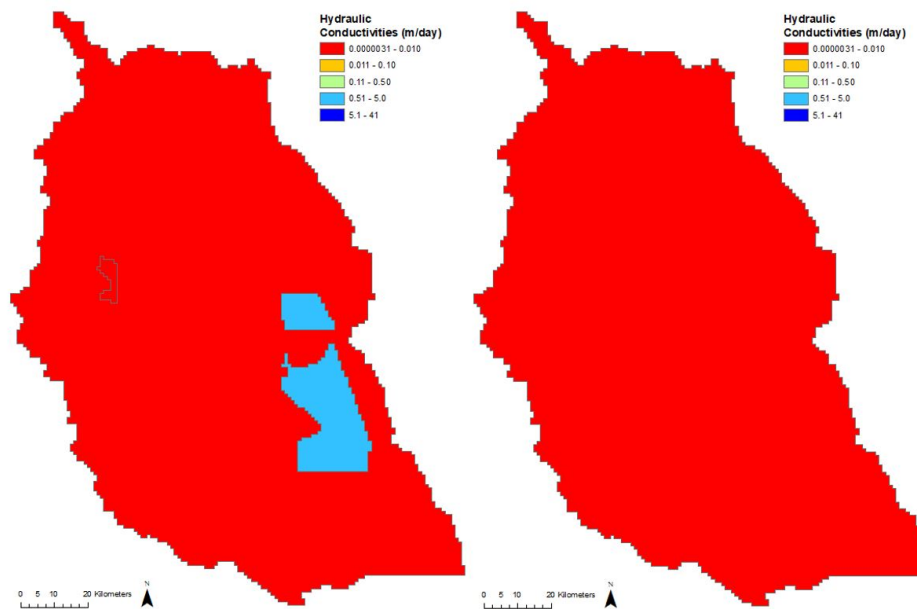


Figure 4.5: Distribution of hydraulic conductivities for the predevelopment steady-state and historical transient model for layer 5 (left) and layer 6 (right).

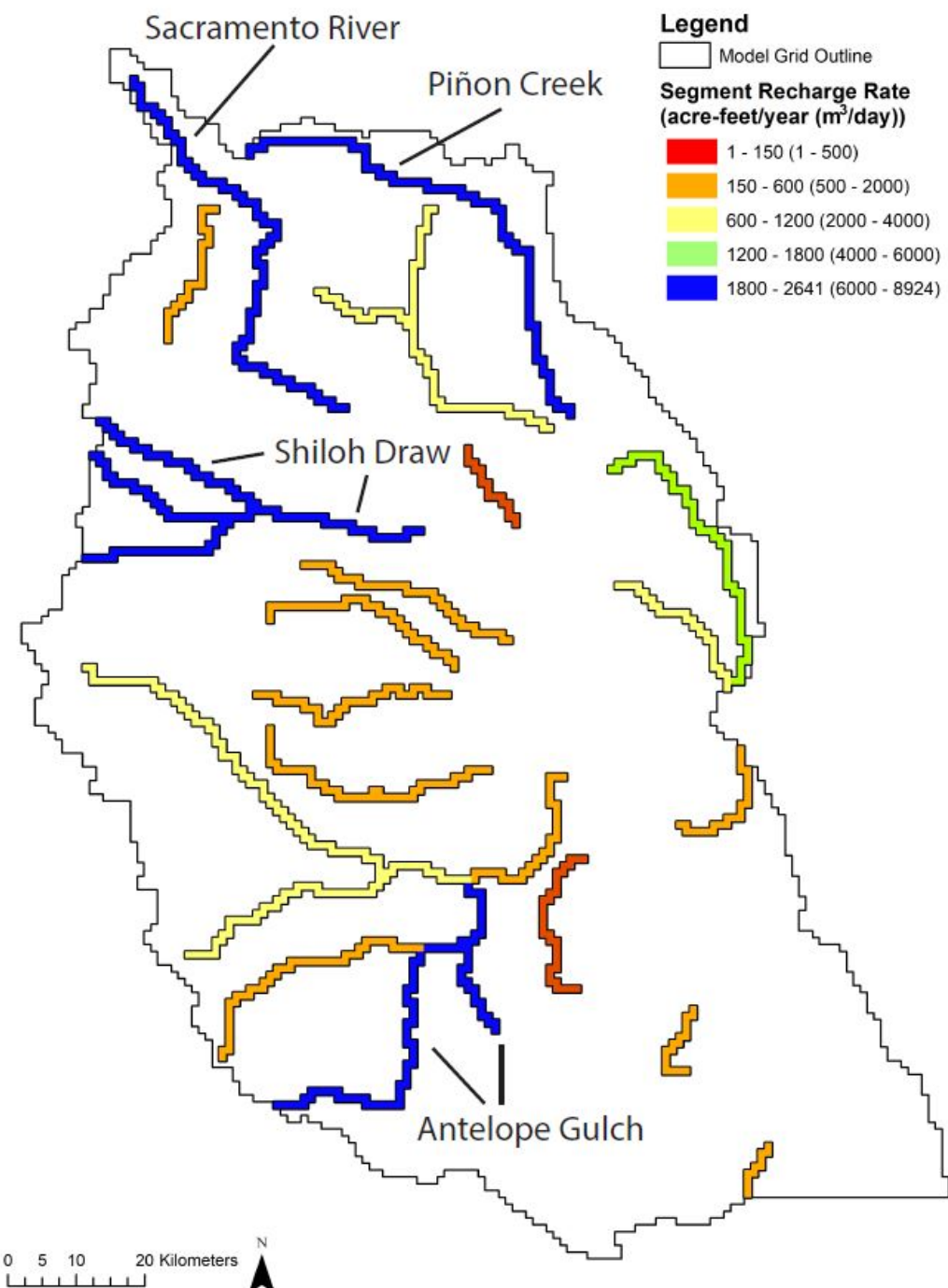


Figure 4.6: Distribution of depression-focused recharge in SFR segments in the predevelopment steady-state model. Color denotes amount of recharge from SFR segment. In acre-feet/year and m^3/day .

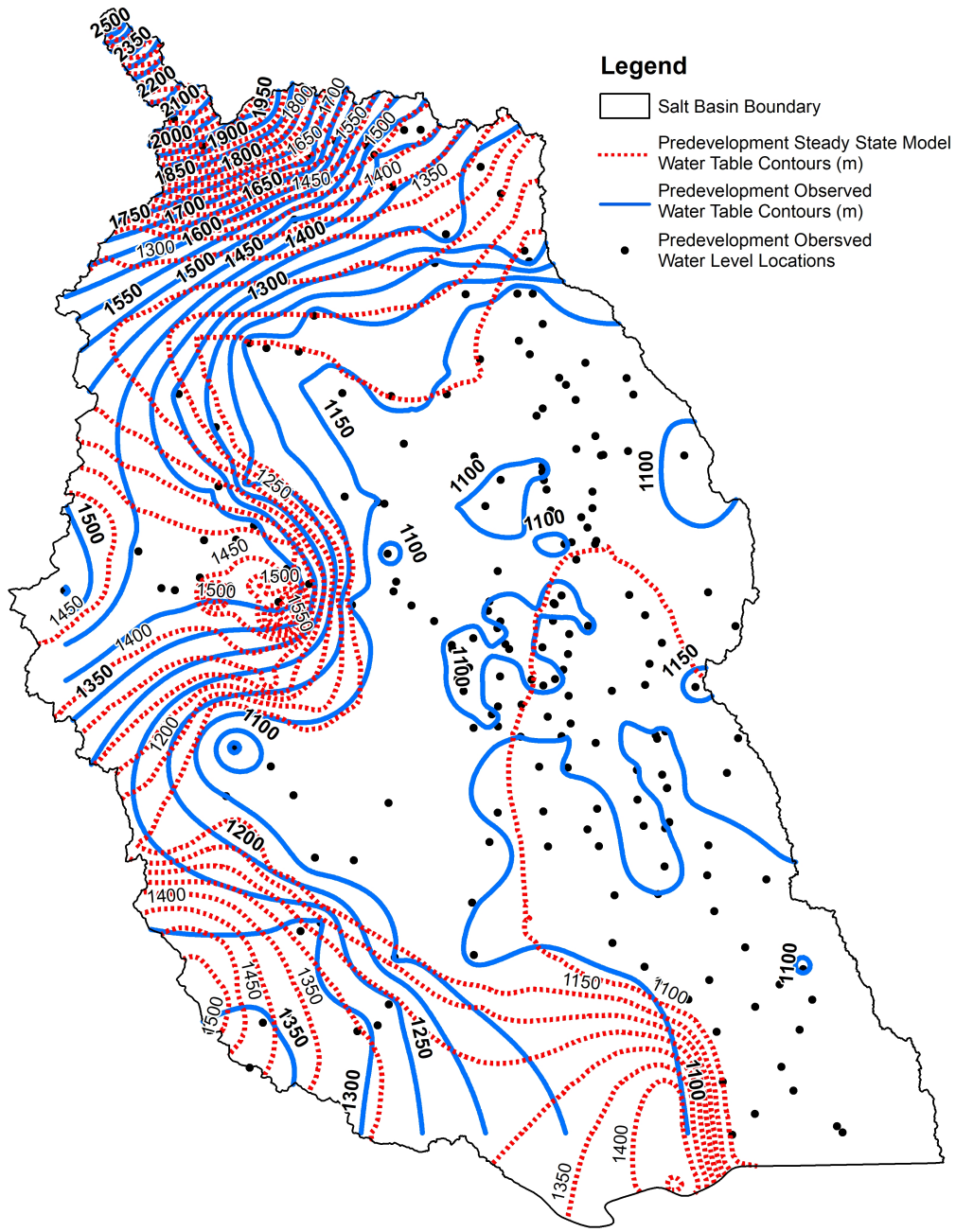


Figure 4.7: Observed and modeled predevelopment water table contour map (in meters). Observed water table contours are denoted by solid blue contour elevation, labels are in meters. Model computed water table contours are denoted by red dashed lines. Black points are locations of observed predevelopment water levels used to create predevelopment observed water table contours. Both set of water table contours developed in this study. The contour interval is 50 meter. This figure shows a relatively good fit between the observed and model predevelopment water tables, and that some of the larger discrepancies may simply reflect interpolation of observed data across regions with only sparse data.

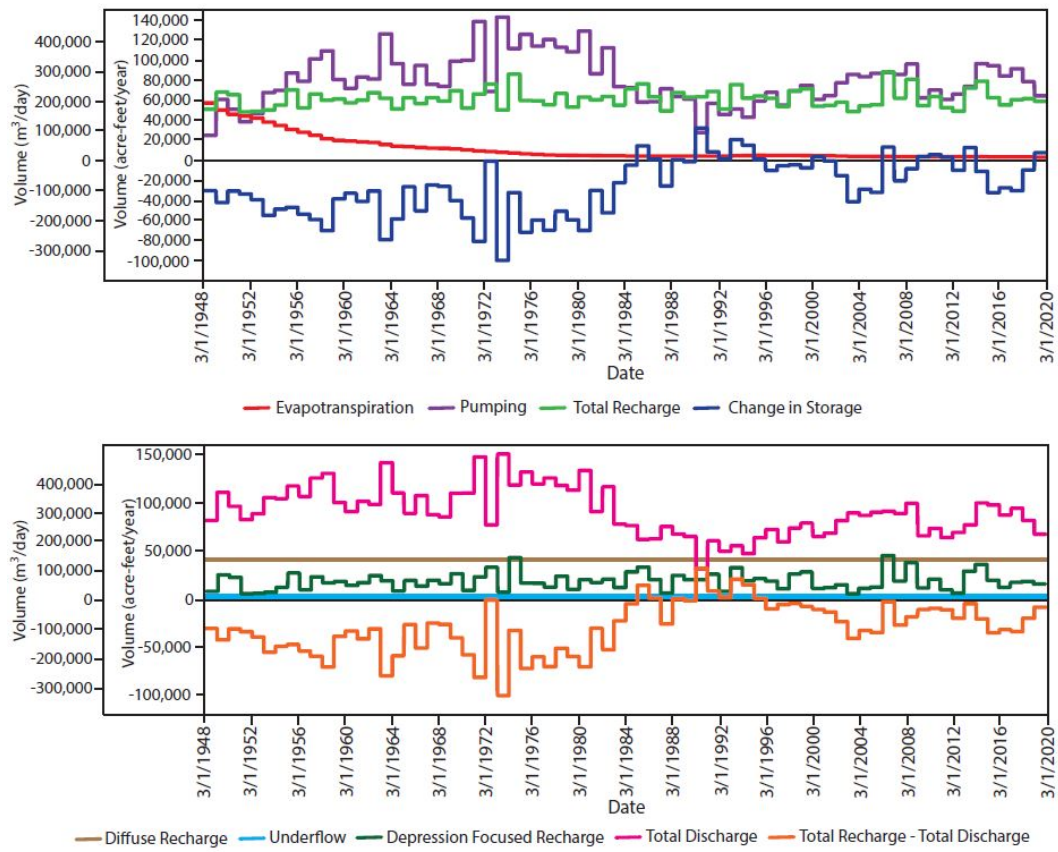


Figure 4.8: (top) Evapotranspiration, pumping, total recharge, and net storage through time of transient model (1948 to 2020). (bottom) Diffuse recharge, underflow, depression-focused recharge, total discharge, and difference between total recharge and total discharge through time of transient model.

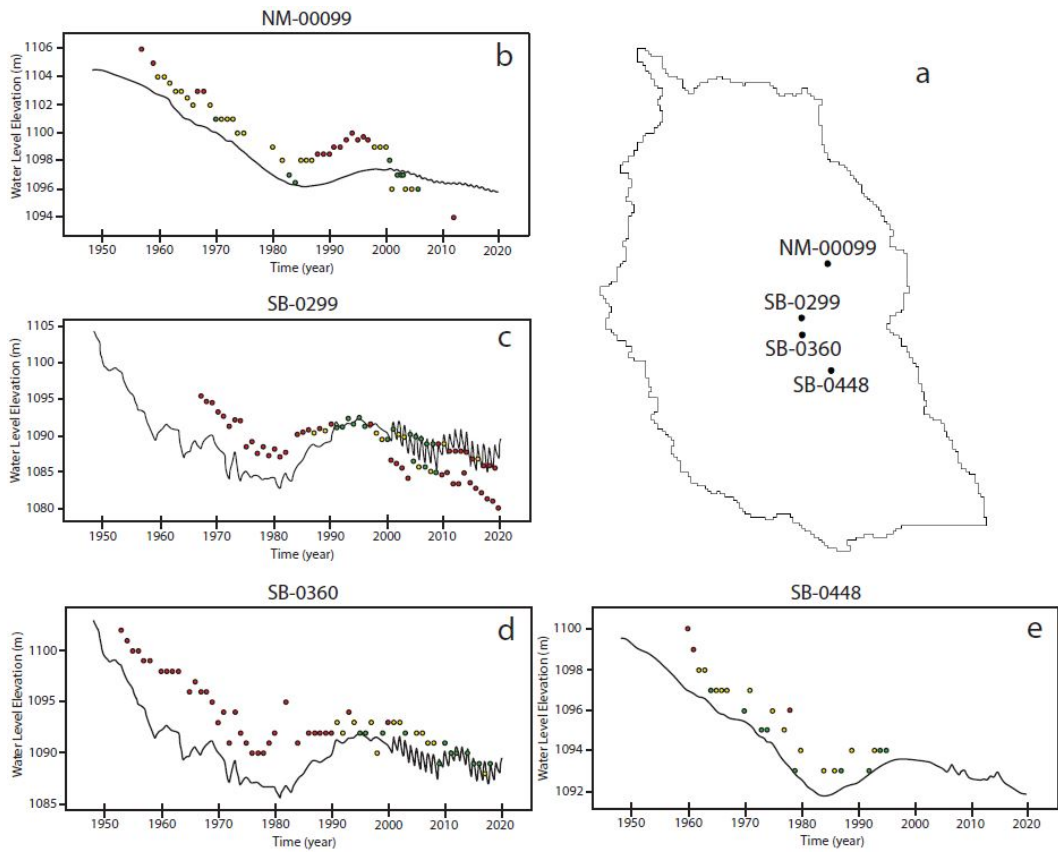


Figure 4.9: Observed versus computed well hydrographs in the Salt Basin (b-d). Locations of four wells displayed as black dots in Figure 4.9a. Black lines show computed water levels through time for the well. Points are observed water levels. Red points have a $>2.5\text{m}$ residual. Yellow points have a 2.5m to 1m residual. Green points have a $<1\text{m}$ residual.

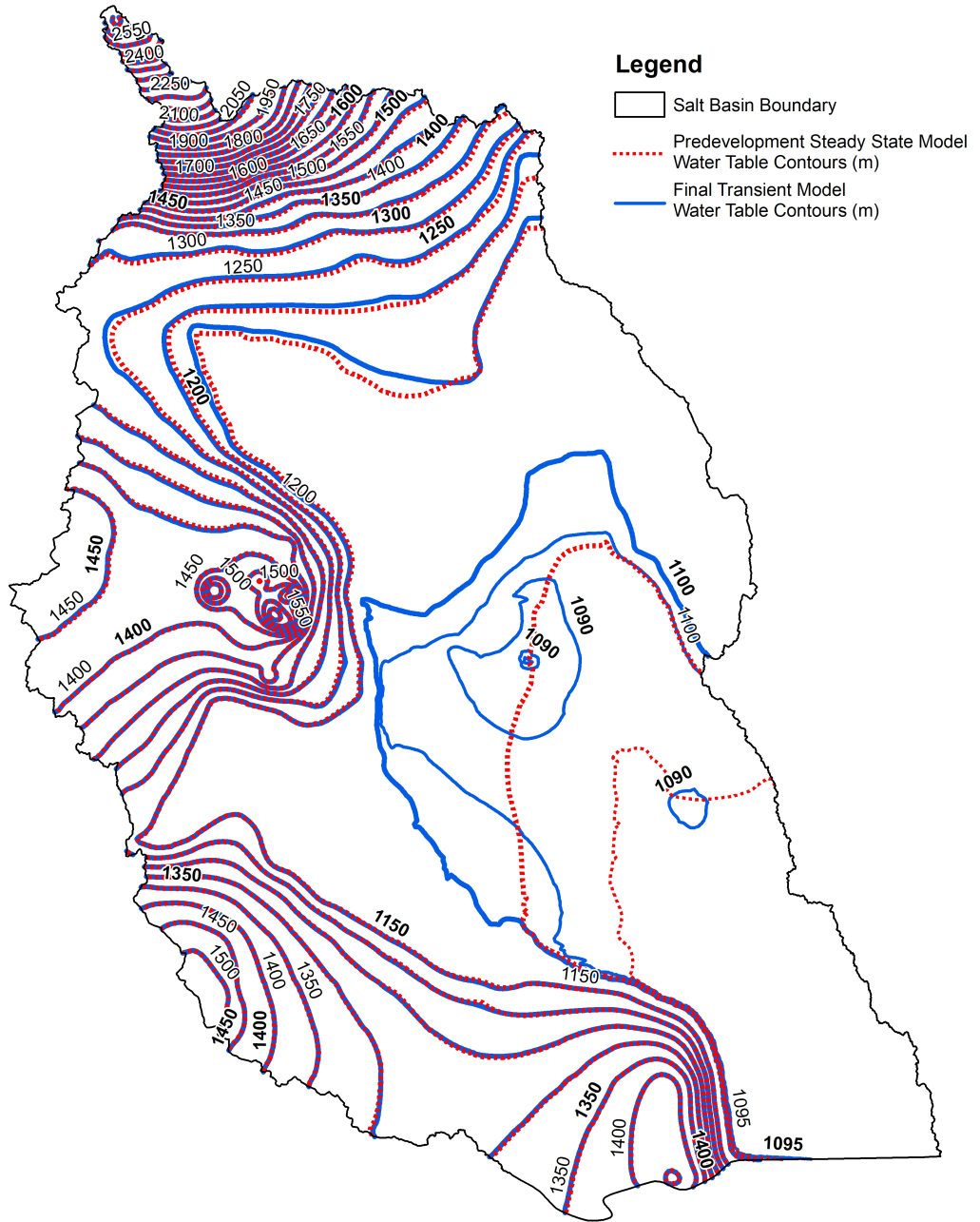


Figure 4.10: Initial (red dashed line) and final 2020 (blue and bolded labels) transient model water table contours. The initial water table contour map is from the predevelopment steady-state model. 50 m contour interval and 5 m contour interval in the salt flats.

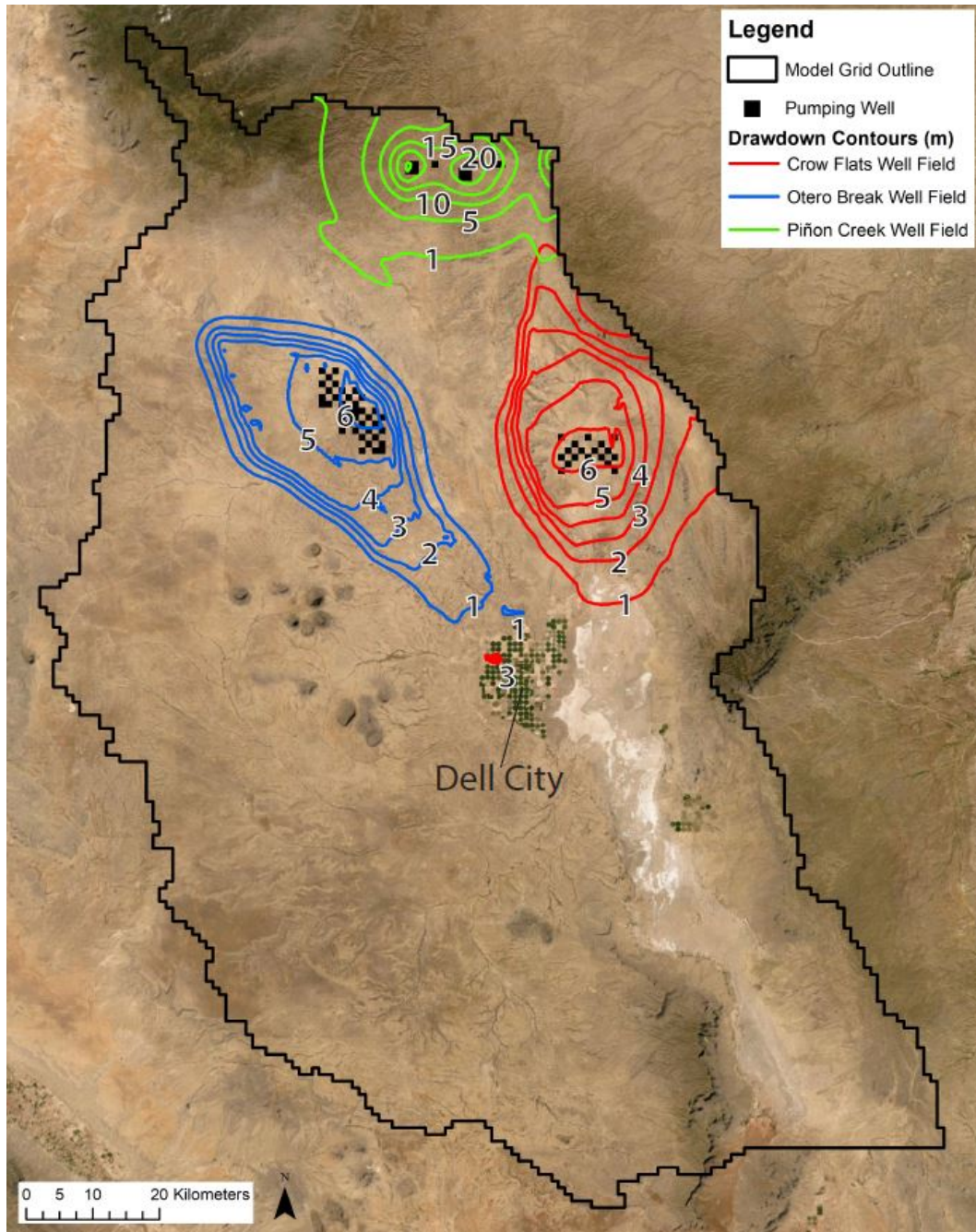


Figure 4.11: Drawdown contours for Scenario 1 (additional 127,072 acre-feet of pumping) water table compared to the historical transient model water table (m) for the three pumping scenarios in the year with the most drawdown, 1974. Crow Flats drawdown contours are red, Otero Break drawdown contours are blue, and Piñon Creek drawdown contours are green.

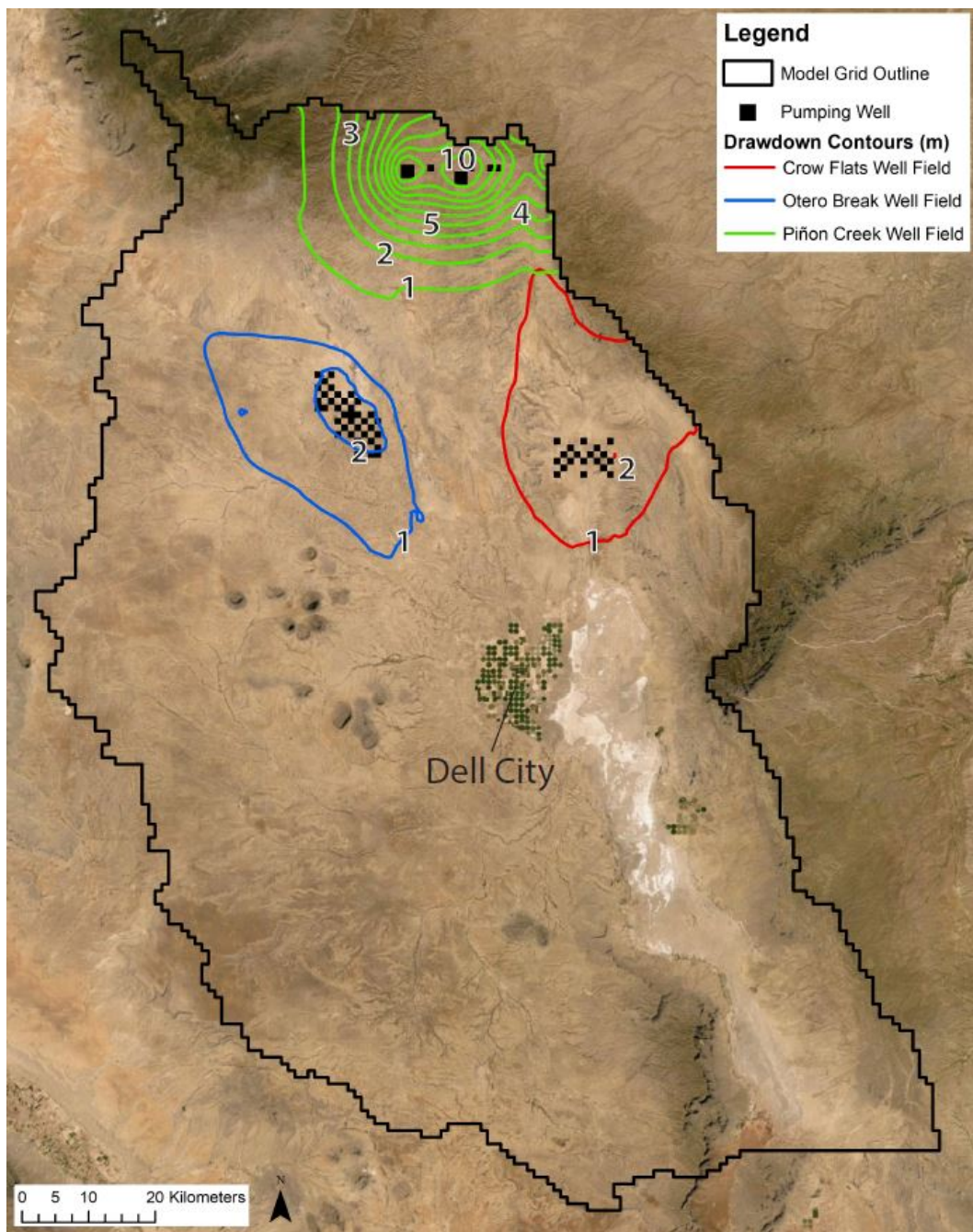


Figure 4.12: Drawdown contours for Scenario 2 (additional 66,345 acre-feet of pumping) water table compared to the historical transient model water table (m) for the three pumping scenarios in the year with the most drawdown, 2014. Crow Flats drawdown contours are red, Otero Break drawdown contours are blue, and Piñon Creek drawdown contours are green.

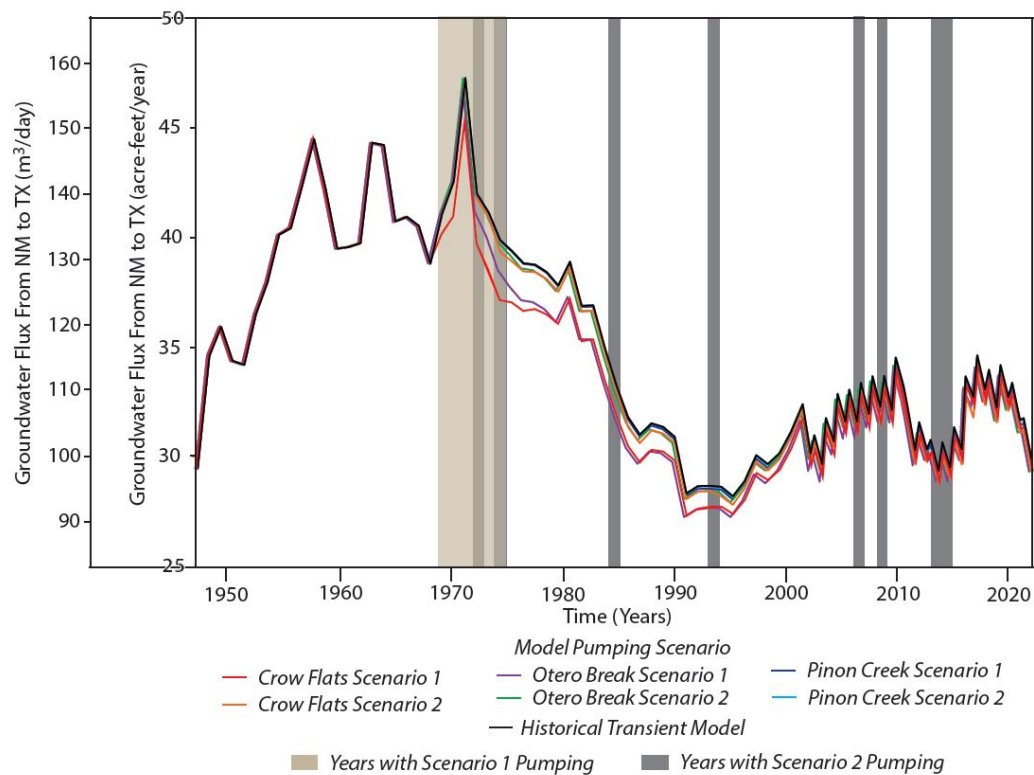


Figure 4.13: Annual subsurface flux of water across the state line from New Mexico to Texas through the entire transient model run, in acre-feet/year.

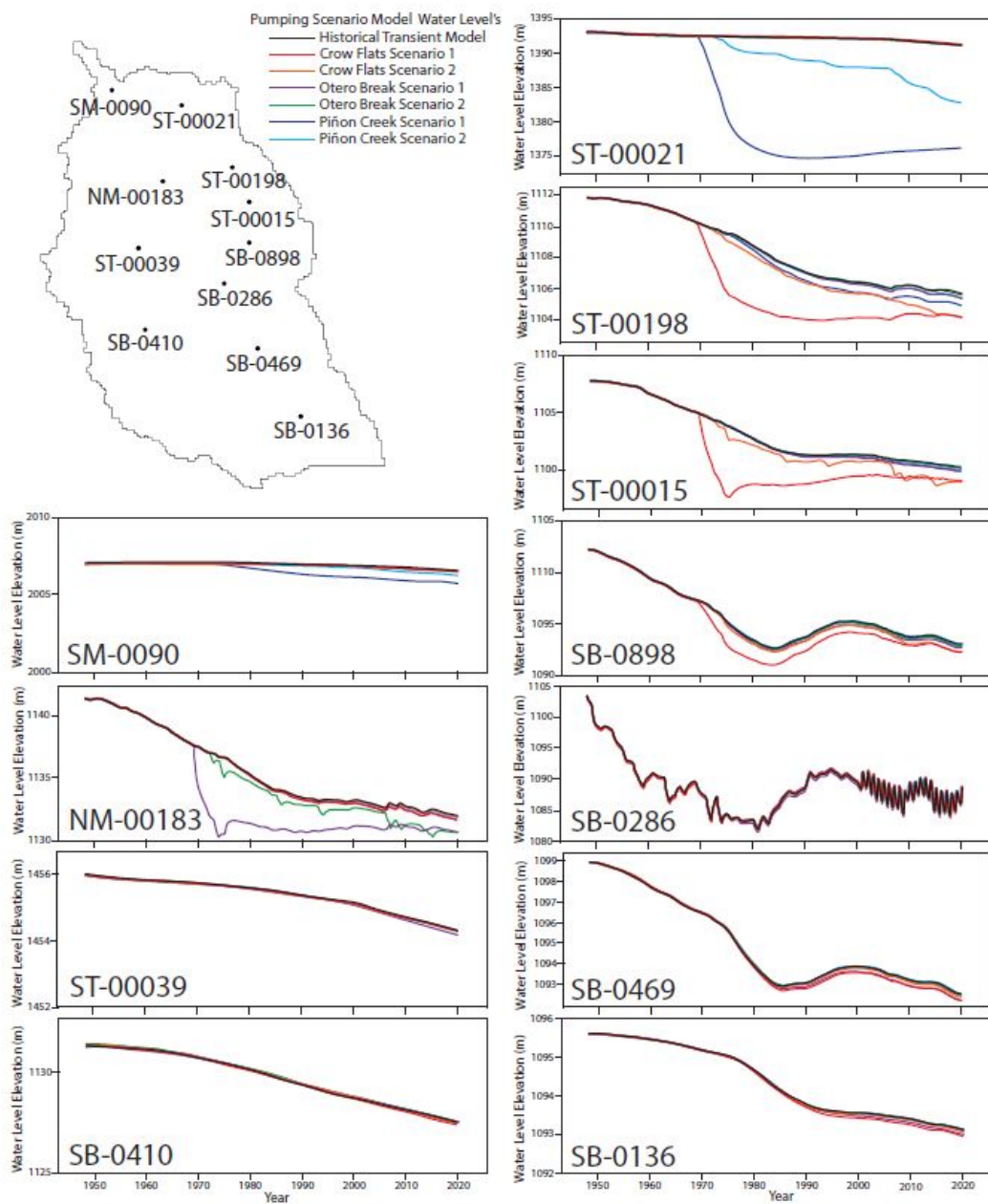


Figure 4.14: Transient water levels for the historical transient model and the six pumping scenario models. Color denotes the model scenario. Well ID is in bottom left of each graph. Top left is a map of model grid and locations of wells plotted in figure. Well ST-00021 is near the Piñon Creek well field. Well ST-00015 is within the Crow Flats well field. Well NM-00183 is within the Otero Break well field. Water levels are in meters.

CHAPTER 5

DISCUSSION

The purpose of this study is to determine the hydrologic budget of the Salt Basin and if a hypothetical well field can maintain safe aquifer yields.

5.1 Predevelopment Steady-State Model

Based on the predevelopment steady-state model, our best estimate of recharge to the aquifer around 1948 was 60,487 acre-feet/year. For the predevelopment steady-state model, three recharge levels were considered. Three models simulating about 40,000, 60,000, and 80,000 acre-feet/year (135,000, 203,000, and 270,000 m³/day) of recharge were constructed. Each model had a good fit of observed versus computed water levels, all with R-squared values over 0.992. The ~60,000 acre-feet/year (203,000 m³/day) of recharge model was selected because of its statistical fit and findings in prior studies of the Salt Basin suggesting a similar recharge value. The ~60,000 acre-feet/year (203,000 m³/day) recharge model had the best R-squared value and RMSE for the fit of observed versus computed water levels and ¹⁴C ages. Three prior studies on the Salt Basin agreed with ~60,000 acre-feet/year (203,000 m³/day) recharge. Hutchison [2008] predevelopment steady-state model of the Salt Basin that calculated recharge by using the Maxey-Eakin approach and critical elevations and found the recharge rate, not including underflow, to be ~63,000 acre-feet/year (213,000 m³/day). Stephens [2010a] developed a basin-scale balance model that evaluated precipitation, evapotranspiration, and recharge which estimated the average annual recharge to be 63,000 acre-feet/year (213,000 m³/day). Shomaker [2010] developed a groundwater model flow budget that was based on extensive work with the water budget and found a recharge rate of ~62,000 acre-feet/year (210,000 m³/day). In a parallel study to this study, a recharge estimate was calculated with the chloride mass balance method, which used the rate of chloride deposition in the Sacramento Mountains, chloride concentration in deep brines under Cloudcroft, NM, the average chloride atmospheric deposition rate, and the chloride/bromide ratio from groundwater samples to estimate the recharge rate. A recharge rate of ~32,000 acre-feet/year (139,000 m³/day) was estimated using this method. Kreitler et al. [1987] suggested that the high density of fractures in the Salt Basin may cause mixing of fresh

and old groundwater, making estimates of recharge from groundwater chemistry inaccurate. PyRANA estimated the total diffuse and depression-focused recharge to be between 34,000 to 68,000 acre-feet/year (115,000 to 230,000 m³/day). The lower recharge estimates cited above indicates using the ~40,000 acre-feet/year (135,000 m³/day) of recharge transient model of the Salt Basin in the future.

Based on PRISM data, the Salt Basin had an average precipitation volume of 3,293,764 acre-feet/year (4,062,794,294 m³/year) from 1895 to 2019. This means that the predevelopment steady-state model, with a recharge rate of 60,487 acre-feet/year (204,000 m³/day), simulated 1.8% of precipitation as recharge. Shomaker [2010] and Stephens [2010a] similarly found that 1.5% of total precipitation in the Salt Basin became recharge.

The majority of the recharge in the model came from diffuse, then depression-focused recharge, and only a small portion came from underflow from adjacent basins. Diffuse recharge was distributed over areas of high elevation. The Cornudas Mountains had the highest volume of recharge, 20,617 acre-feet/year (69,672 m³/day) for the predevelopment steady-state model. This was because it had the largest area for water to infiltrate into the aquifer. A large volume of diffuse recharge was needed to match the observed water table mound under the Cornudas Mountains. The observed water table mound under the Cornudas Mountains is enigmatic and collection of more water level and environmental tracer data there is warranted. The Sacramento Mountains had the next highest volume of diffuse recharge (9,554 acre-feet/year or 32,288 m³/day) and this was due to the high precipitation rate. The Sacramento River and Piñon Creek ephemeral streams had high amounts of depression-focused recharge because they extend into the highest elevations of the Salt Basin, which received more precipitation. Shiloh Draw and Antelope Gulch had high depression-focused recharge because their watersheds extend over portions of the high Otero Mesa and Diablo Plateau.

For the predevelopment steady-state model, evapotranspiration was the only way water could exit the model, so evapotranspiration should be a close approximation of recharge. The evapotranspiration rate used in this model was 1.45 mm/day with a five meter extinction depth. Stephens [2010b] studied the evaporation from the playa deposit core samples in the salt flats to determine an average evaporation rate of 0.63 mm/day. Considering the surface extent of the salt flats, an average of 28,300 acre-feet/year of evapotranspiration loss was estimated, translating to an equivalent amount of recharge. Stephens [2010b] described potential factors that might cause this estimate to be too low, making 28,300 acre-feet/year (96,000 m³/day) a minimum recharge rate. PyRANA and gridMET determined the initial model evapotranspiration rate of 5.5 mm/day. The Blaney-Criddle method and NDVI maps were used to calculate an evapotranspiration rate in Dell City of 3.55 mm/day with an average of 69,000 acre-feet/year (233,000 m³/year) [Cadol, 2021]. The PyRANA, gridMET, and Blaney-Criddle methods included transpiration from plants, which increases the rate above the rate of evaporation from the salt flats. In semi-arid environments, the hydrologic

budget is dominated by monsoonal precipitation and evapotranspiration. The spatial and temporal variations in precipitation and evapotranspiration are hard to quantify and small errors in their values can lead to large errors in recharge values [Gee and Hillel, 1988, Jovanovic and Israel, 2012, Sophocleous, 2004]. Calculated evapotranspiration rates can neglect extreme variants in weather. This can lead to 40 to 60% errors when there are windy, humid, dry, sunny, or cloudy days [Brouwer and Heibloem, 1986]. Thus, errors in the calculated evapotranspiration should be expected. The evapotranspiration rate of 1.45 mm/day used in this model falls above the minimum Stephens [2010b] rate and below the high PyRANA, gridMET, and Blaney-Criddle rates.

It is difficult to estimate recharge and hydraulic conductivities using a steady-state groundwater flow model because the model solution is non-unique. Models using different recharge rates can have similarly good fits of observed to computed water levels by adjusting hydraulic conductivities. The analytical solution to the steady-state groundwater flow equation shown in Equation 5.3 indicates that if recharge and hydraulic conductivities are proportionally increased, the hydraulic head will not change. Darcy's Law in Plan View is given by:

$$Q = -T \left(\frac{\partial h}{\partial x} \right) \quad (5.1)$$

$$T \left(\frac{\partial^2 h}{\partial x^2} \right) = R \quad (5.2)$$

Integrating both sides of Equation 5 with respect to x and assuming $h = h_o$ at $x = 0$ and $\frac{\partial h}{\partial x} = 0$ at $x = L$ yields:

$$h = h_o + \frac{R}{T} \left(xL - \frac{x^2}{2} \right) \quad (5.3)$$

where L is the basin length (m), Q is discharge (m^3/day), T is transmissivity (m^2/day), R is recharge rate (m/day), ∂h is change in hydraulic head (m), and ∂x is distance of flow (m).

This becomes problematic when one is trying to determine values for both hydraulic conductivities and recharge with observed water levels, which is the situation in this study.

All three predevelopment steady-state models with different levels of recharge had poor fits to ^{14}C ages. The models lacked porosity data and used a uniform porosity across the entire model and the flow paths from the MODPATH computed ages were not quality checked. In addition, natural tracers should be assumed to have a $\pm 50\%$ error [Sophocleous, 2004]. The Salt Basin is also highly fractured which could cause mixing of young and old water [Kreitler et al., 1987]. Other groundwater models in New Mexico also had difficulty fitting groundwater ages such as Sanford [2011].

5.2 Historical Transient Model

The historical transient model was unable to fit seasonal oscillations in the water table after the year 2000, but was able to reproduce the annual trends in water levels. The historical transient model revealed that holding the diffuse recharge rates constant and varying depression-focused recharge based on annual precipitation rates provided a good match to transient water level observations. It was found that pumping reduced the water levels under the salt flats, significantly decreasing the evapotranspiration rate from 1948 to 2020. Between 1948 to 1980 the evapotranspiration rate drops quickly from ~57,000 to ~4,500 acre-feet/year (193,000 to 15,000 m³/day). Then from 1980 to 2020, evapotranspiration rates decrease more slowly to ~3,000 acre-feet/year (10,000 m³/day) in 2020. Shomaker [2010] observed a similar phenomenon in their model, which used a nine meter evapotranspiration extinction depth from the land surface. Pumping in their transient groundwater model decreased water levels under the salt flat, decreasing evapotranspiration rates until it reached zero in 1980. Based on observed data, the salt flats should reach zero evapotranspiration in the year 2000 [Shomaker, 2010]. Shomaker [2010] believed that the early decrease in water levels in their model under the salt flats was due to over-estimated consumptive pumping used in their model. Our model did not reach zero evapotranspiration for the entire transient simulation, let alone the year 2000. This could be because of an over estimation of return flow from pumping, which was 50% for DCMI wells and accounted for in irrigation wells by only pumping the water that would be evapotranspired.

The computed predevelopment steady-state water table compared favorably to observed conditions. The final computed 2020 water level map from the historical transient model, compared favorably to the measured cone of depression (Figure 4.10). Water table maps and model results show the water table minima shifted from under the salt flats to under Dell City. Reversal of the groundwater flow direction probably has taken place and water is now flowing towards Dell City instead of towards the salt flats. This could be dangerous because saline water from the salt flats could be pulled into Dell City wells.

Safe aquifer yield is the maximum pumping rate at which the consequences are considered acceptable [Alley et al., 1999]. In this study, the unacceptable consequence is loss of groundwater storage leading to unacceptable water table declines (i.e., water level declines below well screens or pump intake valves). The safe aquifer yield estimate can be pumped indefinitely with the assumption that the climate conditions do not change. This definition means the safe aquifer yield estimates are conservative. In the state of New Mexico a new well must be applied for with a annual pumping rate requested to the Office of the State Engineer [Green and Castle, 2017]. The Office of the State Engineer determines if the annual pumping rate can be reasonably produced and applied to a beneficial use while maintaining water quality and implementing water conservation measures [NMOSE, 2001]. This indicates that pumping leading to the mining of groundwater storage may be acceptable in New Mexico provided that adjacent wells are not negatively affected.

The historical transient model indicates the Salt Basin has not reached, but is approaching a new dynamic equilibrium since pumping started in the Salt Basin. This phenomenon can be seen in the net storage oscillating back and forth over storage gain and loss since about 1985 in Figure 4.8. There is still more net loss in storage than net gain in storage since 1985 suggesting the Salt Basin has not reached a new dynamic equilibrium. The approach to a new dynamic equilibrium is also seen in the evapotranspiration rate slowing its decrease after about 1980. This suggests a slow decrease in water levels in the Salt Basin lowlands. The decrease in water levels from 1985 to 2020 is also seen in observed water levels in Dell City (Figure 2.4). The storage change and evapotranspiration rates from 1985 to 2020 indicate the aquifer had on average been pumped slightly above the safe aquifer yield for this time. The pumping rate from 1985 to 2020 averaged 69,276 acre-feet/year ($233,000 \text{ m}^3/\text{day}$) with a minimum of 27,319 acre-feet/year ($92,000 \text{ m}^3/\text{day}$) and a maximum of 96,263 acre-feet/year ($325,000 \text{ m}^3/\text{day}$). A safe aquifer yield estimate can be made by subtracting the average storage change from 1985 to 2020 (-5,422 acre-feet/year), which is theoretically the volume of water that was pumped over the safe aquifer yield, from the average recharge rate from 1985 to 2020. Using this method and assuming a recharge rate of about 60,000 acre-feet/year ($203,000 \text{ m}^3/\text{day}$), the safe aquifer yield of the Salt Basin is estimated to be 64,000 acre-feet/year ($216,000 \text{ m}^3/\text{day}$).

Safe aquifer yield can also be estimated from the sum of recharge and the safely captured evapotranspiration. The average total recharge rate for the historical transient model from 1948 to 2020 is 61,259 acre-feet/year ($207,000 \text{ m}^3/\text{day}$), which includes diffuse recharge, depression-focused recharge, and underflow. Conservatively, 50% of evapotranspiration can be safely captured [Bredehoeft, 2002]. 50% of the average evapotranspiration rate from 1948 to 2020 in the historical transient model is 5,534 acre-feet/year ($19,000 \text{ m}^3/\text{day}$). Safe aquifer yield for the Salt Basin, assuming a recharge rate of about 60,000 acre-feet/year ($203,000 \text{ m}^3/\text{day}$), is therefore estimated to be about 67,000 acre-feet/year ($226,000 \text{ m}^3/\text{day}$).

If the recharge rate used in the model was lower or higher, this would decrease or increase the safe aquifer yield estimates. Increases in temperatures and associated reduction in recharge could also lower our estimates of safe aquifer yield in the future.

Fichera [2021] used this studies groundwater model layers and storage properties along with well depth and water quality data to determine the potable groundwater volume available in the Salt Basin. She found that there is a total of 69 million-acre-feet (Maf) (85 km^3) of groundwater in the entire Salt Basin, 13 Maf (16 km^3) on the New Mexico side of the Salt Basin [Fichera, 2021]. Based on the Texas Water Code §36.108 (d), which considers environmental and socioeconomic impacts of pumping groundwater, it is likely that only 25 to 75% of the total groundwater volume is available for pumping [Boghici et al., 2014]. This means 17 to 52 Maf (21 to 64 km^3) of groundwater in the entire Salt Basin and 3 to 10 Maf (4 to 12 km^3) of groundwater available on the New Mexico side of the Salt Basin

[Fichera, 2021].

Based on the estimate of groundwater volume available for pumping in the Salt Basin determined by Fichera [2021], a pumping rate of 100,000 acre-feet/year (338,000 m³/day) could be pumped for about 90 to 300 years using groundwater storage just from the New Mexico side of the Salt Basin or about 500 to 1,600 years using groundwater storage from the entire Salt Basin. Note that this does not take into consideration changes in water quality, depth to water, groundwater flux across the state line, underflow from adjacent basins, and groundwater flow paths. Excessive groundwater pumping in the vicinity of Dell City will eventually lead to salt water intrusion.

5.3 Pumping Scenarios

One can estimate the time required to approach steady state conditions in response to pumping (and hence changes in groundwater storage) using the response time (τ) for a basin. The response time for pumping effects in the Salt Basin was calculated with calibrated hydraulic diffusivity, transmissivity, specific yield, and a characteristic distance of 50 km (basin half width).

$$\tau = \frac{L^2}{D_h} \quad (5.4)$$

where τ is the response time to pumping, D_h is the hydraulic diffusivity (m²/day), and L is the characteristic basin length (m).

The Salt Basin is over 150 km long from north to south and over 100 km wide from east to west, so a characteristic length of 50 km seems reasonable.

The unconfined aquifer response time is given by:

$$D_h = \frac{T}{S_y} \quad (5.5)$$

where D_h is the hydraulic diffusivity (m²/day), T is transmissivity (m²/day), and S_y is specific yield.

Using a hydraulic diffusivity of 26,000 m²/day and a S_y of 0.1, the response time for pumping was 263 years.

The confined aquifer the response time is given by:

$$D_h = \frac{K}{S_s} \quad (5.6)$$

where D_h is the hydraulic diffusivity (m²/day), K is hydraulic conductivity (m/day), and S_s is specific storage (1/m).

Using a hydraulic conductivity of 41 m/day and a S_s of 10^{-6} m^{-1} , the response time for pumping was 61 days. However the response time could have been longer (685 years) if the hydraulic conductivity was set to 0.01 m/day.

The models were run for 72 years. We conclude that the pumping scenarios were not run long enough to reach a dynamic equilibrium due to additional pumping. Thus our 72 year model simulation period was too short to determine what the long-term effects of pumping could be. Keep in mind, the effects from the additional pumping in the hypothetical pumping scenarios could be exacerbated in the future if this additional pumping was continued using 2020 climate conditions.

The three hypothetical well fields used in the six pumping scenarios are a long distance from the Dell City pumping center, ranging from 34 to 76 km apart. This distance was designed to minimize drawdown in both the hypothetical well fields and Dell City. Based on the computed state line fluxes, the new NM well field pumping had a minimum effect on groundwater water flowing from NM to TX. Pumping a total additional 127,072 acre-feet (157 million m^3) (Scenario 1) in the Crow Flats well field had the largest decrease in flux from NM to TX, for all six scenarios, with a total of 65 acre-feet (80,000 m^3) from 1948 to 2020. That was only 0.05% of the total additional pumping volume of 127,072 acre-feet (157 million m^3). Wells in the Salt Basin that were not directly in the well field could be affected by the additional pumping (Figure 4.14). Including wells 20 km from the southern border of the basin, but this was a drawdown $<0.5 \text{ m}$. The drawdowns $<0.5 \text{ m}$ are seen throughout the entire basin. The observation well in Dell City showed minimal ($<1 \text{ m}$) to no changes in water levels due to the pumping scenarios. Together the flux across the NM-TX border and observation well water levels suggest that the additional pumping will not have much affect on wells in TX.

Figures 4.11 and 4.12 show the extent of the drawdown for the pumping scenarios. The wells within the drawdown would be affected by the hypothetical well field pumping. Outside of the 1 meter contours, drawdown of $<1\text{m}$ is seen sporadically throughout the Salt Basin. Overall, pumping an additional 127,072 acre-feet (157 million m^3) (Scenario 1) cause drawdowns that are more severe than pumping a total additional 66,345 acre-feet (82 million m^3) (Scenario 2). The shape of the drawdown contours are highly affected by geology in the Crow Flats and Otero Break well fields. The contours extend further in geologic zones with higher conductivities. The Otero Break well field contours extends further down the Otero Break, towards Dell City and the Crow Flats well field extends towards the salt flats. Pumping a total additional 66,345 acre-feet (82 million m^3) (Scenario 2) at the Crow Flats and Otero Break well fields do not cause drawdowns larger than two meters outside of the well field itself. The small drawdown is promising but it should be noted that the Otero Break well field has a preferential drawdown pattern heading towards Dell City, which could cause problems if drawdowns increase. Nevertheless, pumping a total additional 66,345 acre-feet (82 million m^3) (Scenario 2) at the Crow Flats and Otero Break well fields are the most promising. Pumping a total additional 127,072 acre-feet (157 million m^3) (Scenario 1) for all

three well fields or lowering the pumping rate (Scenario 2) at the Piñon Creek well field either create too large of drawdown or encroach on Dell City.

Based on the historical transient model which assumes the recharge rate to be about 60,000 acre-feet/year ($203,000 \text{ m}^3/\text{day}$) the safe aquifer yield is estimated to be 64,000 and 67,000 acre-feet/year ($216,000$ to $226,000 \text{ m}^3/\text{day}$). Therefore, historical pumping in the Salt Basin is on average above the safe aquifer yield estimates. The average estimated historical pumping for the last five years (2015 to 2020) is estimated to be about 82,000 acre-feet/year ($277,000 \text{ m}^3/\text{day}$). Pumping a total additional 127,072 acre-feet (157 million m^3) (Scenario 1) or the lower additional pumping volume of 66,345 acre-feet (82 million m^3) (Scenario 2), based on pumping volumes, could not maintain safe aquifer yields. Historical pumping rates would need to decrease to maintain safe aquifer yields.

Considering the loss of evapotranspiration versus storage loss, drawdown contour trends, and the state line flux, total additional pumping of 66,345 acre-feet (82 million m^3) (Scenario 2) at the Crow Flats and Otero Break well fields appear to be sustainable in the short term. But, considering the safe aquifer yield estimates of 64,000 and 67,000 acre-feet/year ($216,000$ to $226,000 \text{ m}^3/\text{day}$), no additional pumping in the Salt Basin can maintain safe aquifer yield.

In addition, if the pumping scenarios were run starting in the year 2021 and going into the future, they may show more negative effects, such as increased drawdown and decreased state line flux, because those years could potentially have less recharge due to climate change in the future. It is also important to note that our analysis did not consider water quality change due to pumping.

5.4 Uncertainties and Improvements

The models we constructed contain uncertainties. First, the predevelopment recharge rate of 60,487 acre-feet/year ($204,000 \text{ m}^3/\text{day}$) was mostly based on prior work and is not significantly statistically better than the other recharge scenarios. Recharge values of 40,000 or 80,000 acre-feet/year ($135,000$ or $270,000 \text{ m}^3/\text{day}$) of are potentially reasonable solutions, as well. Recharge and evapotranspiration are spatially and temporally variable, especially in a semi-arid climate, with monsoons providing most of the water in the basin, making these parameters hard to quantify and estimate [Jovanovic and Israel, 2012, Sophocleous, 2004]. The pumping rates used in our models needed to be estimated for most wells. Although the methods used to determine pumping were thorough, they are still estimates. For the historical transient model, the water level oscillations seen in Huff and Chace [2006] were not able to be simulated. This suggests the geology zones may be too coarse and cannot perfectly model the fluctuations in water levels in the Salt Basin. This causes uncertainty in the geologic framework used. Finally, for the pumping scenarios, the additional pumping was not applied to the model for a long enough time to achieve dynamic equilibrium conditions. Thus,

assumptions were made based on the short term additional pumping to determine how the additional pumping would affect the Salt Basin in the long term.

Several other studies have attempted to more or less answer the questions posed in this study. Not surprisingly, there has been a wide variety of answers (Figure 2.5). The current model is the only model of the Salt Basin to use PEST. PEST helps determine a better fit to observed data, improving the model quality. In many instances it can reveal spatial data gaps. This model improved estimates of pumping rates by using available public pumping rates, NDVI maps, the Blaney – Criddle method, and Shomaker [2010]’s pumping data.

CHAPTER 6

CONCLUSIONS

A predevelopment steady-state and a historical transient 3D groundwater flow model that included pumping were developed in order to estimate the overall water budget and determine if potential new NM well fields in the Salt Basin can honor estimates of safe aquifer yield. For the calibration of the predevelopment steady-state model, three recharge levels were considered; using values of about 40,000, 60,000, and 80,000 acre-feet/year (135,000, 203,000, and 270,000 m³/day) of recharge. The predevelopment steady-state model was first manually calibrated and then further calibrated with observed water levels using PEST. Based primarily on estimates of recharge from prior studies [Hutchison, 2008, Shomaker, 2010, Stephens, 2010a], the recharge rate was assumed to be ~60,000 acre-feet/year (203,000 m³/day). This estimate also had a slightly better statistical fit to water level data than the other two recharge rates. The ~60,000 acre-feet/year (203,000 m³/day) of recharge predevelopment steady-state model underwent more calibration and was then used as a starting point for the historical transient model. The historical transient model was manually calibrated to water levels to refine the estimates for hydraulic conductivities, specific storage, specific yield, evapotranspiration, and stream conductances. The calibrations of hydraulic conductivities and stream conductances made to the historic transient model were applied to the predevelopment steady-state model. The historical transient model was then used for the six hypothetical pumping scenarios. The pumping scenarios used three hypothetical well fields, the Crow Flats well field, the Otero Break well field, and the Piñon Creek well field. Each well field had two pumping scenarios applied: Scenario 1 (total additional pumping of 127,072 acre-feet (157 million m³)) accounts for the shortages from the Pecos River Compact from 1969 to 1974 and Scenario 2 (total additional pumping of 66,345 acre-feet (82 million m³)) accounts for additional pumping in years when runoff is high.

Using information from prior studies and the results from our predevelopment steady-state model we believe that the recharge rate of about 60,000 acre-feet/year (204,000 m³/day) is most likely with a possible range of 40,000 to 80,000 acre-feet/year (135,000 to 270,000 m³/day). The evapotranspiration rate matched the recharge rate in the predevelopment steady-state model. The historical transient model had an average recharge rate of 61,259 acre-feet/year (207,000 m³/day), an average evapotranspiration rate of 11,067 acre-feet/year (37,000 m³/day) due to declining water table elevation, and an average pumping

rate of 79,529 acre-feet/year ($269,000 \text{ m}^3/\text{day}$). Evapotranspiration rates decreased from $\sim 57,000$ to $\sim 3,000$ acre-feet/year ($192,000$ to $10,000 \text{ m}^3/\text{day}$) from 1948 to 2020. This was because pumping in the Salt Basin lowered the water levels under the salt flats below the evapotranspiration extinction depth. From 1985 to 2020, a dynamic equilibrium with change in storage is approaching but not yet reached. This suggests that historically the aquifer was being slightly over pumped over the safe aquifer yield.

Based on the approaching new dynamic equilibrium in net storage changes since 1985, the safe aquifer yield was estimated to be equal to the average of pumping rate minus the average groundwater storage loss from 1985 to 2020. This estimates the safe aquifer yield to be 64,000 acre-feet/year ($216,000 \text{ m}^3/\text{day}$). Another method to determine safe aquifer yield is sum the average recharge rate (61,259 acre-feet/year or $207,000 \text{ m}^3/\text{day}$) from 1948 to 2020 and 50% of the average evapotranspiration rate (5,534 acre-feet/year or $19,000 \text{ m}^3/\text{day}$) from 1948 to 2020. This suggests a safe aquifer yield of 67,000 acre-feet/year ($226,000 \text{ m}^3/\text{day}$). Therefore the safe aquifer yield is between 64,000 and 67,000 acre-feet/year ($216,000$ to $226,000 \text{ m}^3/\text{day}$).

Six hypothetical pumping scenarios were applied to the historical transient model. Scenario 1 applied a total of 127,072 acre-feet (157 million m^3) of additional pumping from 1969 to 1974 to each of the hypothetical NM well fields. Scenario 2 applied a total of 66,345 acre-feet (82 million m^3) of additional pumping to years with high runoff. These pumping scenarios were applied to three different hypothetical well fields, the Crow Flats well field, Otero Break well field, and Piñon Creek well field. Any additional pumping from the Salt Basin will result in a decrease of evapotranspiration and groundwater storage. For all six pumping scenarios, the decrease in groundwater flowing from NM to TX is minimal, with a maximum of 65 acre-feet ($80,000 \text{ m}^3$) for the Crow Flats well field with 127,072 acre-feet (157 million m^3) of additional pumping (Scenario 1). The drawdown contours showed that the 66,345 acre-feet (82 million m^3) (Scenario 2) of additional pumping in the Crow Flats and Otero Break could potentially maintain safe aquifer yield. The other well fields showed sub-optimal drawdowns. But, based on the safe aquifer yield estimates from this study, no additional pumping at any of the well fields could maintain safe aquifer yields.

Future work should focus on repeating the historical and hypothetical pumping scenario transient models using 40,000 and 80,000 acre-feet/year (135,000 and $270,000 \text{ m}^3/\text{day}$) of recharge to quantify, in part, to determine the range of uncertainty in our model predictions. Running transient models into the future would also be useful to determine when dynamic equilibrium conditions occur. Installing stream gauges and/or pressure transducers to the Sacramento River and arroyos during high precipitation events would provide useful ground truth on depression-focused recharge. Monitoring lake levels and underlying groundwater heads in the salt flats would confirm whether or not the vertical head gradients are downward and if water is migrating away from the salt flats towards Dell City. This model could also be improved by creating a model ground surface

directly from a digital elevation model instead of the nodes with digital elevation model values used currently. Pursuing model calibration with the ^{14}C ages and analyzing flow paths may prove fruitful, however, this analysis unlikely to reduce our uncertainty regarding parameter calibration.

REFERENCES

- John T Abatzoglou, David E Rupp, and Philip W Mote. Seasonal climate variability and change in the pacific northwest of the united states. *Journal of Climate*, 27 (5):2125–2142, 2014.
- William M Alley, Thomas E Reilly, and O Lehn Franke. *Sustainability of ground-water resources*, volume 1186. US Department of the Interior, US Geological Survey, 1999.
- Edward S Angle. Hydrogeology of the salt basin. *Aquifers of West Texas: Texas Water Development Board Report*, 356:232–247, 2001.
- John B Ashworth. Ground-water resources of the bone spring-victorio peak aquifer in the dell valley area, texas. Report, Texas Water Development Board, 1995.
- John B Ashworth. Bone spring-victorio peak aquifer of the dell valley region of texas. *Aquifers of West Texas. Report*, 356:135–152, 2001.
- Edward R Banta. *MODFLOW-2000: The US Geological Survey Modular Ground-water Model—documentation of Packages for Simulating Evapotranspiration with a Segmented Function (ETS1) and Drains with Return Flow (DRT1)*. US Department of the Interior, US Geological Survey, 2000.
- DS Barker. Cenozoic igneous rocks, sierra blanca area, texas. In *Trans-Pecos region, southeastern New Mexico and West Texas. New Mexico Geol Soc Guidebook, 31st Field Conference*, pages 219–223, 1980.
- LJ Bjorklund. Reconnaissance of ground-water conditions in the crow flats area otero county, new mexico: State of new mexico, state engineer office technical rept. 1957.
- Bruce Allen Black. *Geology of the Northern and Eastern Parts of the Otero Platform, Otero and Chaves Counties, New Mexico*. The University of New Mexico, 1973.
- Harry French Blaney and Wayne D Criddle. *Determining consumptive use and irrigation water requirements*. US Department of Agriculture, 1962.
- Radu Boghici, Ian C Jones, Robert G, Jerry Shi, Rohit Raj Goswami, David Thorkildsen, and Sarah Backhouse. Gam task 13-028: Total estimated recoverable storage for aquifers in groundwater management area 4. 2014.
- Felicia Michelle Boyd and Charles W Kreitler. *Hydrogeology of a gypsum playa, northern Salt Basin, Texas*. Bureau of Economic Geology, University of Texas at Austin, 1986.

- John D Bredehoeft. The water budget myth revisited: why hydrogeologists model. *Groundwater*, 40(4):340–345, 2002. ISSN 0017-467X.
- RF Broadhead. Petroleum geology of the mcgregor range, otero county, new mexico: New mexico geological society. In *53rd Field Conference, Guidebook*, pages 331–338, 2002.
- C Brouwer and M Heibloem. Irrigation water management: irrigation water needs. *Food and Agriculture Organization of the United Nations Training manual*, 3, 1986.
- Daniel Cadol, 2021.
- Daniel Cadol, Gabriel Parish, Sarah Reuter, Talon Newton, Fred M. Philips, and HJan M.H. Hendrickx. Estimating soil water holding capacity and runoff in new mexico to improve modeled recharge rates. Report, New Mexico Water Resources Research Institute, 2020.
- RE Denison, EA Hetherington, and JB Otto. Age of basement rocks in northeastern oklahoma. *Oklahoma Geology Notes*, 29(5):120–128, 1969.
- Rodger E Denison, ME Bickford, Edward G Lidiak, and Eva B Kisvarsanyi. Geology and geochronology of precambrian rocks in the central interior region of the united states. 1987.
- Patricia Wood Dickerson, Margaret Skeels Stevens, and James Bowie Stevens. Frontmatter: South texas geological society field trip guidebook: Geology of the big bend, and trans-pecos, texas. 1989.
- John E Doherty and Randall J Hunt. *Approaches to highly parameterized inversion: a guide to using PEST for groundwater-model calibration*, volume 2010. US Department of the Interior, US Geological Survey Reston, 2010.
- Jennifer L Druhan, James F Hogan, Christopher J Eastoe, Barry J Hibbs, and William R Hutchison. Hydrogeologic controls on groundwater recharge and salinization: a geochemical analysis of the northern hueco bolson aquifer, texas, usa. *Hydrogeology Journal*, 16(2):281–296, 2008. ISSN 1431-2174.
- Thomas Emery Eakin and George Burke Maxey. *Ground Water in Goshute–Antelope Valley, Elko County, Nevada*. State of Nevada, Office of the State Engineer, 1949.
- CJ Eastoe and BJ Hibbs. Stable and radiogenic isotope evidence relating to regional groundwater flow ssystems originating in the high sacramento mountains, new mexico. In *AGU Fall Meeting Abstracts*, volume 2005, pages H33G–04, 2005.
- Marissa Fichera. Total groundwater volume and recoverable storage estimate for the salt basin (nm & tx), Jul 2021.
- Steven T Finch. *Hydrogeologic framework of the salt basin and development of three-dimensional ground-water flow model*. John Shomaker & Associates, Incorporated, 2002.

- Gerald M Friedman. Occurrence and origin of quaternary dolomite of salt flat, west Texas. *Journal of Sedimentary Research*, 36(1):263–267, 1966.
- Joseph Spencer Gates, WD Stanley, and HD Ackermann. Availability of fresh and slightly saline ground water in the basins of westernmost Texas. Technical report, US Geological Survey, 1978.
- Glendon W Gee and Daniel Hillel. Groundwater recharge in arid regions: review and critique of estimation methods. *Hydrological processes*, 2(3):255–266, 1988. ISSN 0885-6087.
- Peter Gillham George, Robert Earl Mace, and William F Mullican. *The Hydrogeology of Hudspeth County, Texas*. Citeseer, 2005.
- Lisa K Goetz. New Mexico geological society guidebook, 31st field conference, trans-Pecos region, 1980 83 quaternary faulting in salt basin graben, west Texas. In *Trans-Pecos Region, Southeastern New Mexico and West Texas: New Mexico Geological Society, Thirty-First Field Conference, November 6-8, 1980*, volume 31, page 83. The Society, 1980.
- Lisa Karen Goetz. Quaternary faulting in salt basin graben, west Texas. 1977.
- LK Goetz. Salt basin graben: A basin and range right-lateral transtensional fault zone: Some speculations. *Structure and tectonics of Trans-Pecos Texas: West Texas Geological Society Publication*, pages 85–81, 1985.
- Monica Green and Anne Castle. Assured water supply laws in the western states: The current state of play. *Colo. Nat. Resources Energy & Envtl. L. Rev.*, 28:67, 2017.
- David P. Groeneveld and William M. Baugh. Mapping and estimating evapotranspiration for Dell City, Texas. Report, HydroBio Advanced Remote Sensing, Santa Fe, New Mexico, 2002.
- David S Gutzler. New Mexico's changing climate. *Natural Resources Journal*, 45(2): 277–282, 2005.
- Arlen W Harbaugh. *MODFLOW-2005, the US Geological Survey modular ground-water model: the ground-water flow process*. US Department of the Interior, US Geological Survey Reston, VA, 2005.
- Arlen W Harbaugh, Edward R Banta, Mary C Hill, and Michael G McDonald. Modflow-2000, the U. S. Geological Survey modular ground-water model—user guide to modularization concepts and the ground-water flow process. *Open-file report. U. S. Geological Survey*, (92):134, 2000.
- Robert Harrington and Aaron Steinwand. Development of hydrologic and vadose models to improve groundwater management in the Owens Valley. 2004.
- Philip Thayer Hayes. Geology of the Guadalupe Mountains, New Mexico. Technical report, US Geological Survey, 1964.

Mary C Hill and Claire R Tiedeman. *Effective groundwater model calibration: with analysis of data, sensitivities, predictions, and uncertainty*. John Wiley & Sons, 2006.

Glenn F Huff and DA Chace. Knowledge and understanding of the hydrogeology of the salt basin in south-central new mexico and future study needs. Report, United States Geological Survey, Office of the State Engineer Interstate Stream Commission, Sandia National Laboratories, 2006.

WR Hutchison. Preliminary groundwater flow model,dell city area, hudspeth and culberson counties, texas, 2008.

INTERA. Remote-sensing based evaluation of groundwater discharge from the salt basin, new mexico. Report, New Mexico Interstate Stream Commission, 2010.

ISC. *Pecos River Compact*. 1949.

Nebo Jovanovic and Sumaya Israel. Critical review of methods for the estimation of actual evapotranspiration in hydrological models. *Evapotranspiration: Remote Sensing and Modeling*, 2012.

S. Kelley, M. Fichera, E. Evenocheck, B.A. Eberle, M. Person, D. Cadol, B.T. Newton, S. Timmons, and C. Pokorny. Assessment of water resources in the salt basin region of new mexico and texas: Data summary report. Report, New Mexico Bureau of Geology and Mineral Resources, 2020.

Vincent Cooper Kelley. *Geology of the Pecos country, southeastern New Mexico*, volume 24. State Bureau of Mines and Mineral Resources, 1971.

Charles Kerans, F Jerry Lucia, and RK Senger. Integrated characterization of carbonate ramp reservoirs using permian san andres formation outcrop analogs. *AAPG bulletin*, 78(2):181–216, 1994.

PB King, RE King, and JB Knight. Geology of the hueco mountains. *El Paso and Hudspeth counties, Texas: Washington, DC, United States Geological Survey, Oil and Gas Investigations, Preliminary Map*, (36):1, 1945.

Philip B King. *Geology of the southern Guadalupe Mountains, Texas*, volume 215. US Government Printing Office, 1948.

William Edward King and Vicki M Harder. *Oil and Gas Potential of the Tularosa Basin–Otero Platform–Salt Basin Graben Area, New Mexico and Texas*, volume 198. New Mexico Bureau of Mines & Mineral Resources, 1985.

Leonard F Konikow and John D Bredehoeft. Modeling flow and chemical quality changes in an irrigated stream-aquifer system. *Water Resources Research*, 10(3): 546–562, 1974. ISSN 0043-1397.

Leonard F Konikow and Christopher E Neuzil. A method to estimate groundwater depletion from confining layers. *Water Resources Research*, 43(7), 2007.

FE Kottlowski. Summary of late paleozoic in el paso border region. In *Border stratigraphy symposium: New Mexico Bureau of Mines and Mineral Resources Circular*, volume 104, pages 38–51, 1969.

Frank Edward Kottlowski. *Paleozoic and Mesozoic strata of southwestern and southcentral New Mexico*. State Bureau of Mines and Mineral Resources, New Mexico Institute of Mining, 1963.

CW Kreitler, JA Raney, R Nativ, EW Collins, WF Mullican, TC Gustavson, and CD Henry. Siting a low-level radioactive waste disposal facility in texas, volume four-geologic and hydrologic investigations of state of texas and university lands: The university of texas at austin, bureau of economic geology. *IAC (86-87)*, 1987.

Stanley William Lohman. *Ground-water hydraulics*, volume 708. US Government Printing Office, 1972.

Greg H Mack and Katherine A Giles. The geology of new mexico. *A Geologic History*, 86, 2004.

Peter Hotchkiss Masson. Age of igneous rocks at pump station hills, hudspeth county, texas. *AAPG Bulletin*, 40(3):501–518, 1956.

James R Mayer and JM Sharp Jr. The role of fractures in regional groundwater flow. *Mechanics of Jointed and Faulted Rock*, 1995.

James R Mayer and John M Sharp Jr. Fracture control of regional ground-water flow in a carbonate aquifer in a semi-arid region. *Geological Society of America Bulletin*, 110(2):269–283, 1998.

James W Mercer and Charles R Faust. Ground-water modeling: An overview a. *Groundwater*, 18(2):108–115, 1980. ISSN 0017-467X.

Richard F Meyer. *Geology of Pennsylvanian and Wolfcampian rocks in southeast New Mexico*. State Bureau of Mines and Mineral Resources, 1966.

David S Morgan and Michael D Dettinger. Ground-water conditions in las vegas valley, clark county, nevada; part ii, hydrogeology and simulation of ground-water flow. Report 2331-1258, US Geological Survey; USGS Earth Science Information Center, 1994.

William R Muehlberger and Patricia W Dickerson. A tectonic history of trans-pecos texas. *Structure and Stratigraphy of Trans-Pecos Texas: El Paso to Guadalupe Mountains and Big Bend July 20–29, 1989*, 317:35–54, 1989.

WF Mullican III and RK Senger. Saturated-zone hydrology of south-central hudspeth county, texas. *Hydrogeology of Trans-Pecos Texas: Kreitler, CW, and Sharp, J. M., Jr., eds., The University of Texas at Austin, Bureau of Economic Geology Guidebook*, 25:37–42, 1990.

- Norman Dennis Newell. *The Permian reef complex of the Guadalupe Mountains region, Texas and New Mexico: a study in paleoecology*. Hafner Publishing Company, 1972.
- BT Newton, GC Rawling, SS Timmons, L Land, PS Johnson, TJ Kludt, and JM Timmons. Sacramento mountains hydrogeology study. *NM Bur Geol Min Resour Open-File Rep*, 543, 2012.
- PD Nielson and JM Sharp Jr. Tectonic controls on the hydrogeology of the salt basin, trans-pecos texas. *Structure and Tectonics of Trans-Pecos Texas*, pages 85–81, 1985.
- Richard G Niswonger and David E Pradic. Documentation of the streamflow-routing (sfr2) package to include unsaturated flow beneath streams-a modification to sfr1. Report 2328-7055, US Geological Survey, 2005.
- NMOSE. *Natural Resources and Wildlife, Underground Water - General Provisions*. New Mexico Statutes, 2001.
- CJ Nutt, JM O'Neill, MD Kleinkopf, DP Klein, WR Miller, BD Rodriguez, and VT McLemore. Geology and mineral resources of the cornudas mountains, new mexico. Technical report, US Geological Survey,, 1997.
- Richard A Pauloo, Graham E Fogg, Zhilin Guo, and Thomas Harter. Anthropogenic basin closure and groundwater salinization (abcsal). *Journal of Hydrology*, 593:125787, 2021. ISSN 0022-1694.
- David W Pollock. Source code and ancillary data files for the modpath particle tracking package of the ground-water flow model modflow; version 3, release 1. *US Geological Survey Open-File Report*, pages 94–0463, 1994.
- Lloyd Charles Pray. *Geology of the Sacramento Mountains Escarpment: Otero County, New Mexico*. State Bureau of Mines and Mineral Resources, New Mexico Institute of Mining . . . , 1961.
- André Blue Ocean Ritchie. *Hydrogeologic Framework and Development of a Three-dimensional Finite Difference Groundwater Flow Model of the Salt Basin, New Mexico and Texas*. Thesis, 2011.
- Ward Sanford. Calibration of models using groundwater age. *Hydrogeology Journal*, 19(1):13–16, 2011. ISSN 1435-0157.
- Ralph A Scalapino. *Development of ground water for irrigation in the Dell City area, Hudspeth County, Texas*. Texas Board of Water Engineers, 1950.
- Timothy M Shepard and Jack L Walper. Tectonic evolution of trans-pecos, texas. 1982.
- J. W. Shomaker. Hypothetical well fields in salt basin and pipeline to pecos river. *John Shomaker & Associates, Inc. Draft Report, Prepared for New Mexico Interstate Stream Commission*, page 17, 2002.

- J. W. Shomaker. Revised hydrogeologic framework and updated groundwater-flow model of the salt basin, new mexico. Final report, John Shomaker & Associates, 2010.
- Sophia Carmelita Sigstedt. *Environmental tracers in groundwater of the Salt Basin, New Mexico, and implications for water resources*. Thesis, 2010.
- M Sophocleous. Groundwater recharge, 2004.
- Daniel B. Stephens. Recharge modeling study, salt basin of southeastern new mexico. Report, 2010a.
- Daniel B. Stephens. Salt basin historical playa evaporation study. Report, 2010b.
- Charles Warren Thornthwaite. An approach toward a rational classification of climate. *Geographical review*, 38(1):55–94, 1948. ISSN 0016-7428.
- Anne Celeste Tillery. *Estimates of mean-annual streamflow and flow loss for ephemeral channels in the Salt Basin, southeastern New Mexico*, 2009. US Department of the Interior, US Geological Survey, 2011. ISBN 1411331559.
- Jozsef Toth. A theoretical analysis of groundwater flow in small drainage basins. *Journal of geophysical research*, 68(16):4795–4812, 1963. ISSN 0148-0227.
- US-Census-Bureau. National population totals: 2010-2012, 2020. URL <https://www.census.gov/programs-surveys/popest.html>.
- USGS. Landsat normalized difference vegetation index, 2021.
- David E Wilkins. Hemiarid basin responses to abrupt climatic change: Paleolakes of the trans-pecos closed basin. *Physical Geography*, 18(5):460–477, 1997. ISSN 0272-3646. doi: 10.1080/02723646.1997.10642630.
- Fei Xu. *Estimation of Focused Recharge for New Mexico Using a Soil-Water-Balance Model: PyRANA*. New Mexico Institute of Mining and Technology, 2018. ISBN 0438286138.

APPENDIX A

SALT BASIN GEOLOGY

The Salt Basin is a geologically complex region that extends from southern New Mexico into northwestern Texas. The surface of the Salt Basin is made up of mostly Permian through Quaternary units (Figure A.1). Permian rock units make up the majority of water-bearing strata. Below is highly fractured Pennsylvanian through Precambrian units. The fractures were caused by three tectonic events that occurred in the region. The Mississippian - Pennsylvanian Marathon - Ouachita (Ancestral Rocky Mountains) orogeny, the Late Cretaceous - Paleogene Laramide orogeny, and the Neogene Basin and Range extension. These fractures form major groundwater flow paths through the Salt Basin. The major aquifer units are made up of stratigraphic units deposited from marine environments from varying sea levels. The geology section of this thesis was strongly influenced by Ritchie [2011] and Kelley et al. [2020].

A.1 Stratigraphy

The major groups of stratigraphy include Neogene alluvial and bolson deposits, Tertiary intrusions, Cretaceous units, Permian shelf facies, Permian shelf-margin facies, Permian basin facies, late Paleozoic units, early Paleozoic units, and Precambrian units.

A.1.1 Neogene Alluvial and Bolson Deposits

Neogene units are alluvial and bolson deposits that consist of unconsolidated clay, silt, sand, and gravel derived from the erosion of, mostly carbonate, local rock. These units were deposited by ancestral drainages into the Salt Basin graben and are of variable thicknesses with a maximum thickness of 2,400 ft [Angle, 2001, Gates et al., 1978]. Basin fill thickness increases from south to north [Angle, 2001]. The thinnest basin fill is just north of the Baylor Mountains and corresponds to the location of the Victorio Flexure (Figure A.2). The thinning of the basin fill and location of the Victorio Flexure has created a groundwater divide [Nielson and Sharp Jr, 1985]. The Neogene units supply moderate to large quantities of fresh to

saline water Angle [2001]. The freshest water is found in coarse-grained fill that is near areas of recharge Gates et al. [1978].

The salt flats lie on the top of the Salt Basin graben, which is the lowest surface elevation in the basin. Sediments in the playas are composed of gypsum, carbonates (calcite and dolomite), quartz and lithic grains, and halite with subordinate aragonite and native sulfur [Boyd and Kreitler, 1986, Friedman, 1966, Stephens, 2010b]. Stephens [2010b] studied the top 4 feet of playa deposits and found that the saturated zone is within 3 to 3.5 feet below the land surface. They also determined the shallow water in the salt flats is not a perched aquifer due to low depth to water in a nearby well.

A.1.2 Tertiary Intrusions

Tertiary intrusions are present in the subsurface of the southwestern Otero Mesa and northwestern Diablo Plateau, and are exposed in the Cornudas Mountains, Granite Mountain, the Sierra Tinaja Pinta Group, the Antelope Hill intrusives, and Sierra Prieta sill [Barker, 1980, Masson, 1956]. The intrusions are made up of phonolite and syenite [King and Harder, 1985, Nutt et al., 1997]. Round Mountain, just east of Dell City, Texas, is a small nepheline-bearing trachyte intrusion [Ashworth, 2001, Mayer and Sharp Jr, 1995].

A.1.3 Cretaceous Units

The lower Cretaceous units make up the Diablo Plateau, which is in the southwest portion of the Salt Basin and unconformably overlies the Permian strata [King and Harder, 1985, Kottlowski, 1963]. The lower Cretaceous units are primarily made up of limestones interbedded with sandstones, shales, and conglomerates [Kottlowski, 1963, Mayer and Sharp Jr, 1995]. The limestone and sandstone are thought to be connected to the Salt Basin and Bone Spring-Victorio Peak aquifer [Mullican III and Senger, 1990].

A.1.4 Permian Shelf Facies

The Artesia Group is made up of interbedded dolomite and sandstone and crops out in the southern Guadalupe Mountains [Kelley, 1971]. This group is 600-800 feet thick and is not a significant water bearing unit.

The San Andres Formation is made up of carbonate and siliciclastic-carbonate units [Kerans et al., 1994]. These units crop out in the southern tip of the Sacramento Mountains and form the present-day topography across most of the Salt Basin. The San Andres has been divided into three subunits of the thick-bedded

Rio Bonito, thin-bedded Bonney Canyon, and the evaporitic Fourmile Draw members by Kelley [1971].

The Yeso Formation crops out across most of the western section of the Salt Basin, and the Sacramento and Guadalupe Mountains. In the Sacramento Mountains, the Yeso Formation consists of over 1,000 ft of red beds, yellow and gray shale, limestone, silty quartz sandstone, and gypsum [Pray, 1961]. In the Guadalupe Mountains, the Yeso Formation consists of dark to light-gray dolomite and dolomitic limestone, interbedded with gypsum and thin beds of gray-yellow sandy quartz-siltstone [Hayes, 1964]. The Yeso Formation was deposited in a transitional marine-terrestrial environment that produced more carbonate rocks in the south and more red beds and evaporites in the north [Pray, 1961]. The units are thickest where the Hueco Limestone and Pennsylvanian is thickest (maximum of 2,410 feet) and thinnest where the Hueco Limestone and Pennsylvanian is thinnest. The Yeso Formation contains abundant evaporites, which causes the groundwater to have higher salinity. The Yeso Formation is also less fractured than other Permian carbonates, making it less permeable [Mayer and Sharp Jr, 1998].

The Hueco Limestone and Abo Formation crop out near the central-western border of the Salt Basin. The Abo Formation red beds were developed from a major uplift in the northwest; the unit then spread southeast and interfingered with marine deposits of the Hueco Limestone [Meyer, 1966]. The Abo Formation is made up of red beds and brown fine grained anhydritic dolomite in the northwest Salt Basin which grades south and east into a coarse-grained dolomite, then into the black massive limestones of the lower Bone Spring Formation [Hayes, 1964, Meyer, 1966, Ritchie, 2011]. The Hueco Limestone consists of a lower unit of fine-crystalline limestone interbedded with shale and of minor sandstone and an upper unit of crystalline dolomite interbedded with shale [Hayes, 1964]. These units are the source of groundwater for several wells [Huff and Chace, 2006].

A.1.5 Permian Shelf-Margin Facies

The Capitan Limestone is the “largest, best-preserved, most intensively studied, Paleozoic reef complex in the world” [Mack and Giles, 2004]. The Capitan Limestone is made up of massive white limestone that was once a wide reef zone [Newell, 1972]. The Capitan Limestone appears in the subsurface of the southeastern portion of the Salt Basin and crops out in the Guadalupe Mountains to form the Capitan Peak. The Capitan Limestone is highly permeable and one of the most substantial aquifer units when in the subsurface. In the southern Guadalupe Mountains, the Capitan Limestone ranges in thickness from 1,000 to 2,000 ft [King, 1948].

The Goat Seep Dolomite Formation is a narrow reef belt made up of massive dolomite. This reef was a precursor to the Capitan Limestone Formation reef. The Goat Seep Dolomite Formation crops out in the Guadalupe Mountains and Sierra Diablo region. The thickness of the Goat Seep Dolomite ranges from 200

to 1,200 feet thick [King, 1948]. The Cutoff Shale is made up of thin-bedded limestone interbedded with dark-siliceous shale, sandy shale, and soft sandstone [Hayes, 1964, King, 1948]. The Cutoff Shale crops out on the northern Sierra Diablo Mountains and in the intensely faulted Guadalupe Mountains.

The Victorio Peak Limestone Formation is made up of white dolomites and limestones. The formation is exposed in the Sierra Diablo Mountains (1,000 to 1,500 feet thick), the Guadalupe Mountains (800 ft thick), and the Diablo Plateau [King, 1948]. The Victorio Peak Limestone Formation is equivalent to the basin-facies Bones Spring Formation that is made up of black limestones and the transition from one formation to another is around the margin of the Delaware Basin [Newell, 1972]. These two formations form a large water-bearing unit called the Bone Spring-Victorio Peak Aquifer. This aquifer is the major source of water for the town of Dell City, Texas. Mayer and Sharp Jr [1998] found a high density of NW-trending fractures on the eastern Otero Mesa, where the Victorio Peak Limestone Formation overlies the Bone Spring Formation. These fractures extend from the Sacramento Mountains to Dell City, Texas and are referred to as the Otero Break.

A.1.6 Permian Basin Facies

The Delaware Mountain Group is made up of three formations: the Brushy Canyon Formation, Cherry Canyon Formation, and Bell Canyon Formation. The Brushy Canyon Formation is a sandstone with local conglomerates at the bottom [King, 1948]. The Cherry Canyon consists of thin-bedded fine-grained sandstone and siltstone [Mack and Giles, 2004]. The Bell Canyon Formation consists of dark to light gray marine limestone fingers that extend from the Capitan Reef into the center of the Salt Basin [Newell, 1972]. The formations are exposed in the Delaware Mountains and range from 600 to 4,000 feet thick [Newell, 1972].

The Bone Spring Limestone is one of the major aquifers in the Salt Basin. It is made up of black cherty limestone with thin interbedded black or brown layers of siliceous shale [Ashworth, 1995]. The unit outcrops in the Delaware Mountains, Guadalupe Mountains, Baylor Mountains, and the Sierra Diablo Mountains [King, 1948]. The Bone Spring grades northwest into the lower portion of the Victorio Peak Limestone [Hayes, 1964]. Thickness of the formation varies from 1,050 to a few hundred feet throughout the Salt Basin [King, 1948].

A.1.7 Later Paleozoic Units

Mississippian through Pennsylvanian rock units are made up of a variety of carbonate rocks that were deposited when seas transgressed onto North America [King and Harder, 1985]. Mississippian through Pennsylvanian rocks are exposed in the Sacramento and Hueco Mountains, and in the Sierra Diablo region [King et al., 1945, Kottlowski, 1963, Pray, 1961]. Mississippian strata are made up of

massive limestone, which grade quickly into the black shales of the Delaware Basin [Kottlowski, 1969, Meyer, 1966]. Mississippian units are thicker to the south due to more deposition and thinner to the north due to more erosion from the Pedernal uplift, [Kottlowski, 1963]. Pennsylvanian carbonates are commonly interbedded with shale and are found in the Salt Basin on top of the Pedernal uplift which formed during the Ancestral Rocky Mountain deformation [Meyer, 1966]. The uplift caused most of the Mississippian through Pennsylvanian units to erode [King and Harder, 1985, Meyer, 1966].

A.1.8 Early Paleozoic Units

During the Early Paleozoic, seas extended over the Salt Basin. This deposited the Cambrian-Ordovician Bliss Sandstone, Ordovician carbonates of the El Paso and Montoya Groups [Kottlowski, 1969], and Silurian carbonates of the Fusselman Formation [King and Harder, 1985]. These units all crop out in the Sacramento Mountains, the Hueco Mountains, and the Sierra Diablo region [King et al., 1945, Kottlowski, 1963, Pray, 1961]. The Bliss Sandstone is predominantly a quartz sandstone, partly glauconitic, with thin interbeds and lenses of siliceous hematite, arenaceous shale, and arenaceous limestone [Kottlowski, 1963]. The El Paso Group is made up of dolomite, limestone, and dolomitic limestone [King et al., 1945, Pray, 1961]. The Montoya Group was deposited as a limestone, but has since been mostly dolomitized [Kottlowski, 1963]. The Fusselman Formation is an aphanitic to coarsely crystalline, massive dolomite [Kottlowski, 1963].

A.1.9 Precambrian Units

The Precambrian units in the Salt Basin have very few surface exposures. Some of these exposures are on the Diablo Plateau, southern Sierra Diablo region, and the Sacramento Mountains escarpment [Denison et al., 1969, Masson, 1956, Pray, 1961]. The Precambrian surface exposure rocks have been described as metamorphosed sedimentary rocks intruded by igneous sills [Pray, 1961], red micrographic perthite granite [Denison et al., 1969], rhyolite porphyry with some micrographic granite porphyry [Masson, 1956]. Oil-and-gas exploratory well cores are the primary means of determining the distribution and type of Precambrian units in the Salt Basin. The wells found that the Chaves Granite and Granitic Gneiss, Carrizo Mountain Group metamorphic rocks, DeBaca-Swisher metasedimentary and basaltic rocks, and the Franklin Mountains igneous rocks are present in the Salt Basin [Denison et al., 1987, Ritchie, 2011].

A.2 Structure

The structural features of the Salt Basin have been strongly controlled by tectonic activity [Shepard and Walper, 1982]. The primary aquifer units, which

are Permian in age, were deposited during the Delaware Basin subsidence. The Neogene alluvial and bolson deposits form another aquifer unit that lies within the Salt Basin graben, which formed during the Basin and Range extension.

Deformation in the Salt Basin can be split up into four major periods: Pennsylvania to Early Permian (Ancestral Rocky Mountain), Mid-to-Late Permian (subsidence of the Delaware Basin), Late Cretaceous (Paleogene compressional deformation during Laramide orogeny), and Cenozoic (Basin and Range extension). Structures developed during these periods are superimposed upon one another, causing major structural trends to be reactivated [George et al., 2005].

A.2.1 Pennsylvania to Early Permian

Pennsylvanian-to-Early Permian faulting and folding is associated with the collision of the southern margin of North America with South America-Africa during the Ouachita-Marathon orogeny [George et al., 2005]. This resulted in the uplift and subsidence in the foreland of the fold and thrust belt that formed the Pedernal landmass, Diablo Platform, and the faulted Sierra Diablo region [Dickerson et al., 1989, Goetz, 1977, King, 1948]. The Pedernal uplift is a dominant feature with faulted and folded Precambrian through Early Permian units that formed a subsurface high that runs down the middle of the Salt Basin. This uplift provided the material that would ultimately be shed into the Delaware Basin and caused preferential erosion of Paleozoic rocks overlying Precambrian basement [Black, 1973, Kottlowski, 1963]. Major features resulting from this orogeny include the Pedernal Uplift and various Ancestral Rocky Mountain faults.

A.2.2 Mid-to-Late Permian

During the Mid-to-Late Permian, differential uplift of the Pedernal landmass and the Diablo and Central Basin Platforms, and the subsidence of the Orogen, Delaware, and Midland Basins, continued into the Late Permian and developed more structures in the Salt Basin [Dickerson et al., 1989]. The Bone Spring Flexure, a southeastward-dipping monocline along the Guadalupe Mountains, was developed through the continued subsidence of the Delaware Basin [Hayes, 1964, King, 1948]. The Babb and Victorio flexures are major down-to-the-northeast faults that formed in Mid-to-late Pennsylvanian, then reactivated during the Mid-Permian [Muehlberger and Dickerson, 1989]. The Babb and Victorio flexures are monoclines that trend NW-SE with a bend on the eastern side of the fault to east-west for the Victorio flexure; the structures are northeastward dipping [King, 1948]. The Otero Fault has a NW-SE trend, is down to the northeast, and is exposed just south of Dell City [Goetz, 1985]. These faults formed during the Mid-Permian and the Babb and Victorio Flexure were displaced 1,000 feet and 1,700 feet respectively [King et al., 1945]. The Victorio Flexure cuts through the Salt Basin

graben and intersects the Apache Mountains on the eastern side of the graben [Goetz, 1980]. The Victorio Flexure is considered the groundwater divide for the Salt Basin. Other Permian features that were developed include the Bitterwell Break, an E-W trending subsurface fault crossing the Salt Basin graben just east of the Sierra Diablo Mountains, Piñon Cross Folds, and the “AV” lineament.

A.2.3 Late Cretaceous

Late Cretaceous deformation was during the Laramide orogeny, which produced northwest trending thrust faults, northwest to westerly trending folds, and monoclinal warping in the Otero Mesa region [Black, 1973, Broadhead, 2002]. East-to-northeast compression caused crustal shortening and north-to-northwest trending features, such as the Otero Mesa folds, Fleming folds, Cornucopia folds, and the Chert Plateau folds [Kelley et al., 2020].

A.2.4 Cenozoic

Cenozoic Basin-and-Range extension produced the current physiographic form of the region; the deformation overprinted all earlier structures, but pre-existing structures were highly influential [Shepard and Walper, 1982]. The features formed during this period were because of two tectonic events. One, the Otero Mesa/Diablo Plateau was translated northward and rotated counterclockwise between the Rio Grande rift zone and the Salt Basin Fault system. Two, the Basin and Range extension created a strong east-west component.

In regards to groundwater flow, one of the most important features created is the Otero Break, which is defined as a series of down-to-the-southwest normal faults and fractures reaching from the Sacramento Mountains to Dell City, Texas [Mayer and Sharp Jr, 1995].

The Basin and Range extension created normal faults and uplifted the Sacramento, Hueco, Sierra Diablo, Brokeoff, Guadalupe, Delaware, and Apache Mountains [Black, 1973, Kelley, 1971, King, 1948, Pray, 1961]. The Basin and Range extension also created the following structural features: Otero Mesa Folds, Sacramento Canyon Fault, Guadalupe and Dog Canyon Fault Zones, Border Fault Zone, North Sierra Diablo Fault Zone, East Sierra Diablo and East Flat Top Mountains Faults, Delaware Mountains Fault Zone, and several unnamed Salt Basin graben faults [Kelley et al., 2020, Ritchie, 2011].

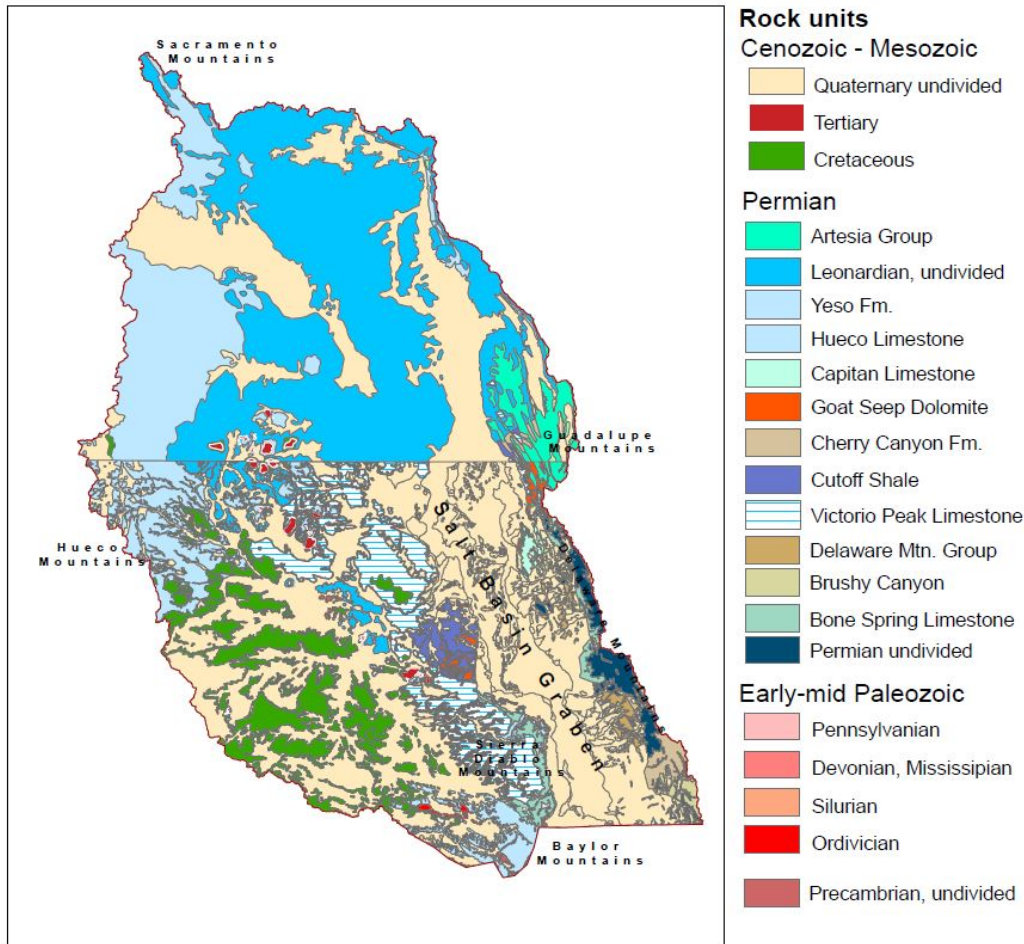


Figure A.1: Generalized surface geology map of the Salt Basin study area. Modified from [Kelley et al., 2020].

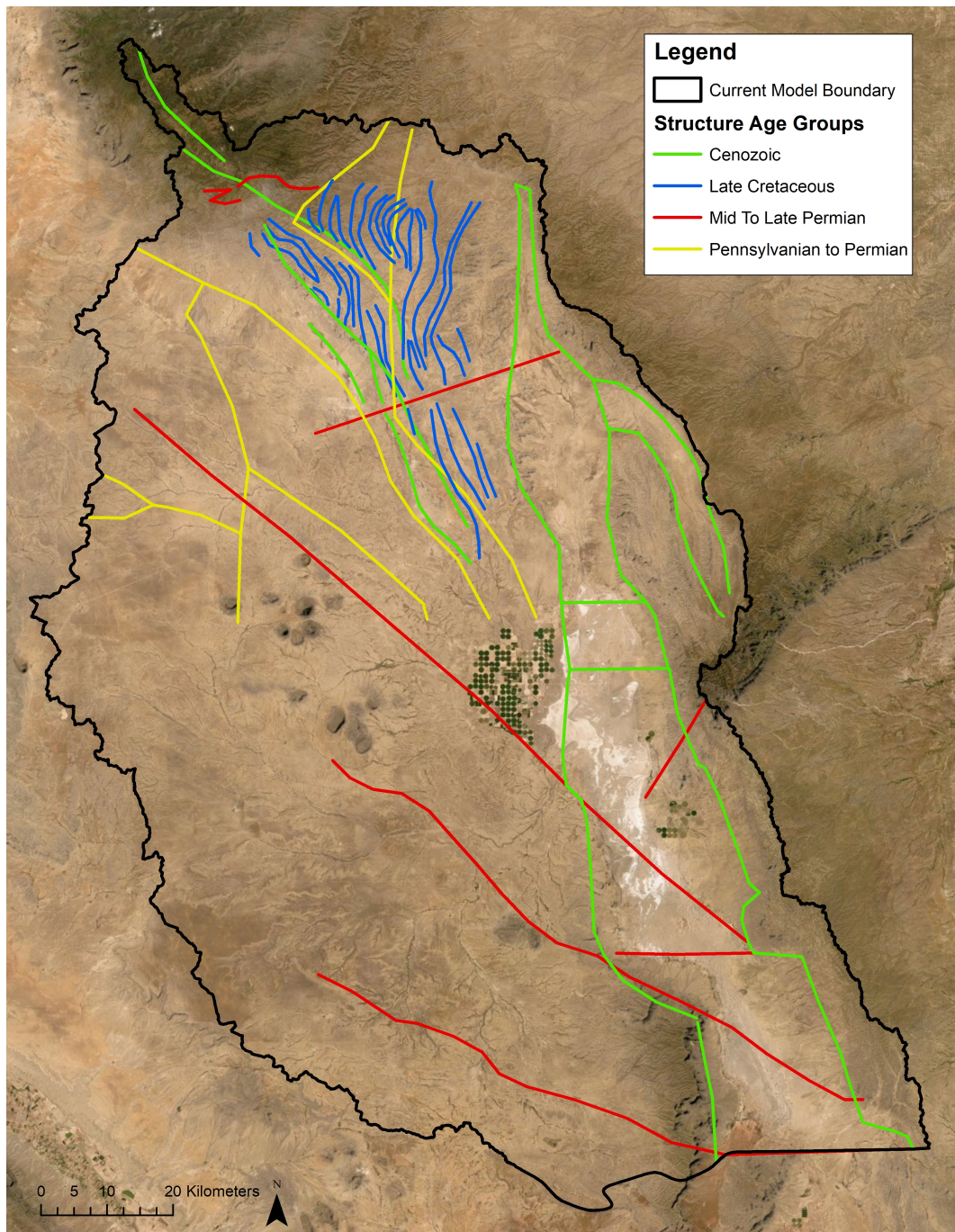


Figure A.2: General structures within the Salt Basin. Structures grouped by age, Cenozoic (green), Late Cretaceous (blue), Mid-to Late Permian (red), and Pennsylvanian to Permian (yellow). Pennsylvanian to Permian structures extend into Texas, but we did not gather data for Texas. (Modified from Ritchie [2011]).

APPENDIX B

PAST GROUNDWATER MODELS OF THE SALT BASIN

The Salt Basin has been extensively studied, including five prior groundwater flow models. This section summarizes the characteristics and findings of prior groundwater modeling studies within the Salt Basin. The purpose of these studies was to better quantify recharge rates and the effects of pumping on the quantity and distribution of groundwater. Below we summarize and discuss five prior modeling studies that have been undertaken by various researcher groups in New Mexico and Texas. The models vary widely in their level of complexity, hydrostratigraphic framework, and calibration data used.

Mayer and Sharp Jr [1995] developed a steady-state transmissivity-based model that included a highly permeable north-northwest oriented fracture zone from the Sacramento Mountains to Dell City, TX to assess hydraulic conductivity patterns and their effects on groundwater flow patterns. John Shomaker & Associates, Inc. developed several groundwater flow models of the Salt Basin that were described in two reports. One of the main objectives of these models was to assess the impacts of pumping on interstate transfers of groundwater. Finch [2002] developed a multi-layer transient and a steady-state model of the Salt Basin that focused on different pumping scenarios and their effects on groundwater flow from NM to TX using MODFLOW. Shomaker [2002] extended the Finch [2002] model, adding additional well fields in NM and evaluating the effects. Hutchison [2008] created a model to determine how much groundwater in the Salt Basin can be pumped sustainably. Shomaker [2010] revised the Shomaker [2002] with new model parameters from a large collaborative study of the Salt Basin. Finally, Ritchie [2011] developed a steady-state MODFLOW model of the Salt Basin to estimate groundwater recharge rates within this system. The footprints of each of these models' outlines are shown in Figure B.1. Below, we discuss the characteristics and findings of each of these models. We have attempted to compare and contrast various model parameters, including hydraulic conductivity and recharge rates.

B.1 Mayer and Sharp (1995) - The Role of Fractures in Regional Groundwater Flow

Mayer and Sharp Jr [1995] analyzed the effects that regional fracture systems may have on large-scale groundwater flow patterns within the Salt Basin. The re-

search was partially funded by the Geological Society of America and the National Ground Water Association. Mayer and Sharp Jr [1995] considered a broad fracture zone (Otero Break; white pattern in Figure B.2) extending from the Sacramento Mountains to the salt flats near Dell City, TX that is thought to be a conduit of fresh water to the city. Scalapino [1950] was one of the first to investigate the possibility that the Sacramento Mountains are the source of fresh groundwater in Dell City, TX. Mayer and Sharp Jr [1995] compiled geologic data from Scalapino [1950], Muehlberger and Dickerson [1989], Pray [1961], Black [1973], and Goetz [1980, 1977] to support their model. Mayer and Sharp Jr [1995] also mapped the fracture zones using aerial photos and field measurements of the lineaments on the surface. The model was a steady-state, one-layer, two-dimensional finite-element groundwater-flow model that integrated fracture transmissivities. The edge of the model domain follows the surface water divide on the northern and western sides of the basin, including the Sacramento Mountains, Otero Mesa and the Diablo Plateau. The eastern and southern model boundaries follow the groundwater system boundary where groundwater flow is perpendicular to eastern boundary and parallel with the southern boundary. The northern, southern, and western boundaries of the model were defined as no-flow boundaries. The no-flow boundaries neglect several possible interbasin groundwater flow paths into the Salt Basin, such as flow from the Peñasco Basin to the north. Mayer and Sharp Jr [1995] thought this interbasin flow to be a negligible amount of flow. The northern portion of the eastern boundary is no-flow and the southern portion of the eastern boundary is constant head. The constant head corresponds to the water table near the salt flats on the east side of the basin.

Total recharge, including that derived from precipitation and irrigation return flow, was estimated to be about 88,366 to 100,527 acre-feet/year (1.1×10^8 to 1.2×10^8 m³/year). Total outflow, including irrigation pumping and evapotranspiration, was estimated to be 105,392 acre-feet/year (1.3×10^8 m³/year). Recharge and evapotranspiration were found to be "strongly elevation dependent" [Mayer and Sharp Jr, 1995] with increased recharge and decreased evapotranspiration with increased elevation. Recharge and discharge were held constant during the simulations. Transient change in storage due to pumping was neglected [Konikow and Neuzil, 2007]. To determine the transmissivity of the regional fracture systems, several steady-state simulations were run with different potential regional transmissivities. Simulations were run with homogeneous isotropic, heterogeneous isotropic, and heterogeneous anisotropic transmissivities. The heterogeneous models' zones with higher fracture densities were given higher transmissivity values. For the anisotropic model, higher values of transmissivity were chosen for the direction parallel to the fracture direction. The final transmissivity values were found by trial-and-error and comparing output to the measured potentiometric surface. Transmissivities ranged from 9.3 to 9,300 fr²/day (10^{-5} to 10^{-2} m²/s). The best fit models used transmissivity zones defined by fracture density and fracture orientation (Figure B.2). Mayer and Sharp Jr [1995] concluded that in the Otero Break region fractures correspond to a highly transmissive zone, with magnitudes of one to three orders higher transmissivity than the rest of the Salt Basin. Therefore, fractures are the primary factor controlling regional groundwater

flow patterns in the Salt Basin.

B.2 John Shomaker & Associates, Inc. (2002)

John Shomaker & Associates, Inc. in 2002 developed several hydrogeologic framework models for the Interstate Stream Commission to assess the effects that additional pumping at current well fields or new well fields would have on the water resources in the Salt Basin. There were two reports, one by Finch [2002] and one by Shomaker [2002]. Finch [2002] developed two four-layer models to assess the viability of pumping more water from deep wells that were already being pumped and to evaluate the effects. One of the models was steady-state and the other was transient. A sensitivity analysis was run on the transient model to find the effects of extra pumping in different locations in the Salt Basin.

B.2.1 Finch (2002) - Hydrogeologic framework of the Salt Basin and development of three-dimensional ground-water flow model

The first model was a steady-state, four-layer finite difference model (MODFLOW). This was created to determine the amount of subsurface water that flows across the New Mexico state line (i.e. underflow) from NM to TX within the Salt Basin with pre-development conditions. Three-dimensional spatial dimensions were considered. The governing equations were solved using the finite difference method. The model includes the Salt Basin watershed and a portion of the Peñasco Basin. Most of the model boundary was assigned a specified flux to simulate recharge and groundwater inflow. This is unusual as recharge is generally imposed at the land surface across the interior of model domains. Evapotranspiration in the salt flats was used to represent outflow from the Basin. The Finch [2002] model domain and boundary conditions are summarized in Figure B.3.

The model was calibrated using pre-development head data that varied recharge and discharge rates as well as hydraulic conductivity. Best fit recharge and discharge rates were found to be 54,943 acre-feet/year ($6.8 \times 10^7 \text{ m}^3/\text{year}$). Adjustments were made to the hydraulic conductivity, recharge, and evapotranspiration across the playas to fit the hydraulic budget and estimated groundwater contours. The layer thicknesses varied gradually in the model and did not follow lithologic contacts as presented by Ritchie [2011] below. The total saturated thickness was approximately 2,500 ft (762 m). Layer 1 of the model represented the water table aquifer and was about 100 ft (30 m) thick. Layer 2 was 500 – 900 ft (152 – 274 m) thick, Layer 3 was 300 – 600 ft (91 – 183 m) thick, and Layer 4 was 100 – 1,400 ft (30 – 427 m) thick. Thicknesses of Layers 2, 3, and 4 were used to enforce permeability with depth inferred from well data. Hydraulic conductivity decreases with depth within each layer, ranging from 0.05 to 10 ft/day (0.02 – 3 m/day), except for the Otero Break, which was assigned a hydraulic conductivity

of 100 ft/day (30 m/day). The model includes valley fill and Permian-age San Andres and Bone Spring-Victorio Peak limestone aquifers. Groundwater flow from NM into TX was calculated to be about 34,501 acre-ft/year (4.3×10^7 m³/year) in predevelopment (1945) conditions using this model.

The second model is a transient four-layer finite difference model. The goal of this model was to calculate the amount of drawdown from 1945-2000 and to find the changes in the amount of subsurface water that flows across the state line (i.e. underflow) from NM to TX within the Salt Basin from 1945-2000. The steady-state model parameters were also used in the transient model. Additional pumping was considered. Recharge and discharge were increased from the predevelopment steady-state model rates to 94,147 acre-feet/year (1.2×10^8 m³/year). The storage coefficients used in these transient simulations varied between 0.05 and 0.15 for unconfined units and 3×10^6 per meter of saturated thickness for confined units [Lohman, 1972]. Based on this model, drawdown reached a maximum of about 100 ft (30 m) in 2000 (Figure B.4).

Groundwater flow from NM into TX was calculated by the steady-state model to be about 34,501 acre-ft/year (4.3×10^7 m³/year) in 1945. The transient model, which included additional pumping, predicted an increase of groundwater flow across the NM-TX state line by 9,000 acre-feet/year (1.11×10^7 m³/year) (Figure B.5).

A sensitivity analysis was conducted using the transient model parameters to determine how different amounts of pumping at different locations changed the amount of underflow from NM to TX. Models were run using double the amount of pumping reported in the year 2000 for a 40-year period considering three scenarios: (1) increased pumping only on the NM side; (2) increased pumping only on the TX side; and (3) increased pumping on both sides of the NM-TX state lines. For scenario (1), the doubling of pumping on the NM side resulted in 20,320 acre-ft/year (2.5×10^7 m³/year) of additional water withdraws for 40 years while the pumping on the TX side was maintained at 49,730 acre-ft/year (6.1×10^7 m³/year). The model showed groundwater flow across the state line decreased by 8,000 acre-feet/year (1×10^7 m³/year) and 72 miles² (186 km²) of the top layer of the model (Layer 1) of the model went dry around Dell City, TX. For scenario (2), pumping was doubled on the TX side to 99,730 acre-feet/year (1.2×10^8 m³/year). Pumping in NM remained at 10,160 acre-feet/year (1.3×10^7 m³/year). This simulation predicted that the flow from NM to TX would increase by 4,500 acre-feet/year (5.6×10^6 m³/year). About 140 miles² (363 km²) of the top layer of the model (Layer 1) went dry around Dell City, TX. For scenario (3), where the pumping was doubled on both NM and TX, initial flow across state lines decreased by 3,000 acre-feet/year (3.7×10^6 m³/year), but by the end of the 40 years had increased back to the rate in 2000. The model simulation net-differences are illustrated in Figure B.6.

B.2.2 Shomaker (2002) - Hypothetical well fields in Salt Basin and pipeline to Pecos River

Shomaker [2002] used the same transient model as Finch [2002], but studied the effects that would occur by adding new well fields to the New Mexico portion of the Salt Basin. Three locations were considered as potential well fields; the Otero Break, Crow Flats, and Fourmile Draw (Figure B.7). Different amounts of water withdrawals per year were considered at each location, with pumping occurring only 6-months a year, and withdrawing an overall average amount of 7,085 acre-feet/year ($8.7 \times 10^6 \text{ m}^3/\text{year}$).

The first model considered the feasibility of the Otero Break well field. The Otero break well field would have wells in fractured San Andres Formation limestone. The proposed well field had 38 wells over 24 miles² (62 km²) of land that were about 1,200 ft (366 m) deep that were pumped at a rate of 1,000 gpm ($1.9 \times 10^6 \text{ m}^3/\text{year}$). The computed cone of depression that formed after 21 years resulted in drawdowns up to 80–90 ft (24 to 27m) at the Otero Break site and reaching 100 ft (30 m) in Dell City (Figure B.8). The reduction in underflow to Texas was predicted to be 2,000 acre-feet/year ($2.5 \times 10^6 \text{ m}^3/\text{year}$) after 40 years of pumping and steadily increasing thereafter.

The second model considered pumping in the Crow Flats, which hosts a valley fill aquifer. The proposed well field was represented using 19 wells across 28 miles² (73 km²). The wells were about 800 ft (243 m) deep and produced with a combined flow rate of 2,000 gpm ($4.1 \times 10^6 \text{ m}^3/\text{year}$). Results indicate that drawdown reached about 90 ft (27 m) at the Crow Flats site and about 100 ft (30 m) in Dell City (Figure B.9). The reduction in flow to Texas uniformly increased to 1,300 acre-feet/year ($1.6 \times 10^6 \text{ m}^3/\text{year}$) after 40 years of pumping and would most likely continue to rise thereafter.

The last scenario considers additional pumping in Fourmile Draw, which includes the valley fill and Bone Spring-Victorio Peak aquifers. The Fourmile Draw is close to Dell City, TX. This scenario included 47 additional wells distributed across 54 km² (21 miles²) of land that were about 1,000 ft (304 m) deep and producing 800 gpm ($1.6 \times 10^6 \text{ m}^3/\text{year}$). Results showed that the drawdown associated with this new well field would reach 90 ft (27 m) near Fourmile Draw site and 110 ft (34 m) near Dell City. The extra drawdown in Dell City is due to the fact that the Fourmile Draw site and Dell City are in close proximity. The reduction in flow to Texas would be a maximum of 7,100 acre-feet/year ($8.7 \times 10^6 \text{ m}^3/\text{year}$). The figures in the Shomaker [2002] report did not include a figure showing the drawdowns for this scenario.

The produced water from these proposed well fields could be piped eastward to help fulfill the Pecos Compact delivery shortfalls. Shomaker [2002] concluded that over the long term the pumping at any of the potential well fields will be at the expense of water flowing into Texas.

B.3 Hutchison (2008) - Preliminary Groundwater Flow Model, Dell City Area, Hudspeth and Culberson Counties, Texas

Hutchison [2008] was tasked by the El Paso Water Utilities to study the effects of groundwater withdrawals from the Dell City, Texas area and develop estimates of groundwater yields for a potential pumping operation to supply municipal water to El Paso, Texas. Three single-layer, two-dimensional steady-state finite-difference groundwater-flow models were created with MODFLOW-2000. Twelve hydrogeologic zones were included in these models. Hutchison [2008] considered varying degrees of lateral anisotropy (K_x and K_y) with the same orientations as Mayer and Sharp Jr [1995] but with a larger ratio of K_{max} to K_{min} (Figure B.10). The degree of lateral anisotropy was as high as 46:1 for some units. They also utilized environmental tracers (^{18}O and 2H) to infer the locations of recharge to calibrate their models. Hutchison [2008] presented three models he refers to as the "structural geology model", the "geochemistry model", and the "hybrid model". The structural model emphasized structural geology findings of Mayer and Sharp Jr [1995], which posits that water flows preferentially along the Otero Break. The geochemistry model emphasizes the findings of Eastoe and Hibbs [2005], which suggests that a significant amount of recharge for Dell City, TX is derived from the Diablo Plateau. The hybrid method utilizes combinations of the "structural geology model" and the "geochemistry model" parameters. Hydraulic conductivity in the models ranged from 0.00239 to 200 ft/day (0.00073 – 61 m/day) based on zone. Storativity varied from 0.0001 to 0.2.

The model domain mostly followed the Salt Basin watershed but excluded the northern and northwestern portions that covered the Sacramento Mountains. The southern boundary extended to the Babb Flexure and Bitterwell Break, which was assumed to be a groundwater divide. The model boundaries were no flow except for the northwestern, western, and southeastern edges of the model domain. The northwestern border was assigned a specified flux boundary to represent recharge from the Sacramento Mountains. The western boundary was an outflow boundary simulated by a drain package. The southeastern portion, the Bitterwell Break, was a constant head boundary. An initial steady-state model was used to find the initial conditions for the transient simulation. The model ran from 1948 to 2002. The total recharge and boundary inflow from the northern border along the Sacramento Mountains for pre-development conditions ranged from 79,000 to 104,000 acre-feet/year (9.7×10^6 to 1.3×10^8 m³/year) depending on the model. The total recharge and boundary inflow from the northern border along the Sacramento Mountains for years 1948 to 2002 ranged from 87,000 to 114,000 acre-feet/year (1.1×10^8 to 1.4×10^8 m³/year). Elevation dependent recharge was imposed using the Maxey-Eakin approach. Pumping was estimated to average about 80,000 acre-feet/year (9×10^7 m³/year) and total outflow by evapotranspiration and pumping was estimated to be between 79,000 to 120,000 acre-feet/year (9.7×10^7 to 1.5×10^8 m³/year). The discharge in the salt flats was simulated using the evapotranspiration package.

The models were calibrated by comparing computed and observed water

levels in Texas and New Mexico. With the additional pumping, the cone of depression around Dell City increased. Hutchison [2008] concluded that the groundwater yield of Dell City, TX area ranges from 54,000 to 95,000 acre-feet/year (6.7×10^7 to 1.2×10^8 m³/year).

Drawdown was calculated by running the model with and without pumping for 50 years and comparing the simulated heads to find the differences. Maximum drawdown ranged from 40 to 50 ft (12 to 15m). Figures B.10 – B.12 show how each of the model types affected drawdown. In all three of the models, the cone of depression extends far into New Mexico to the base of the Sacramento Mountains. These authors conclude that pumping in Dell City, TX affects New Mexico's water levels.

B.4 John Shomaker & Associates, Inc (2010) – Revised Hydrogeologic Framework and Groundwater-Flow Model of the Salt Basin Aquifer in South-eastern New Mexico and Part of Texas

John Shomaker & Associates, Inc. in 2010 was contracted by the New Mexico Interstate Stream Commission to revise the Shomaker [2002] model. The purpose of the model is to obtain more information about the groundwater availability in the New Mexico portion of the Salt Basin. This information will ultimately be used to determine the effects of long-term groundwater mining and the groundwater protection measures that may be required. This was a collaborative study with the U.S. Geological Survey estimating stormwater runoff [Tillery, 2011], New Mexico Institute of Mining and Technology investigating water quality and creating a structural geologic history and framework [Ritchie, 2011], Daniel B. Stephens & Associates Inc. estimating groundwater evaporation and recharge [Stephens, 2010a,b], and INTERA determining water use from satellite imagery [INTERA, 2010].

Shomaker [2010] created two four-layer finite difference models. The first was a steady-state pre-development model and the other was a transient model that included historical pumping. Shomaker [2010] used model boundary conditions that were similar to those reported in the Shomaker [2002] model, but increased the discretization by cutting the grid cell size in half compared to Shomaker [2002] (Figure B.13). The cell size in the new model is one-half mile by one-half mile (about 0.8 by 0.8 km). The top of layer one was the land surface and layer one was the only layer with variable thickness. Layer two is 300 ft thick, layer 3 is 500 ft thick, and layer four is 4,000 ft thick. The range of hydraulic conductivities used is 0.01 to over 100 ft/day (0.003 to 30 m/day). The new model uses a larger range of hydraulic conductivities than Shomaker [2002], which used a range of 0.05 to 100 ft/day (0.02 to 30 m/day).

The new model considered three major flow paths and identified karst aquifers and sinkholes. The first major flow path flows southeast from the Otero Break to Dell City, TX and the second flows from Piñon Creek-Crow Flats area to

Dell City, TX, and the third flows from the Diablo Plateau to the Dell City area and the salt flats. The karst aquifers and sinkholes were mapped and modeled as being good at capturing recharge and transmitting groundwater. Figure B.14 shows the two major flow paths in the northern Salt Basin and the mapped sinkholes.

The steady-state model used pre-development conditions assuming a recharge of 61,723 acre-feet/year ($7.6 \times 10^7 \text{ m}^3/\text{year}$), with 5,451 acre-feet/year ($6.7 \times 10^6 \text{ m}^3/\text{year}$) of that recharge coming from the Peñasco Basin, which was modeled with injection wells at the northern boundary of the model. The amount of recharge coming from the Peñasco Basin was calculated using Darcy's Law. The rest of the recharge is applied as areal recharge but was used to simulate areal and focused recharge (Figure B.15). The new model uses a discharge rate of 61,719 acre-feet/year ($7.6 \times 10^7 \text{ m}^3/\text{year}$), which is applied as evapotranspiration in the playas. The steady-state model was calibrated to steady-state target heads. The new model uses a higher recharge and discharge rate than Shomaker [2002] that used a recharge and discharge rate of 54,943 acre-feet/year ($6.7 \times 10^7 \text{ m}^3/\text{year}$). The new model also uses areal recharge over areas in the model instead of the injection wells along the boundary used by Shomaker [2002].

The transient finite difference model used historical pumping and included four-layers. This model used the same boundary conditions as the steady-state model. The model was run from 1948 to 2009 and used variable recharge that ranged from 35,000 to 90,000 acre-feet/year (4.3×10^7 to $1.1 \times 10^8 \text{ m}^3/\text{year}$), averaging 61,723 acre-feet/year ($7.6 \times 10^7 \text{ m}^3/\text{year}$). These recharge values were very close to those of Stephens [2010a]; 37,000 to 82,000 acre-feet/year or 4.6×10^7 to $1.0 \times 10^8 \text{ m}^3/\text{year}$ and therefore supports Shomaker [2010]'s model values. Flow from the Peñasco Basin accounted for 3,194 to 5,451 acre-feet/year (3.9×10^6 to $6.7 \times 10^6 \text{ m}^3/\text{year}$) of the recharge. The imposed rates of areal recharge and inflow across the model boundaries (using injection wells) is less than the discharge in the model. In order to balance the higher discharge, water is taken from storage. Total inflow into the model included storage ranges from 77,782 to 142,118 acre-feet/year (9.6×10^7 to $1.8 \times 10^8 \text{ m}^3/\text{year}$). Discharge varies in amount and type through time. Evapotranspiration and pumping is modeled until 1980, when evapotranspiration is decreased to zero because the elevation of the water table drops to the point where evapotranspiration is negligible. Pumping is then used as the only discharge in the model. Total discharge, which includes evapotranspiration and pumping, ranges between 77,784 to 142,112 acre-feet/year (9.6×10^7 to $1.8 \times 10^8 \text{ m}^3/\text{year}$) and averages 109,872 acre-feet/year ($1.4 \times 10^8 \text{ m}^3/\text{year}$). Model simulated pumping averages 89,257 acre-feet/year ($1.1 \times 10^8 \text{ m}^3/\text{year}$) and ranges from 50,287 to 113,613 acre-feet/year (6.2×10^7 to $1.4 \times 10^8 \text{ m}^3/\text{year}$). The new model increases discharge compared to Shomaker [2002], which used an average total discharge of 94,147 acre-feet/year ($1.2 \times 10^8 \text{ m}^3/\text{year}$). Drawdown was calculated at the end of the historical transient model, which was the end of September 2009. The modeled drawdown was up to 90 feet in Dell City, TX (Figure B.16). This estimate is less than the drawdown calculated using the Shomaker [2002] model

for the year 2000, which reached 100 ft in Dell City, TX (Figure B.5).

Along with the modeled drawdown, Shomaker [2010] found, using the calibrated storage coefficients determined from the model analysis, that the upper 1,000 feet of aquifer is estimated to currently hold 37.9 million acre-feet of water.

B.5 Ritchie (2011) - Hydrogeologic Framework and Development of a Three-dimensional Finite Difference Groundwater-Flow Model of the Salt Basin, New Mexico and Texas

Ritchie [2011] and Sigstedt [2010] developed the most three-dimensionally detailed model of the Salt Basin groundwater flow system. This study focused on quantifying recharge rates considering pre-development conditions. Ritchie [2011] used computed and observed hydraulic head contour maps to calibrate his model. In addition, ^{14}C age dates on a series of wells along the flow path were used to quantify groundwater flow rates and recharge [Sigstedt, 2010]. Ritchie [2011] created a hydrogeologic framework model by compiling geologic information from structural features, oil-and-gas exploratory wells, and geologic maps. The hydrogeologic framework model contained information on the horizontal and vertical extent of 16 geologic units grouped by similar lithology and depositional facies. The hydrogeologic framework model was then used to construct a 3-D finite difference groundwater flow model using MODFLOW-2000 [Harbaugh et al., 2000].

The model boundaries follow the surface water divides except for the southern and northwestern portions (Figure B.17). In the south, the boundary follows the groundwater divide of the Bitterwell Break. In the northwest, the domain reaches into the Peñasco Basin to allow for the interbasin flow. The entire boundary is a no-flow boundary. The model included elevation-dependent recharge. Groundwater outflow due to evapotranspiration near the salt flats was represented by a series of wells. MODPATH [Pollock, 1994] was used to calculate advective travel times from the uplands to wells where ^{14}C groundwater ages were collected as part of a model calibration exercise.

Two groundwater model scenarios were run considering different amounts and distributions of recharge. The first was a series of water balance scenarios, where recharge was assigned based on regions and the second considered elevation-dependent recharge. The water-balance-based recharge models had recharge ranging from 49,000 acre-feet/year ($5.84 \times 10^7 \text{ m}^3/\text{year}$) for the minimum scenario to 110,000 acre-feet/year ($1.28 \times 10^8 \text{ m}^3/\text{year}$) for the maximum scenario. These values are at the higher end of the range of values from previous Salt Basin studies. The distribution of the recharge was based on sub-basins delineated by Shomaker [2010] and net infiltration figures from Stephens [2010a]. The elevation-dependent recharge models had recharge ranging from 2,700 acre-feet/year ($3.32 \times 10^6 \text{ m}^3/\text{year}$) for the minimum scenario to 29,000 acre-feet/year ($3.61 \times 10^7 \text{ m}^3/\text{year}$) for the maximum scenario. Ritchie [2011] found that relatively

lower recharge rates are consistent with groundwater elevations and ^{14}C age dates. Both recharge distribution models were calibrated to steady-state groundwater levels by varying horizontal hydraulic conductivity. Calibrated hydraulic conductivities ranged from 3.28×10^{-8} feet/day (1×10^{-8} m/day) for a confining unit to 820 ft/day (250 m/day) in the zones associated with high fracture and fault densities. Discharge changed based on the model; the water-balance model ranged from 48,765 to 105,020 acre-feet/year (6.01×10^7 to 1.29×10^8 m 3 /year). The minimum recharge used the lowest discharge values. The elevation-dependent modeled discharge ranged from 2,688 to 29,414 acre-feet/year (3.31×10^6 to 3.63×10^7 m 3 /year).

The elevation-dependent and water-balance recharge distribution models produced good matches to observed groundwater levels and regional groundwater flow. But, MODPATH advective travel times from the elevation-dependent models with (1) average recharge and minimum porosity, (2) maximum recharge and minimum porosity, and (3) maximum recharge and average porosity statistically better fit the radiocarbon groundwater ages. The water-balance based models poorly fit the radiocarbon groundwater ages measured by Sigstedt [2010]. Therefore, Ritchie (2011) concluded that the elevation-dependent recharge distribution model represented the Salt Basin groundwater-flow system the best.

B.6 Past Model Summary

Mayer and Sharp Jr [1995] concluded that the Salt Basin has highly variable transmissivities due to fracturing in the basin. Mayer and Sharp Jr [1995] used transmissivities ranging from 9.3 to 9,300 fr 2 /day, assuming a constant thickness. This range is on the smaller end when compared to Hutchison [2008] and Ritchie [2011]. The thickness of this model was not stated, but the range of transmissivities compared to the ranges of hydraulic conductivities used in other models, is on the low end. The main fracture zone in their model is the Otero Break that directs flow towards the Dell City, TX area with recharge from the Sacramento Mountains. These authors concluded that a distributed fracture zone trending north-northwest is the primary factor controlling regional groundwater flow patterns in the Salt Basin. Mayer and Sharp Jr [1995] used close to the highest recharge rates reported, with a range from 88,366 - 100,527 acre-feet/year. Mayer and Sharp Jr [1995] used one of the lowest discharge rates of 105,392 acre-feet/year.

Shomaker [2002] found that any additional pumping in New Mexico will ultimately decrease the amount of water flowing into Texas. Finch [2002] concluded that if the wells that are currently used are pumped at a higher rate, the drawdowns will also increase. Shomaker [2002] found that if there is additional pumping at new potential well fields, drawdown will increase at the new well field location and change the amount of water flowing from New Mexico into Texas. Shomaker [2002] used a recharge and discharge rate of 94,147 acre-feet/year for their transient model, which is similar to the recharge rates that Mayer and

Sharp Jr [1995] used. Shomaker [2002] used the smallest range and most moderate hydraulic conductivities with a range from 0.05 to 100 ft/day.

Hutchison [2008] used a slightly higher recharge rate than Mayer and Sharp Jr [1995] and Shomaker [2002] for current conditions with a range of 79,000 to 114,000 acre-feet/year. Hutchison [2008] used the second most diverse range of hydraulic conductivities, having a much lower minimum hydraulic conductivity than Mayer and Sharp Jr [1995] and Shomaker [2002] with a range of 0.00239 to 200 ft/day. Hutchison [2008] uses a moderate discharge rate at 79,000 to 120,000 acre-feet/year. Hutchison [2008] concluded that the groundwater yield of the Dell City, TX area ranges 54,000 to 95,000 acre-feet/year.

Shomaker [2010] revised the Shomaker [2002] model by updating the model with new data that had been collected in the Salt Basin. Shomaker [2010] used the highest discharge and recharge with their transient model ranging from 77,782 to 142,118 acre-feet/year for recharge and 77,784 to 142,112 acre-feet/year for discharge. The model had a hydraulic conductivity range from 0.05 to over 100 ft/day which is slightly larger than Shomaker [2002] but still less than Hutchison [2008] and Ritchie [2011].

Ritchie [2011] developed a conceptual model of the Salt Basin groundwater system that used an elevation-dependent recharge distribution and lower recharge rates relative to past studies that range from 2,700 (minimum scenario) to 29,000 acre-feet/year (maximum scenario). The low recharge rates were constrained by groundwater residence time data (^{14}C age dating). Ritchie [2011] uses the lowest discharge rates in his more successful elevation dependent model, which ranged from 2,688 (minimum scenario) to 29,414 acre-feet/year (maximum scenario). Ritchie [2011] used the largest range of hydraulic conductivities and also has the smallest minimum. Ritchie [2011]'s range of hydraulic conductivities is 3.28×10^{-8} - 820 ft/day.

Tables B.1 and B.2 summarize the results and objectives of past modeling studies of the Salt Basin.

Model	Purpose	General Results
Mayer and Sharp (1995)	Research the effects that regional fracture systems had on permeability using a groundwater flow model. Model results were compared to regional head patterns.	A southeast trending fracture system, the Otero Break, plays an important role in controlling regional groundwater flow patterns in the Salt Basin.
John Shomaker & Associates, Inc. (2002)	Assessed the effects that additional pumping (Finch, 2002) or new proposed NM well fields (Shomaker, 2002) would have on the water resources in the Salt Basin.	Pumping more water on the New Mexico or Texas side would affect the amount of groundwater flowing across the NM-TX state line. Long term pumping at any of the potential well fields will be at the expense of water flowing into Texas.
Hutchison (2008)	Assessed groundwater yields from proposed pumping operations to supply municipal water to El Paso, Texas.	The groundwater yield of Dell City, TX area ranges 6.7×10^7 to $1.2 \times 10^8 \text{ m}^3/\text{year}$ depending on what definition of "sustainability" is used.
John Shomaker & Associates, Inc. (2010)	Assessed groundwater availability in the New Mexico portion of the Salt Basin.	The upper 1,000 ft of aquifer is estimated to currently hold 37.9 million acre-feet of water. Drawdown in Dell City is modeled to reach 90 ft. Concluded that recharge, evapotranspiration, pumping, and hydraulic conductivity values used in this model were consistent with prior studies and observed data.
Ritchie (2011)	Develop the most detailed hydrostratigraphic framework model for the Salt Basin. Considered elevation dependent and zonal recharge scenarios. Used both groundwater residence times and head data to calibrate the model.	The elevation-dependent recharge scenario provided the best fit to head patterns and ^{14}C residence times.

Table B.1: General information about each Salt Basin model's purpose and results.

Model	Model Type	Hydraulic Conductivity Ranges	Discharge/Pumping Ranges	Recharge Ranges
Mayer and Sharp (1995)	1-layer, 2D FEM	Transmissivities with constant thickness 9.3 to 9,300 ft ² /day	105,392 acre-feet/year	88,366 - 100,527 acre-feet/year
John Shomaker & Associates, Inc. (2002)	4-layer, quasi-3D FDM	0.05 to 100 ft/day	Steady-State 54,943 acre-feet/year Transient 94,147 acre-feet/year (increased pumping from this in some areas to see effects)	Steady-State 54,943 acre-feet/year Transient 94,147 acre-feet/year
Hutchison (2008)	3 x 1-layer 2D FDM	0.000239 to 200 ft/day	Steady-State ~88,000 acre-feet/year Transient ~97,000 acre-feet/year	Steady-State ~88,000 acre-feet/year Transient 139,000 acre-feet/year
John Shomaker & Associates, Inc. (2010)	4-layer, 3D FDM	0.05 to over 100 ft/day	Steady-State: 61,723 acre-feet/year Transient: 77,782 to 142,118 acre-feet/year	Steady-State: 61,719 acre-feet/year Transient: 77,784 to 142,112 acre-feet/year water-balanced model: 49,000 acre-feet/year for the minimum recharge scenario to 110,000 acre-feet/year for maximum scenario
Ritchie (2011)	6-layer, 3D FDM	water-balanced model: 3.28×10^{-8} - 820 ft/day elevation dependent model: 3.28×10^{-8} - 82 ft/day 3.28×10^{-8} ft/day for a confining unit	elevation-dependent model: 2,688 acre-feet/year for the minimum recharge scenario to 29,414 acre-feet/year for maximum scenario	elevation-dependent model: 2,700 acre-feet/year for the minimum recharge scenario to 29,000 acre-feet/year for maximum scenario

Table B.2: Hydraulic conductivity, recharge and discharge data for each Salt Basin model. Abbreviations: FEM = Finite element model; FDM = finite difference model.

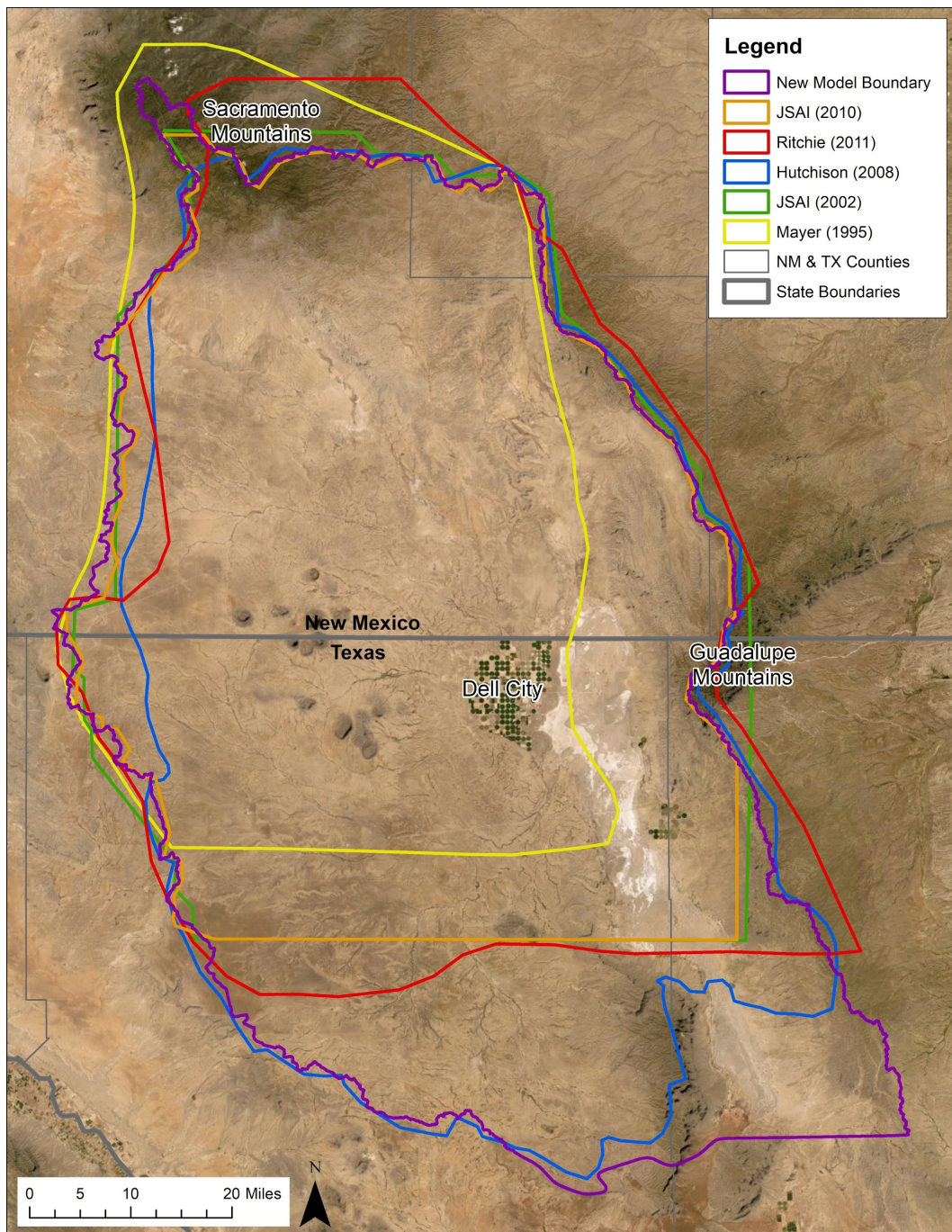


Figure B.1: Boundaries of the five models discussed in this report along with this studies model boundary. Boundaries made from geo-referencing report boundaries into GIS.

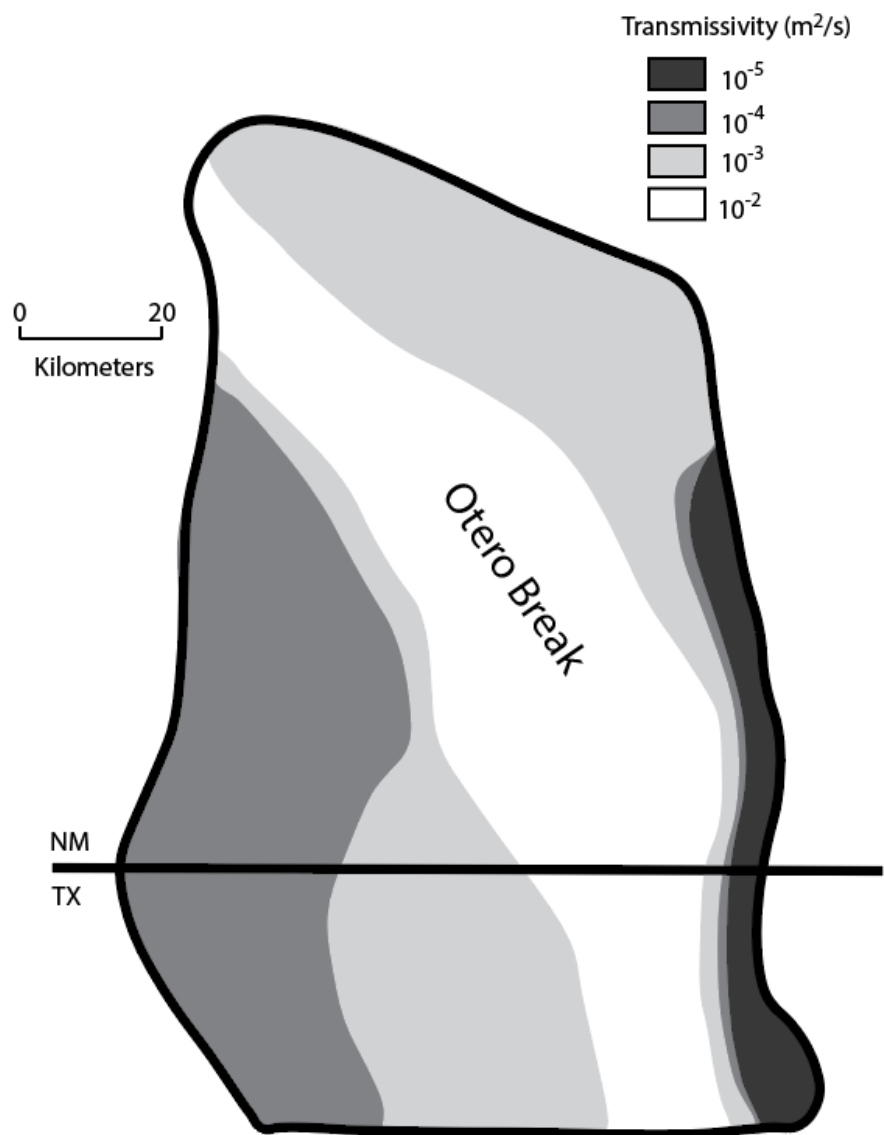


Figure B.2: Transmissivity zones used in the model that was found to be most accurate when compared to observed data. The highest transmissivity zone contains the Otero Break. Modified from [Mayer and Sharp Jr, 1995].

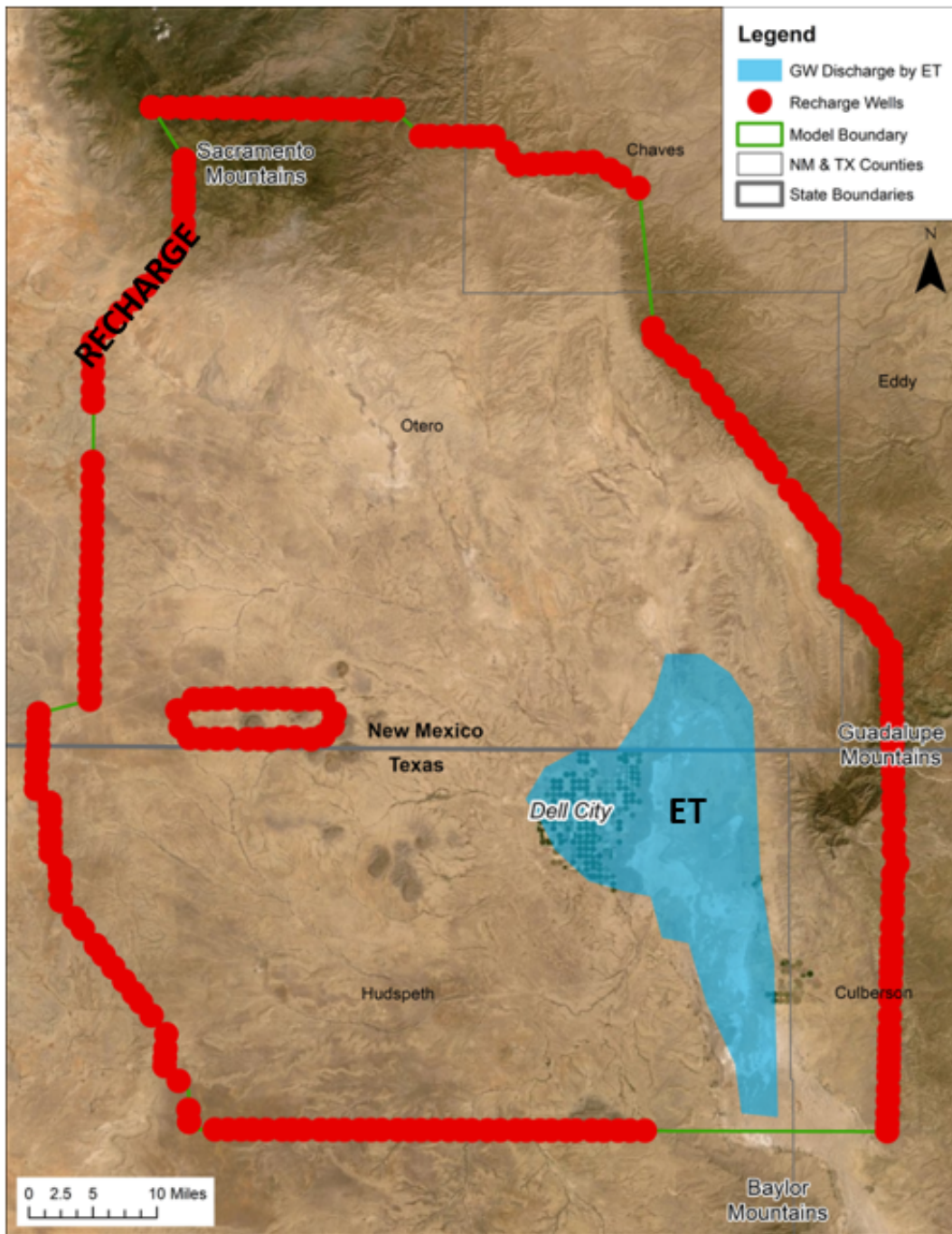


Figure B.3: Outline of model domain used by Finch [2002]. The red dots are recharge wells that simulate recharge and inflow from other basins. The blue cells represent groundwater discharge by evapotranspiration. Modified from [Finch, 2002]. The green lines denote a no-flux boundary condition.

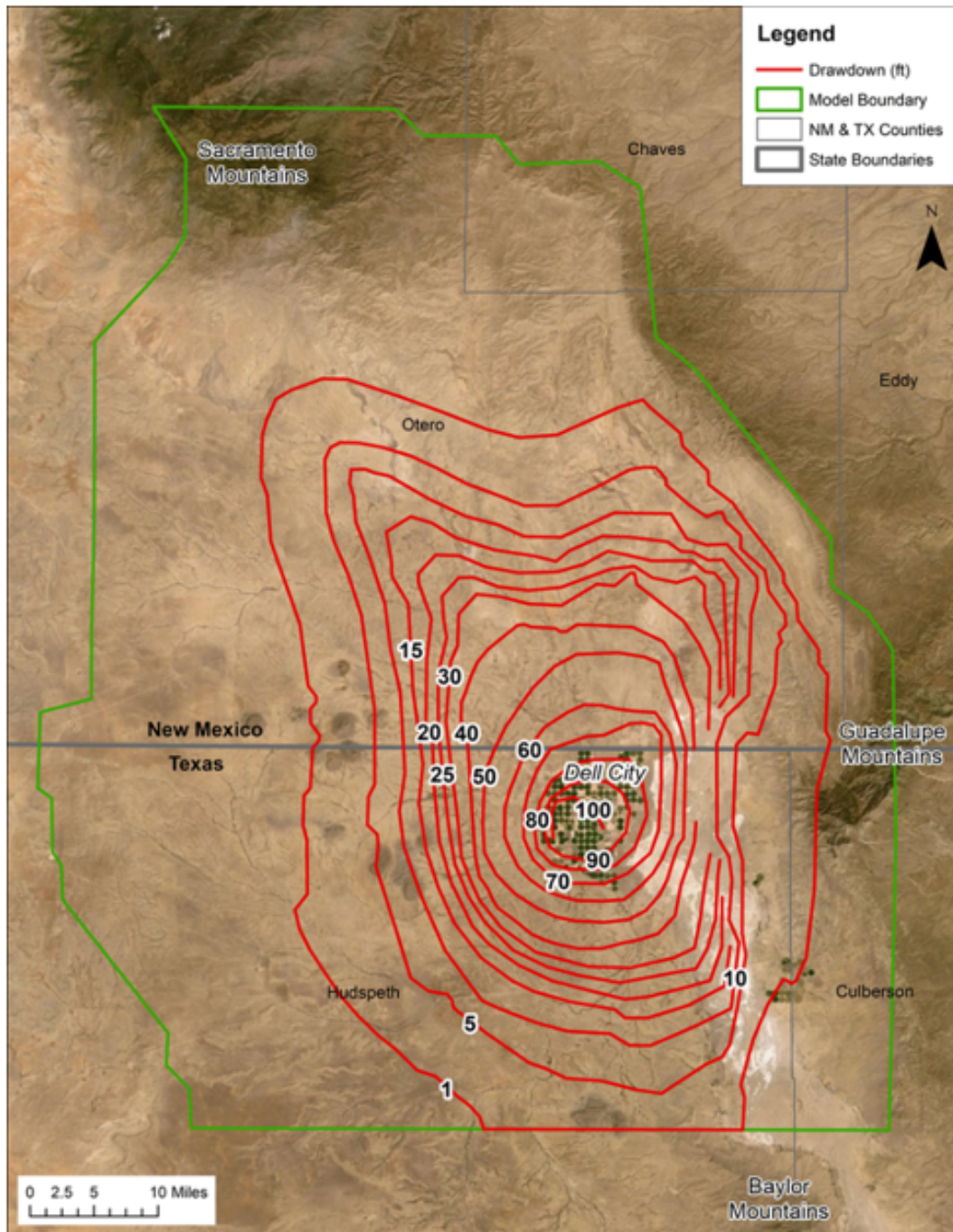


Figure B.4: Computed drawdown resulting from pumping from 1945 – 2000. Maximum drawdown is 100 ft. Contours intervals are 10 ft. Modified from [Finch, 2002].

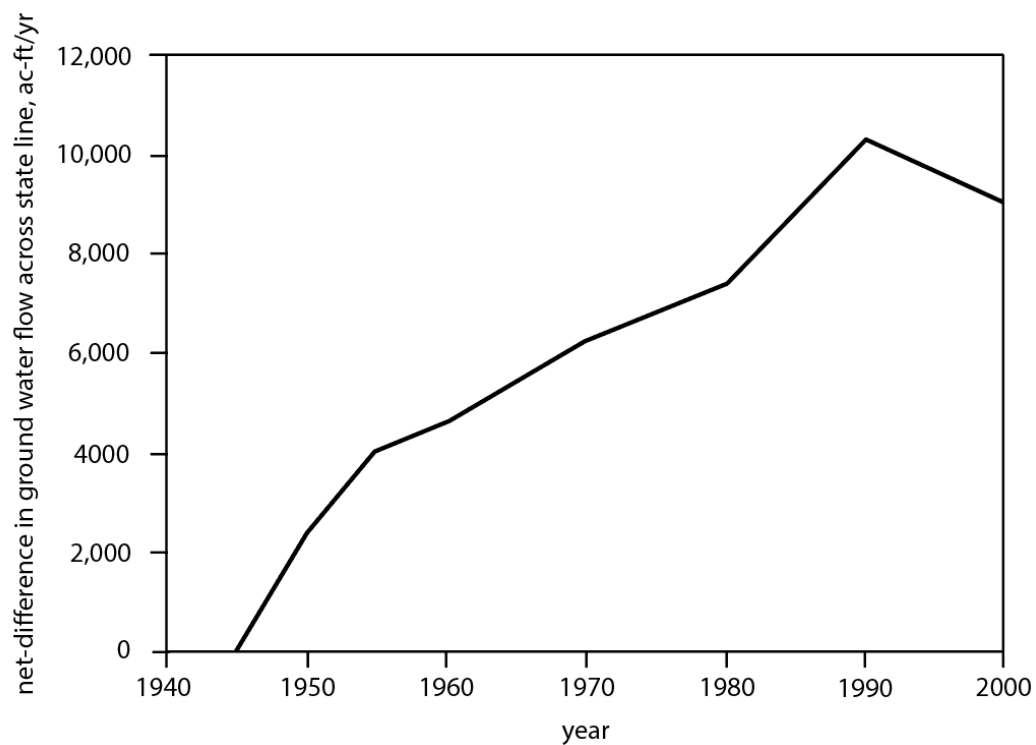


Figure B.5: Net-difference in ground-water flow from NM to TX from 1945 – 2000.
(Modified from Shomaker [2002]).

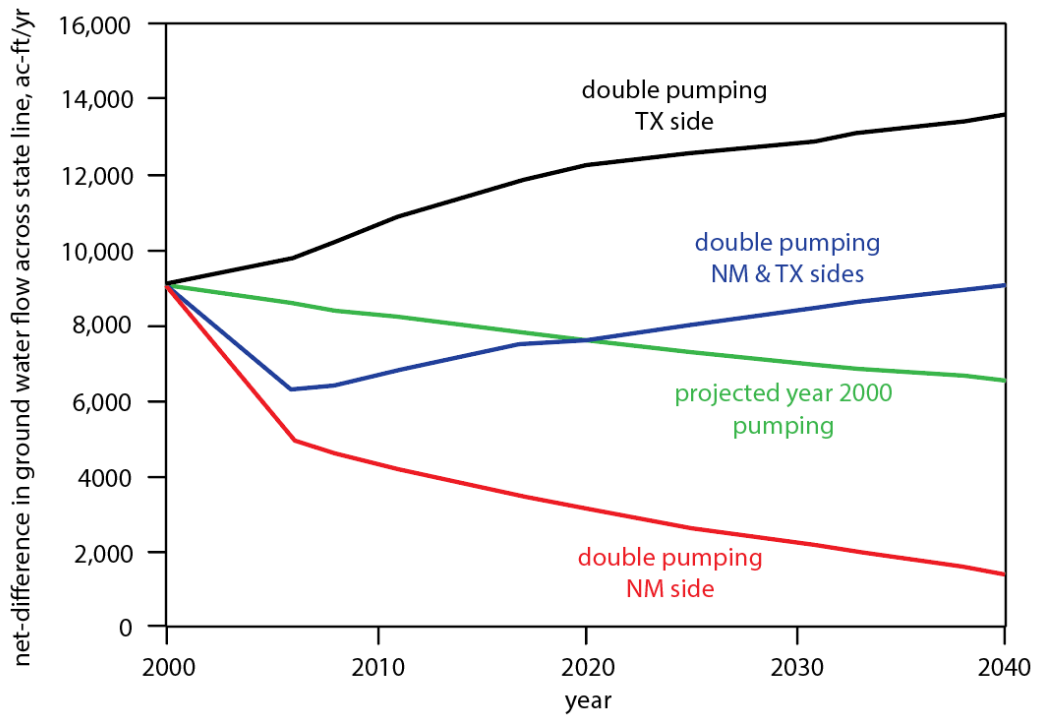


Figure B.6: Model simulated net-difference in groundwater flow from NM to TX as a result of different pumping scenarios. (Modified from Shomaker [2002]).

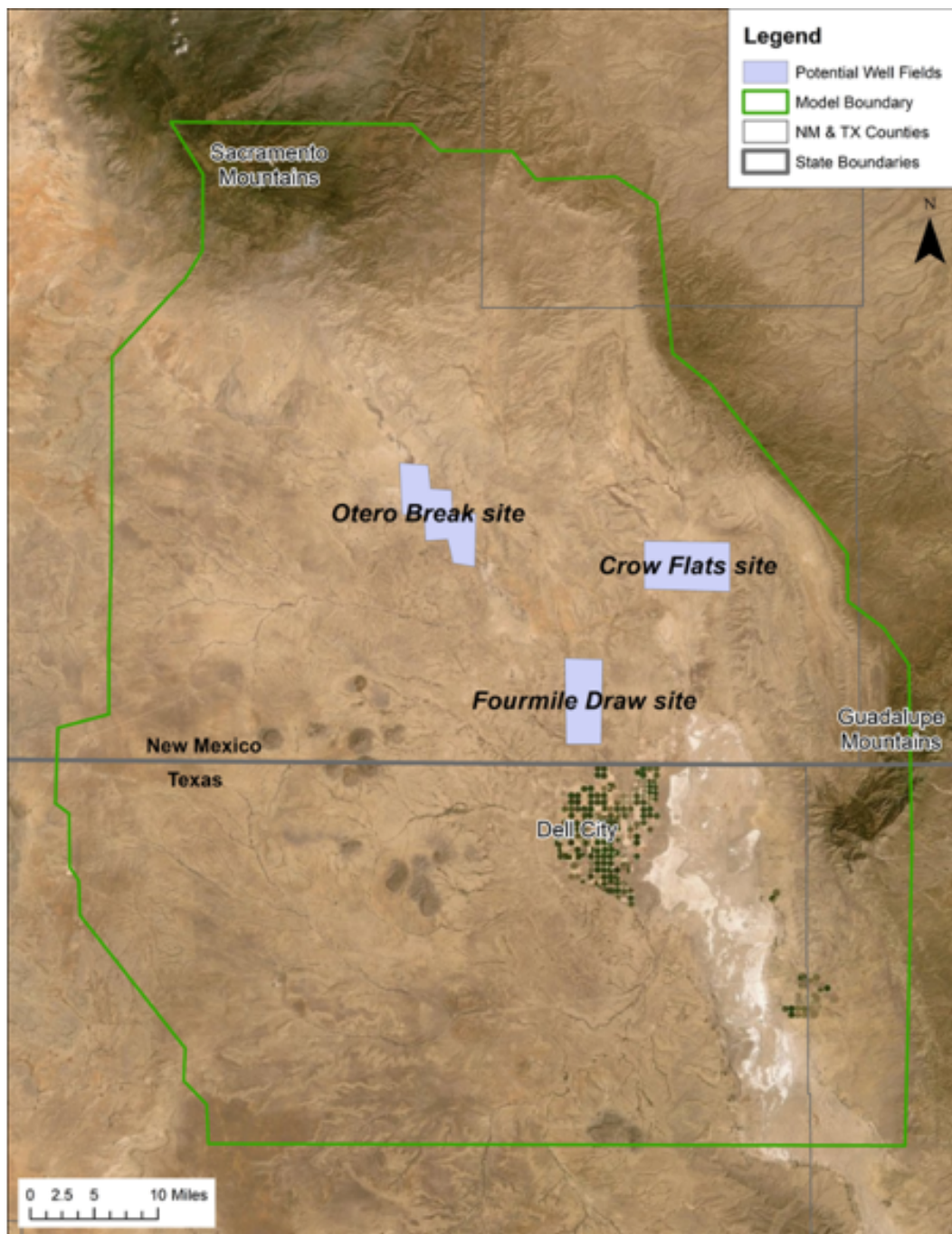


Figure B.7: Locations of the potential well fields represented in Shomaker (2002). The light purple indicates the well fields in the Otero Break, Crow Flats, and Fourmile Draw. Modified from [Shomaker, 2002].

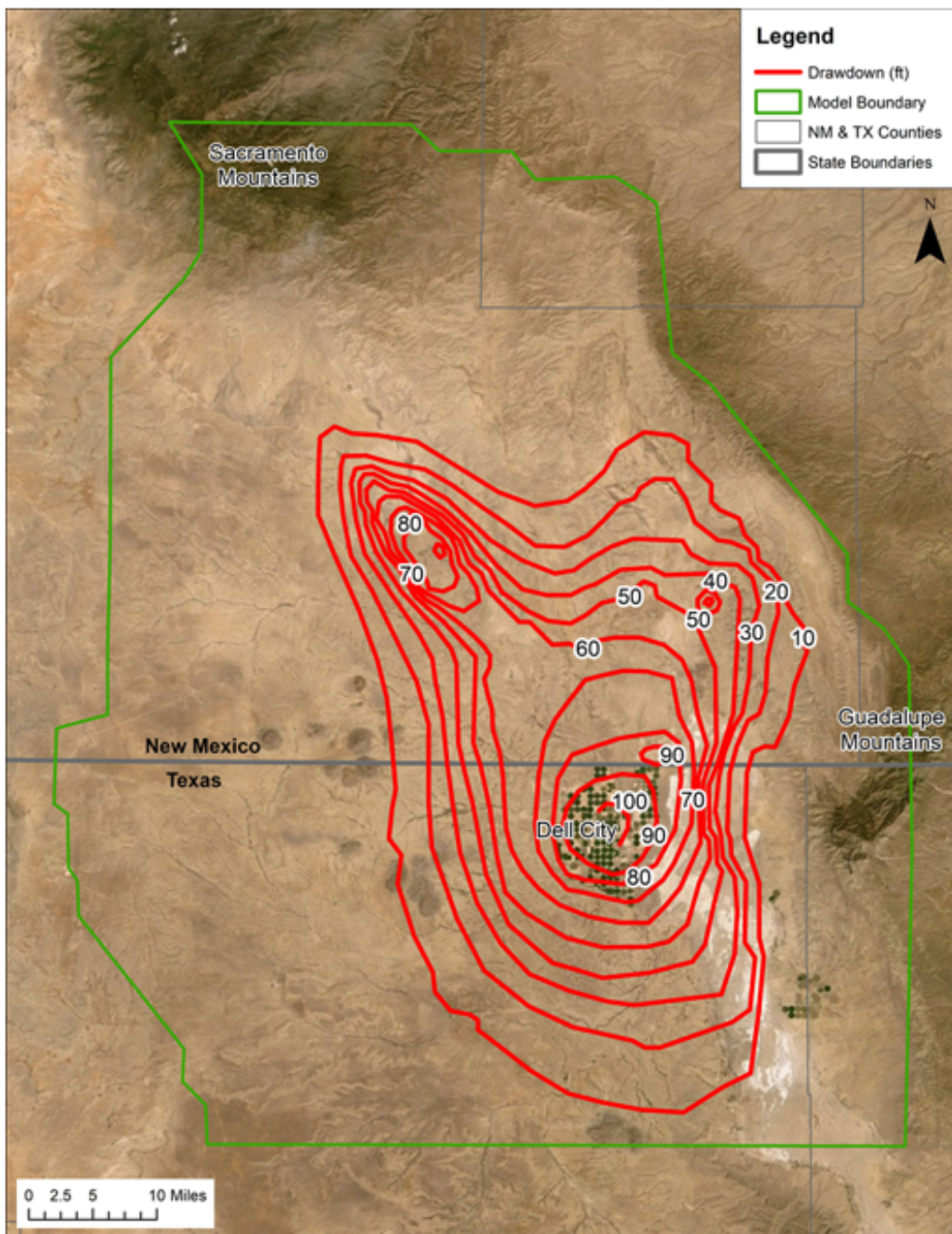


Figure B.8: Maximum simulated drawdown due to historical pumping with a hypothetical well field near Otero Break (scenario (1)). Drawdowns were calculated from pre-development conditions. Contour intervals of 10 ft. Maximum drawdown of about 100 ft. Modified from [Shomaker, 2002].

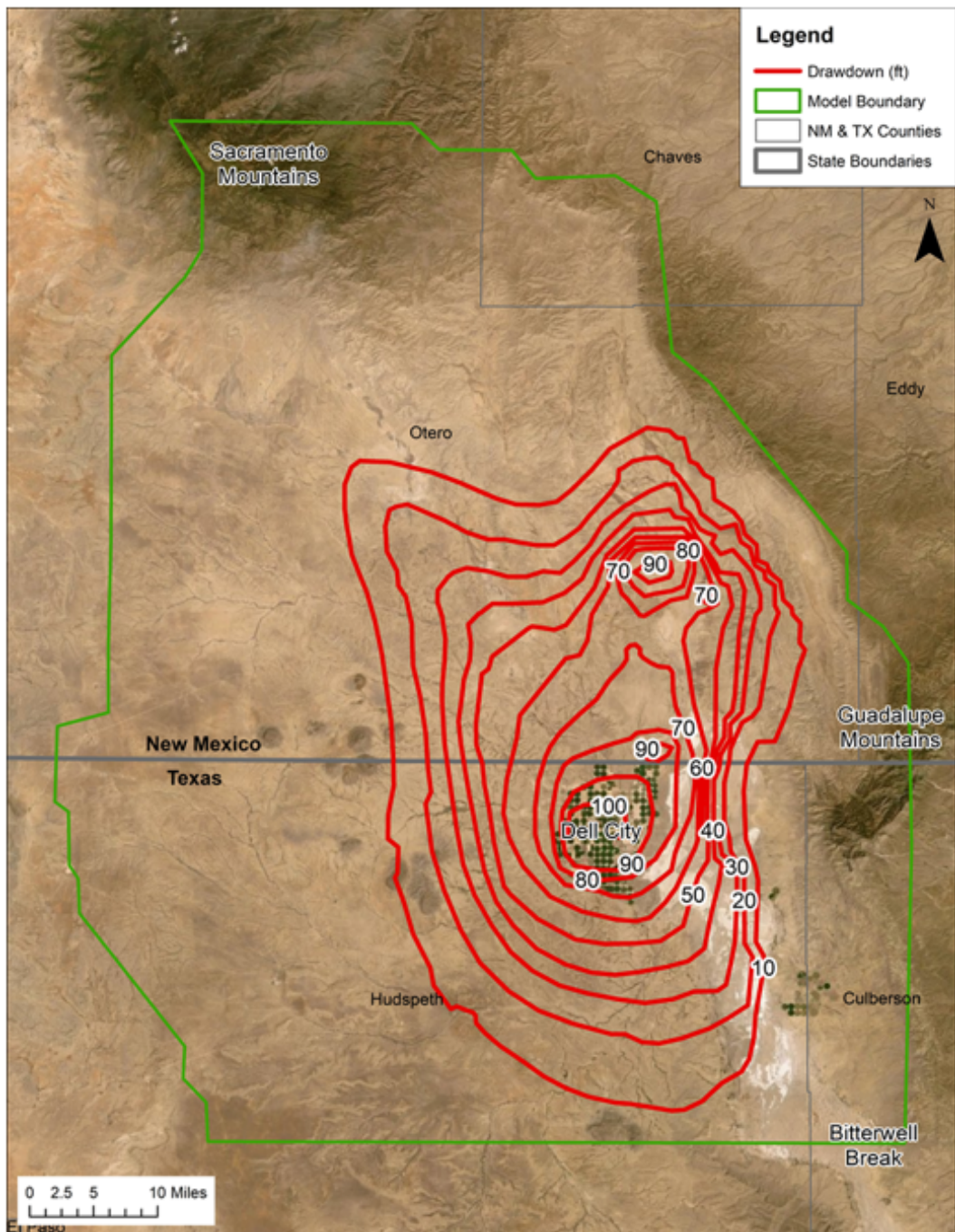


Figure B.9: Maximum simulated drawdown due to historical pumping with a hypothetical well field near Crow Flats. Drawdowns were calculated from pre-development conditions. Contour intervals of 10 ft. Maximum drawdown of 100 ft. Modified from [Shomaker, 2002].

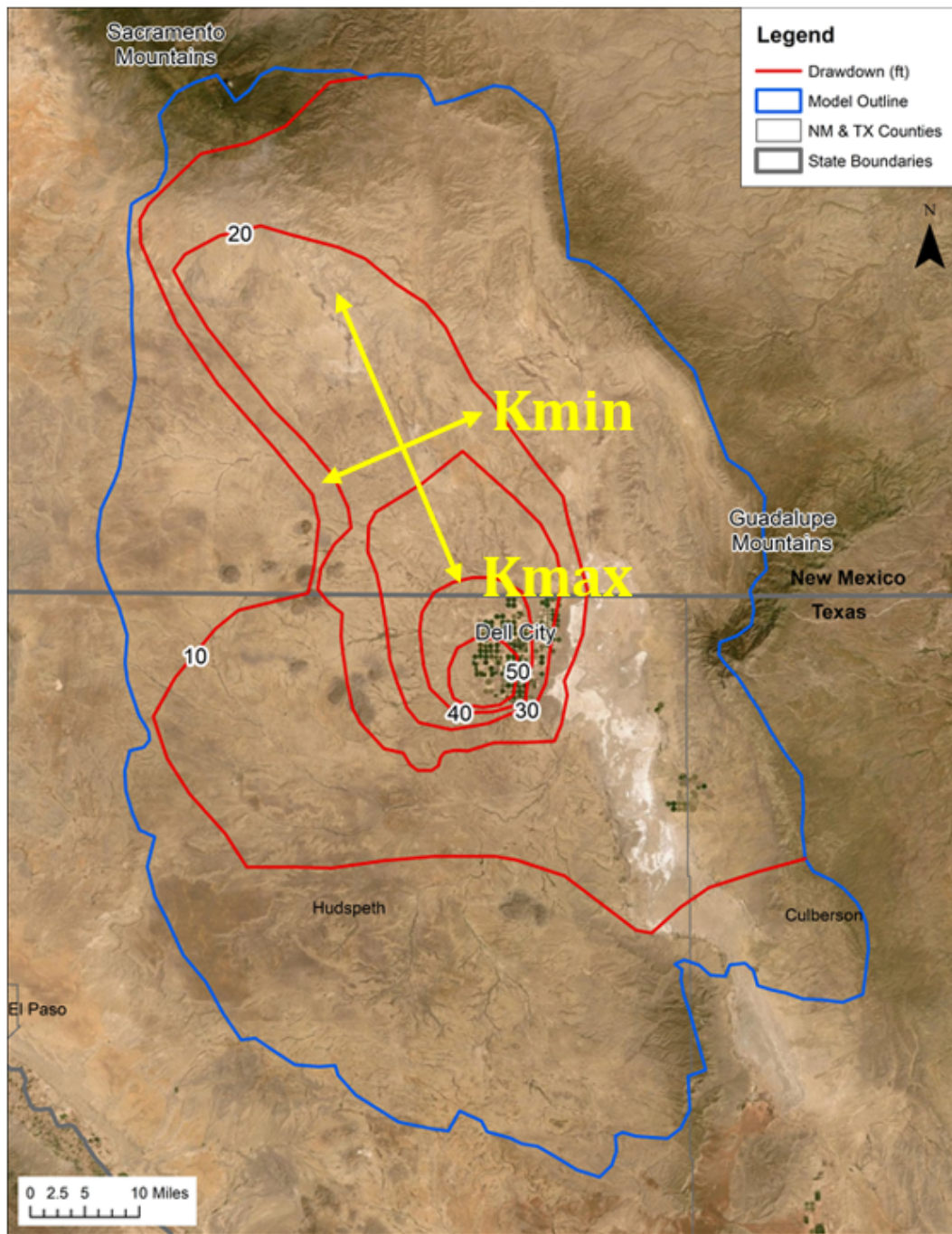


Figure B.10: Drawdowns for the structural model from pumping from 1948 - 2002. Drawdown follows the Otero Break north-northwestward. Maximum drawdown of 50 ft. Contour intervals of 10 ft. The anisotropy used in the model is illustrated by the yellow arrows. Modified from Hutchison [2008].

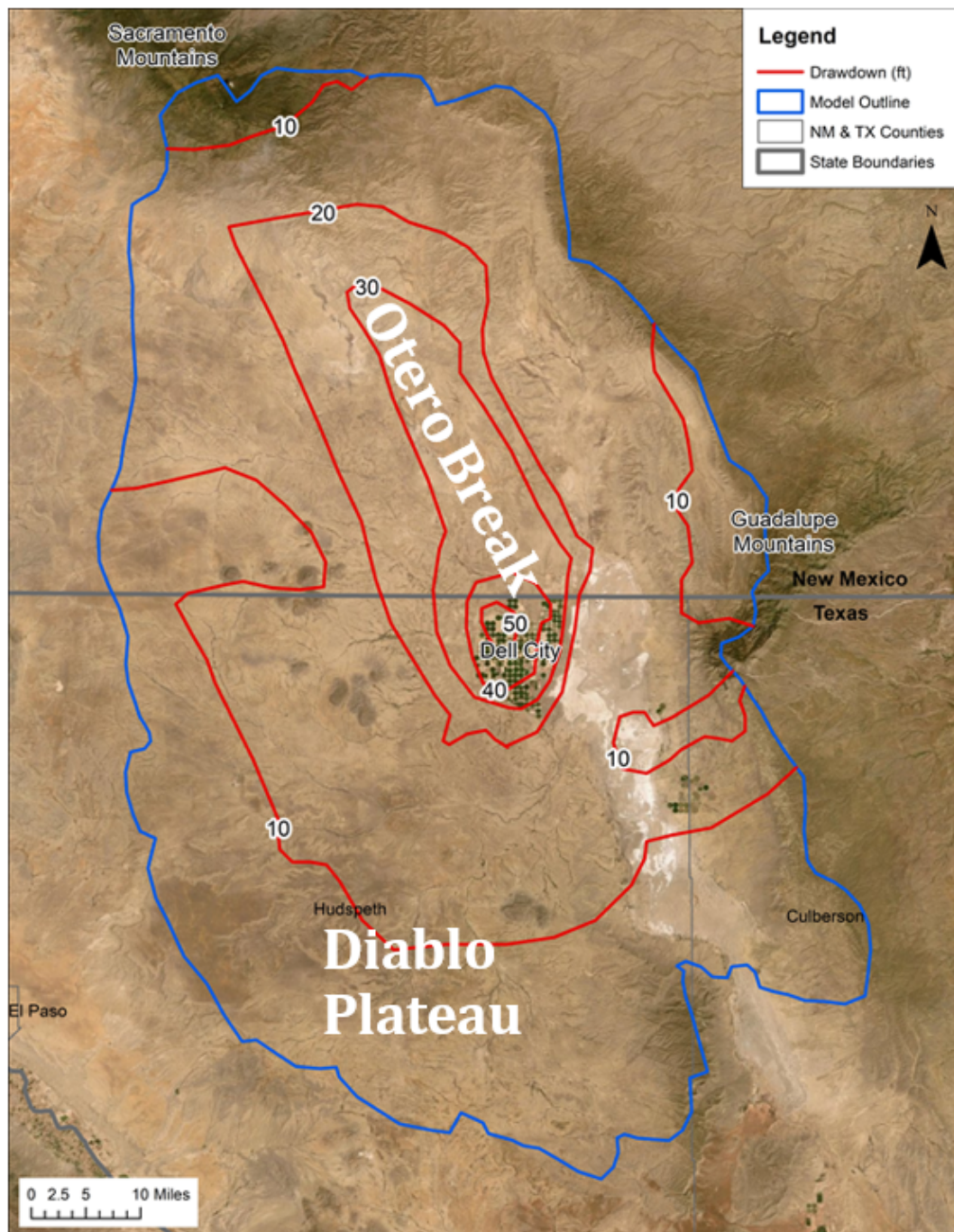


Figure B.11: Drawdowns for the geochemistry model from pumping from 1948 - 2002. Drawdown follows the Otero Break north-northwestward. Maximum drawdown of 50 ft. Contour intervals of 10 ft. The location of the Otero Break and Diablo Plateau are also shown. Modified from Hutchison [2008].

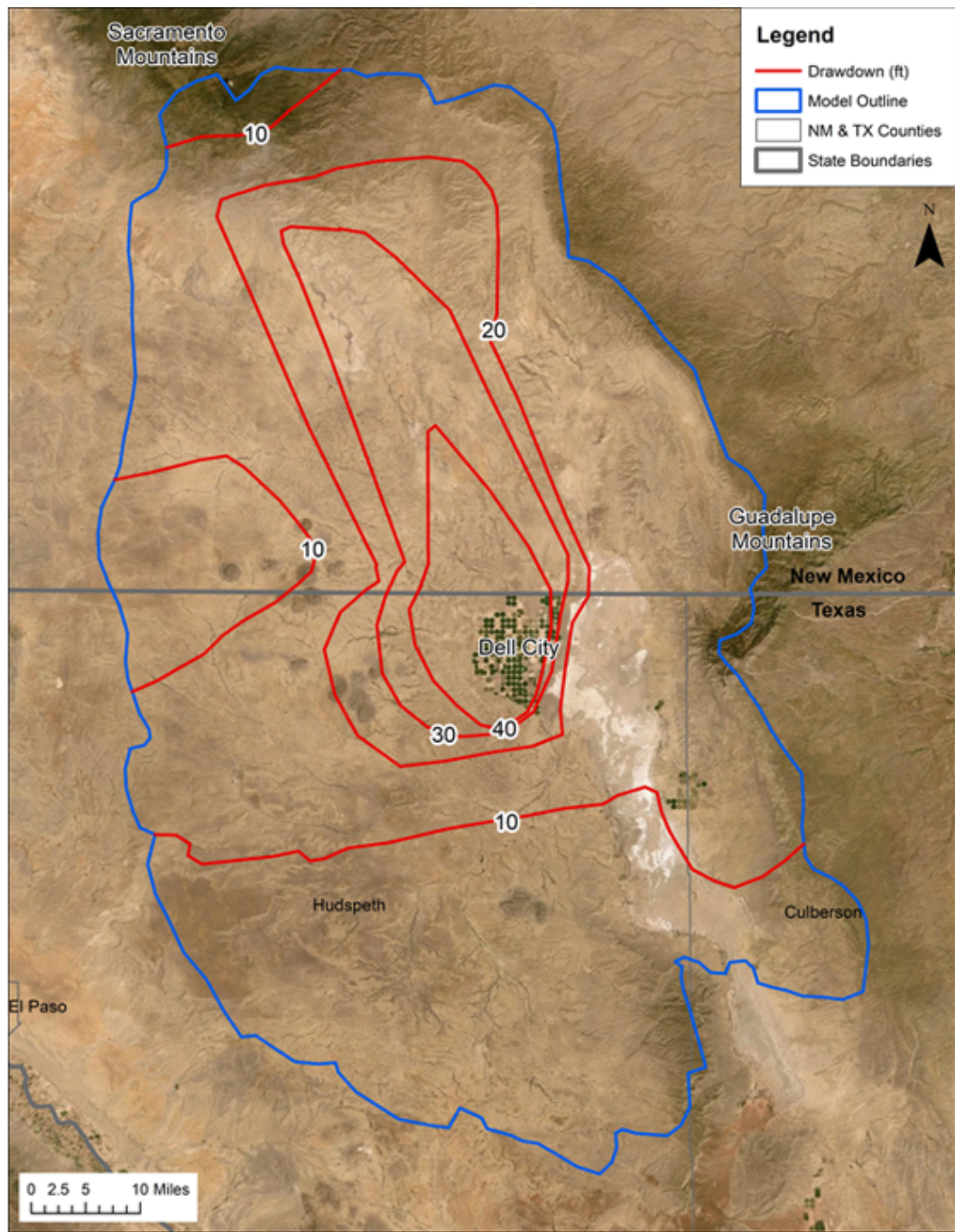


Figure B.12: Drawdowns for the hybrid model from pumping from 1948 - 2002. Drawdown follows the Otero Break north-northwestward. Maximum drawdown of 40 ft. Contour intervals of 10 ft. Modified from Hutchison [2008].

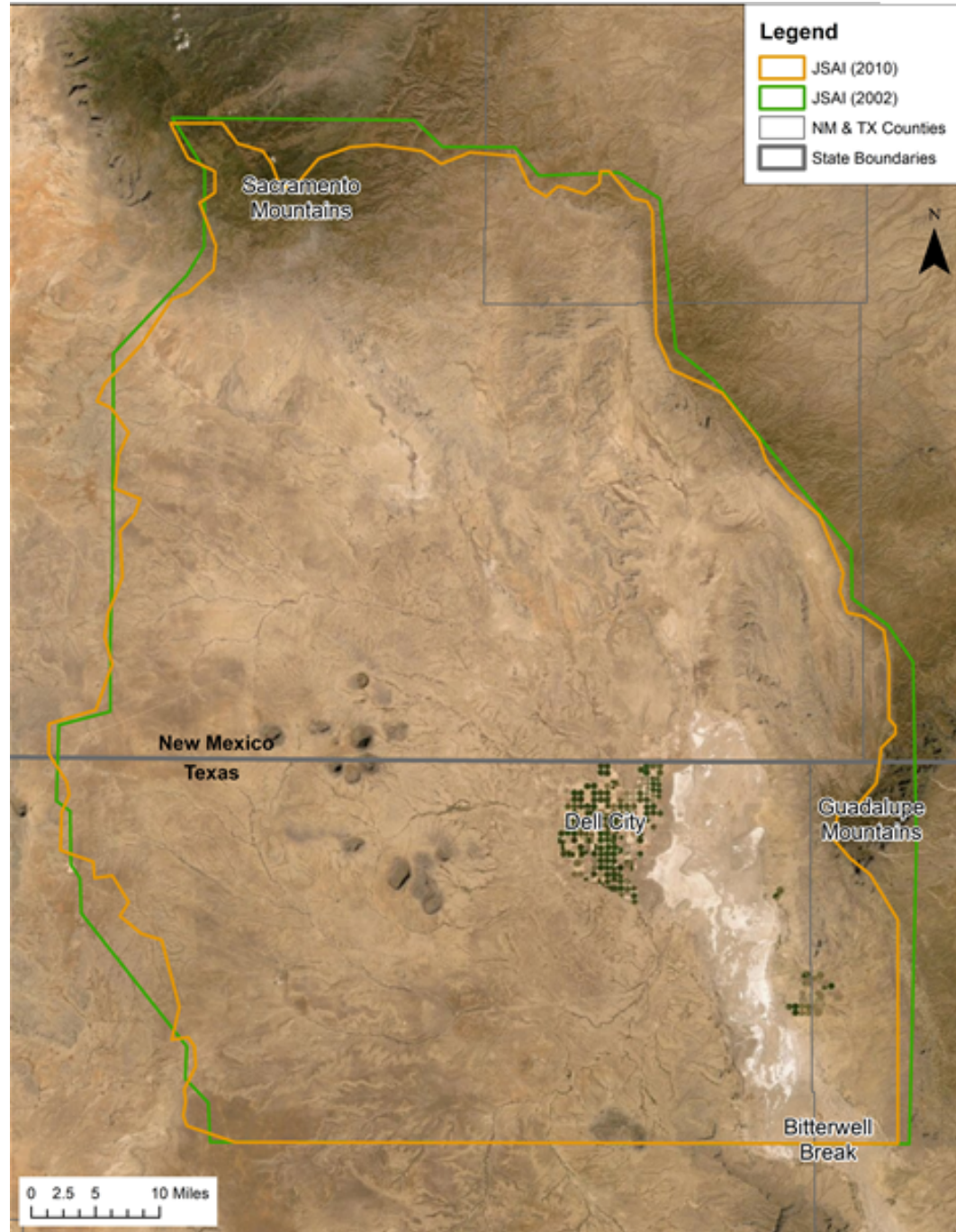


Figure B.13: Shomaker [2010] [orange] and Shomaker [2002] [green] model boundaries. Modified from [Shomaker, 2010] and [Shomaker, 2002]

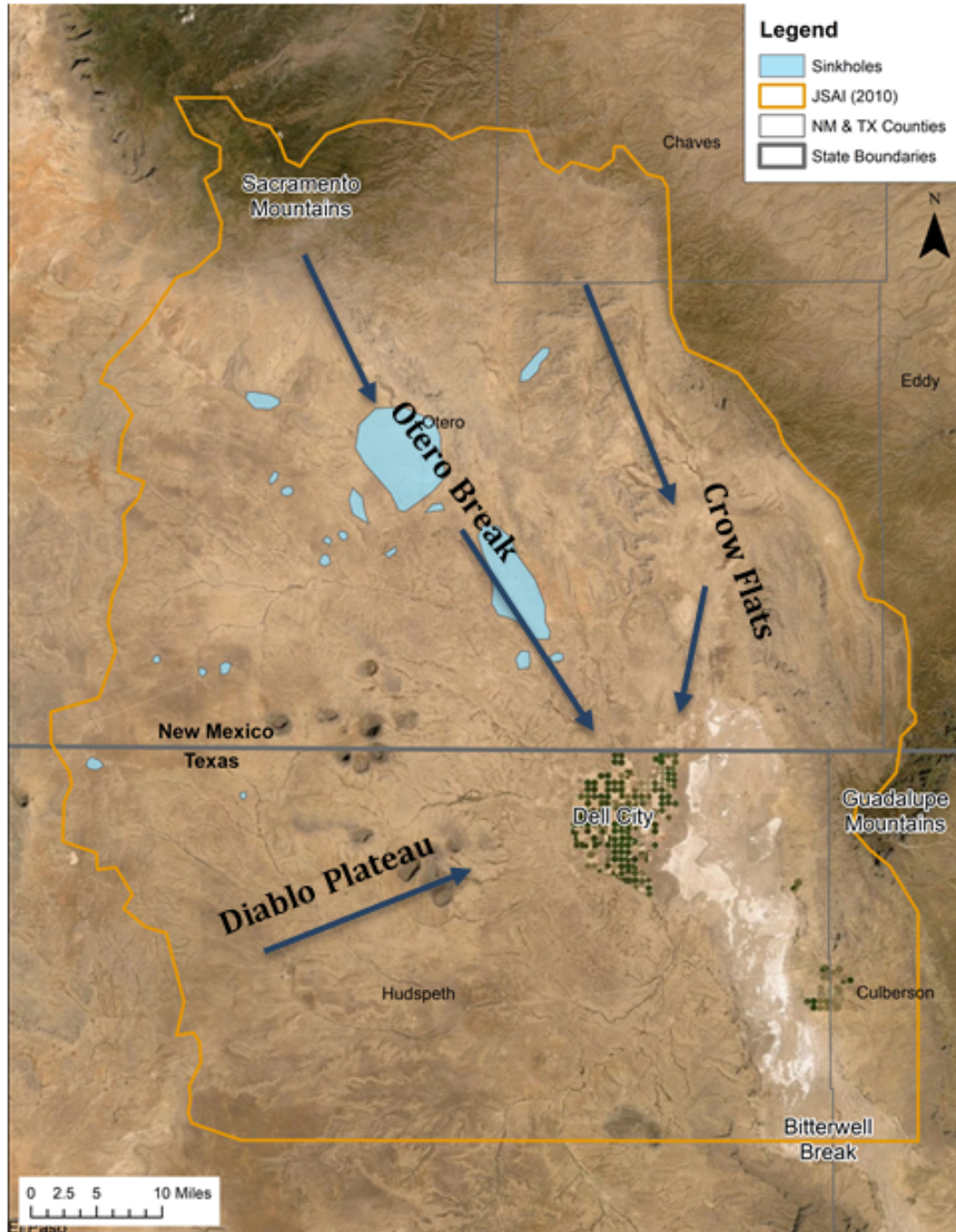


Figure B.14: Shomaker [2010] model boundary (orange), model sinkholes (blue), and major flow paths (arrows). Modified from [Shomaker, 2010].

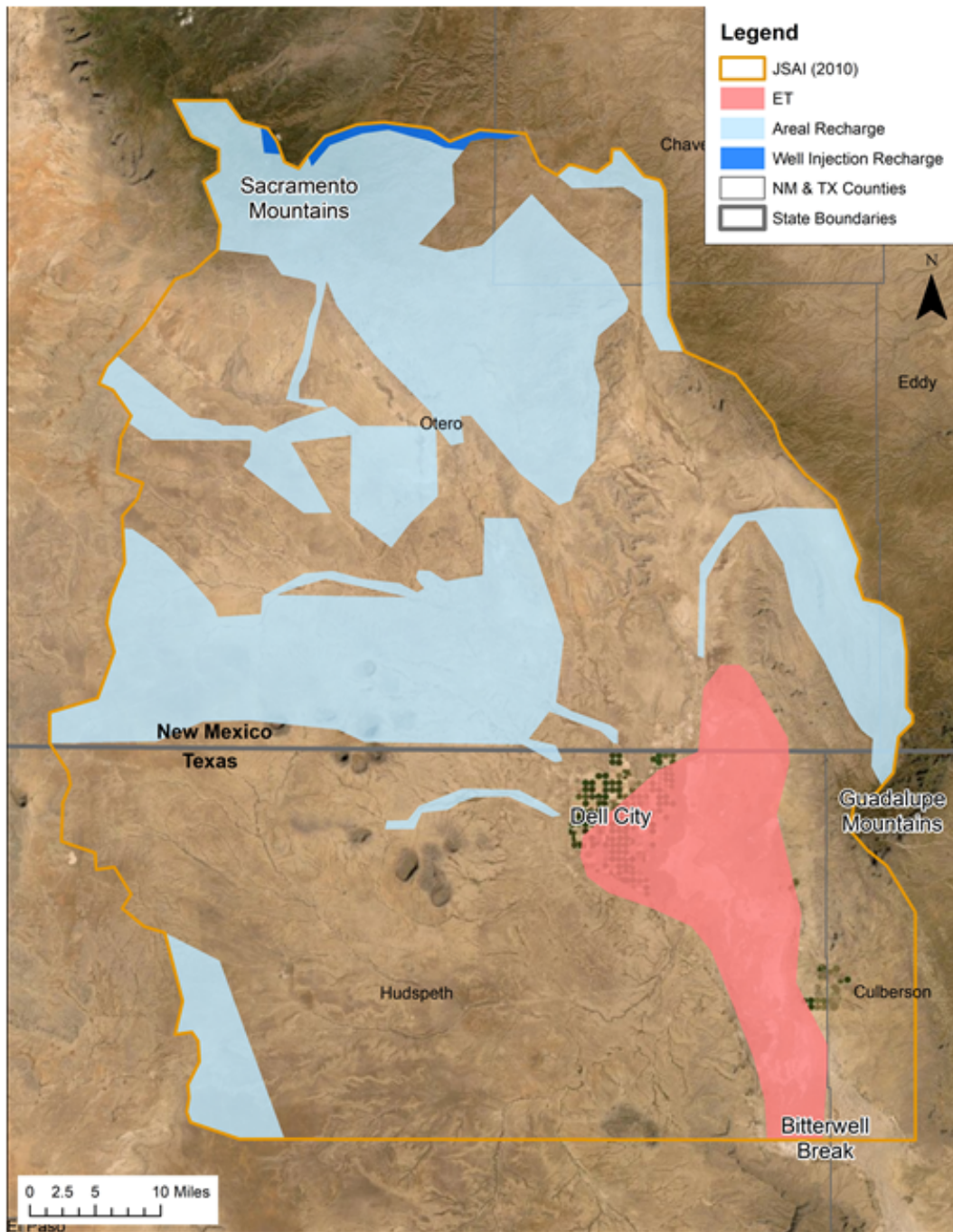


Figure B.15: Shomaker [2010] location of recharge and evapotranspiration. Injection well recharge is in dark blue, areal recharge is light blue, and the light red is evapotranspiration. Modified from Shomaker [2010].

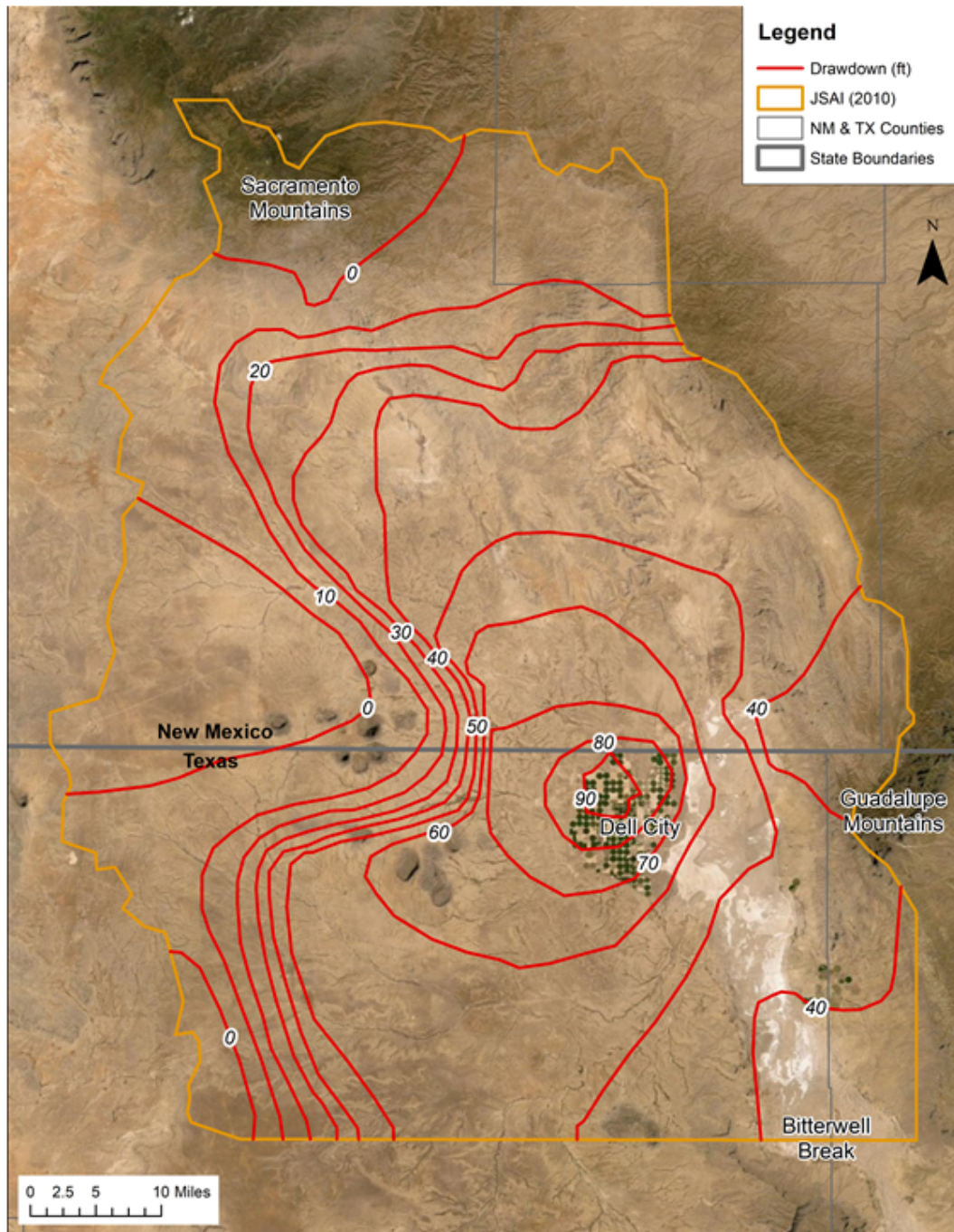


Figure B.16: Model simulated drawdown after running the historical transient model from 1948 to 2009. Contour intervals of 10 ft. Maximum drawdown of 90 ft. Modified from [Shomaker, 2010].

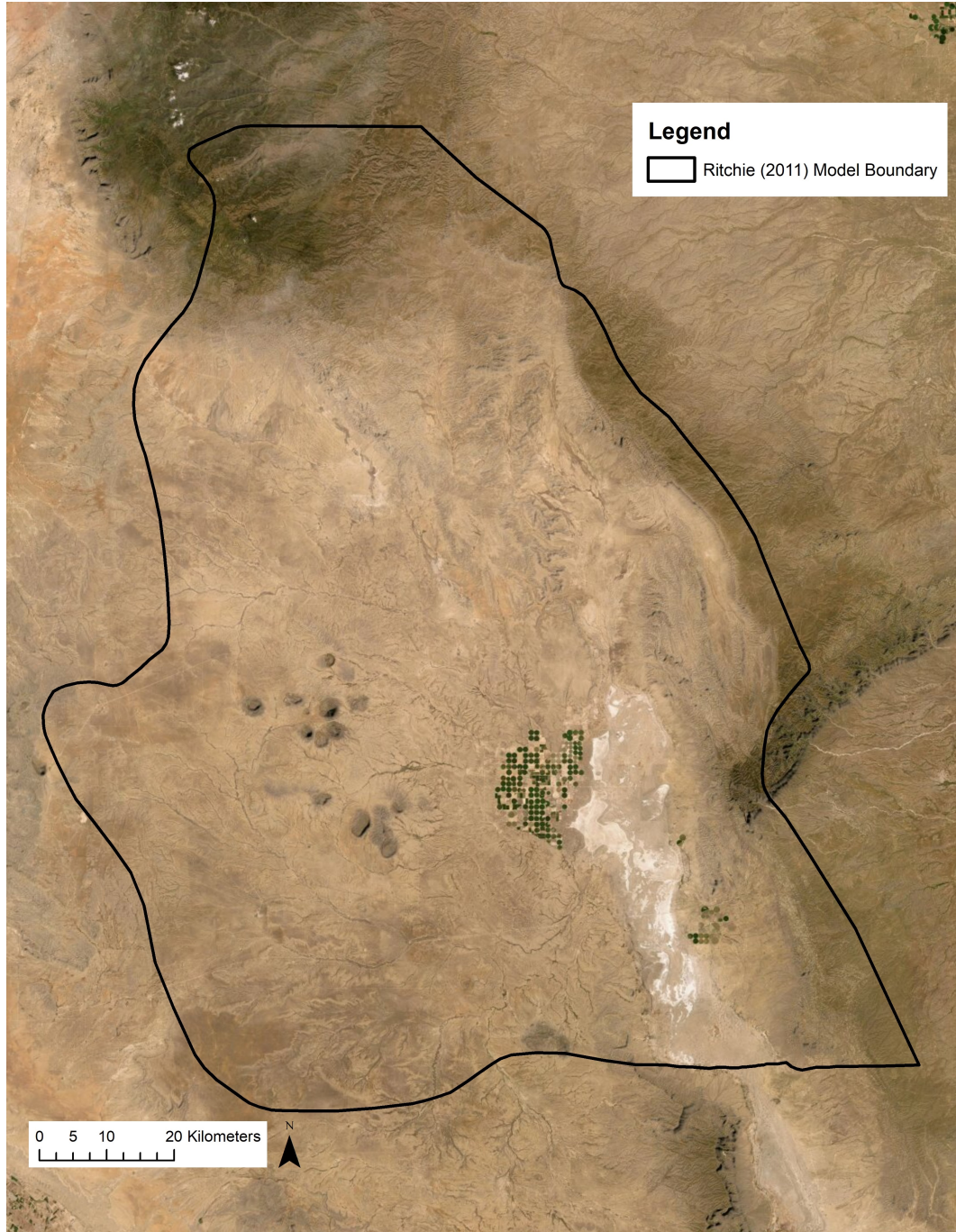


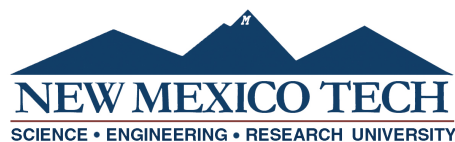
Figure B.17: Ritchie [2011] Salt Basin groundwater flow model boundary.

ASSESSMENT OF SAFE AQUIFER YIELD
WITHIN THE SALT BASIN IN NEW MEXICO AND TEXAS.

by

Elizabeth Evenocheck

Permission to make digital or hard copies of all or part of this work for personal or classroom use is granted without fee provided that copies are not made or distributed for profit or commercial advantage and that copies bear this notice and the full citation on the last page. To copy otherwise, to republish, to post on servers or to redistribute to lists, requires prior specific permission and may require a fee.



ProQuest Number: 28646648

INFORMATION TO ALL USERS

The quality and completeness of this reproduction is dependent on the quality
and completeness of the copy made available to ProQuest.



Distributed by ProQuest LLC (2021).

Copyright of the Dissertation is held by the Author unless otherwise noted.

This work may be used in accordance with the terms of the Creative Commons license
or other rights statement, as indicated in the copyright statement or in the metadata
associated with this work. Unless otherwise specified in the copyright statement
or the metadata, all rights are reserved by the copyright holder.

This work is protected against unauthorized copying under Title 17,
United States Code and other applicable copyright laws.

Microform Edition where available © ProQuest LLC. No reproduction or digitization
of the Microform Edition is authorized without permission of ProQuest LLC.

ProQuest LLC
789 East Eisenhower Parkway
P.O. Box 1346
Ann Arbor, MI 48106 - 1346 USA